BIOASSAY–GUIDED ISOLATION OF CYTOTOXIC

COMPOUND FROM *Hydrocotyle vulgaris*.

By

TEE SHIN LEONG

MASTER OF SCIENCE

FACULTY OF ENGINEERING AND SCIENCE

UNIVERSITI TUNKU ABDUL RAHMAN

2012

BIOASSAY – GUIDED ISOLATION OF CYTOTOXIC COMPOUND

FROM *Hydrocotyle vulgaris*.

By

TEE SHIN LEONG

A dissertation submitted to the Department of Science,

Faculty of Engineering and Science,

Universiti Tunku Abdul Rahman,

In partial fulfillment of the requirements for the degree of

Master of Science

2012

ABSTRACT

BIOASSAY-GUIDED ISOLATION OF CYTOTOXIC COMPOUND FROM

Hydrocotyle vulgaris.

Tee Shin Leong

Hydrocotyle vulgaris is a local medicinal plant, traditionally used for wound healing and as a diuretic herb. Preliminary investigations showed promising cytotoxic activity in the crude ethanolic crude. The cytotoxic compounds were isolated from leaves and root of *Hydrocotyle vulgaris* using a bioassay–guided isolation method. Repeated chromatography of the dichloromethane fraction for leaf and hexane fraction of root using column, thin layer and high performance liquid chromatography resulted in isolation of one partial pure cytotoxic compound, **C1** (isolated from hexane fraction of root) and one pure cytotoxic compound, **L1** (isolated from dichloromethane fraction of leaf). L1 was deduced to be panaxynol from fourier transform infrared spectroscopy (FTIR), polarimetry, mass spectroscopy (MS) and nuclear magnetic resonance spectroscopy (NMR). **C1** and panaxynol was cytotoxic toward human erythromyeloblastoid leukemia cells, K-562 with an IC_{50} value of 13.9 µM and 34.2 µM respectively when tested using the MTT (3-(4, 5-dimethylthiazol-2-yl)-

2, 5-diphemyl-tetrazolium bromide) cell viability assay. The ability of panaxynol to induce apoptosis was determined by flow cytometric detection of phosphatidylserine (PS) externalization using Annexin V-FITC. The cell cycle arrested was quantified from histograms of cell populations stained with propidium iodide. The activation of caspases-3/7, 8 and 9 were quantified by using luminescent cell based assay that detected the presence of caspase enzymatic activity. K-562 cells exposed to panaxynol at IC_{50} and IC_{85} concentrations for 48 hours resulted in membrane blebbing, chromatin condensation and apoptotic bodies which are consistent with apoptotic cell death. Flow cytometric detection of PS externalisation showed that panaxynol at IC_{50} and IC_{85} concentrations resulted in 16.57 % ± 3.01 and 32.87 % ± 5.45 of apoptotic populations when treated for 48 hours. IC_{50} concentrations of panaxynol resulted in 7.15 % ± 1.72 of the K-562 cell population detected in sub G_0 and 53.08 % ± 2.47 in G_0/G_1 phase at 48 hours incubation. IC_{85} concentrations of panaxynol over the same incubation time resulted in doubling of the sub G_0 (15.07 % ± 2.86) population while G_0/G_1 phase population remained almost the same at 54.92 % ± 1.49. Untreated K-562 cells showed a small (1.39 % ± 0.55) sub G_0 population and 47.03 % ± 3.14 of the population in G_0/G_1. This suggested that panaxynol caused a minor G_0/G_1 arrest in K-562 cells only at IC_{85} concentration. Enzymatic activities of caspases-3/7, 8 and 9 in K-562 cells increased to 35.07 RLU/cell ± 2.04, 2.78 RLU/cell ± 0.28 and 51.31 RLU/cell ± 5.23 respectively, when treated with IC_{85} concentration of panaxynol for 24 hours compared with untreated K-562 cells that showed baseline enzyme activities of

4.27 RLU/cell ± 0.09, 0.97 RLU/cell ± 0.07 and 5.36 RLU/cell ± 0.60 respectively. This showed that apoptosis was mediated by activation of the caspase cascade. In conclusion, panaxynol was successfully isolated from dichloromethane fraction of leaves of *Hydrocotyle vulgaris* and killed K-562 cells via induction of apoptosis mediated by the caspase cascade in the absence of any significant cell cycle arrest activity.

ACKNOWLEDGEMENTS

Firstly, I would like to thank my supervisor, Dr Anthony Ho Siong Hock for giving me an opportunity to have my master project being supervised by him. I also want to thank him for providing advice, encouragement, guidance, and information regarding my project during the process of my project and the preparation of this thesis. Besides, I would also like to express my gratitude to Dr Lim Yang Mooi's guidance during the work completion seminar and final part of my dissertation submission.

Furthermore, I would like to express my gratitude to the UTAR laboratory officers, especially Ms Soong and Mr Su for their kind and helpful assistance during my laboratory work.

Special thanks also go to my lab mates, Jia jie, Chin Piow, Ooiean, Wei Hsum, Teck Yew, Su Yin, Siew Ling, Sze Mum, Hoey and Shiau Chooi who have shared their views and supported me during the process of project.

Lastly, my deepest appreciation to Lee Mei and my supportive parent who helping me to prepare the plant material for my project. Once again, a deep heartfelt thanks to all who had contributed one way throughout my preparation of this thesis.

APPROVAL SHEET

This dissertation entitled "**BIOASSAY-GUIDED ISOLATION OF CYTOTOXIC COMPOUND FROM *Hydrocotyle vulgaris*.**" was prepared by TEE SHIN LEONG and submitted as partial fulfillment of the requirements for the degree of Master of Science at Universiti Tunku Abdul Rahman.

Approved by:

_____

(DR. LIM YANG MOOI)   Date:………………………..

Associate Professor

Department of Pre-clinical Sciences

Faculty of Medicine and Health Sciences

Universiti Tunku Abdul Rahman

FACULTY OF ENGINEEERING AND SCIENCE

UNIVERSITI TUNKU ABDUL RAHMAN

Date: _____

SUBMISSION OF THESIS

It is hereby certified that TEE SHIN LEONG (ID No: 08UEM08120) has completed this thesis entitled "Bioassay-Guided Isolation of Cytotoxic Compounds From *Hydrocotyle vulgaris*" under the supervision of LIM YANG MOOI (Supervisor) from the Department of Pre-clinical Sciences, Faculty of Medicine and Health Sciences .

I understand that University will upload softcopy of my thesis in pdf format into UTAR Institutional Repository, which may be made accessible to UTAR community and public.

Yours truly,

_____

(TEE SHIN LEONG)

DECLARATION

I hereby declare that the dissertation is based on my original work except for quotations and citations which have been duly acknowledged. I also declare that it has not been previously or concurrently submitted for any other degree at UTAR or other institutions.

Name: _____

Date: _____

TABLE OF CONTENTS

LIST OF TABLES

LIST OF FIGURES

LIST OF ABBREVIATIONS

%	Percentage
º C	Degree celsius
δ	Chemical shift
+ ve	Positive
- ve	Negative
$[\alpha]_D$	Dry weight
μg	Microgram
μl	Microliter
μm	Micrometre
μM	Micromolar
^1H	Hydrogen with number atom 1
^{13}C	Carbon with number atom 13
A498	Human, kidney carcinoma
AIF	Apoptotic inducing factor
Apaf - 1	Apoptotic protease-activating factor 1
Asp	Aspartate
A – T	Adenine – Thymine
ATCC	American type culture collection
ATP	Adenosine triphosphate
BAX	BCL-2 associated X protein
BEL-7402	Hepatocellular carcinoma

BrdU	Bromodeoxyuridine
C	Carbon
c	Concentration
Ca^{2+}	Calcium ion
Caco-2	Epithelial colorectal adenocarcinoma
CAD	Caspase activated DNase
Caki-1	Human, kidney carcinoma
Calu-1	Human, epidermoid carcinoma
CARD	Caspase recruitment domains
CDK	Cyclin dependent kinase
$CHCl_3$	Chloroform
CKI	Cyclin dependent kinase inhibitor
cm	Centimetre
CO_2	Carbon dioxide
CoQ	Coenzyme Q
COSY	Homonuclear shift correlation spectroscopy
CURC II	Human, renal cell carcinoma
DED	Death effector domain
DNA	Deoxyribonucleic acid
DISC	Death inducing signaling complex
DMSO	Dimethyl sulfoxide
ELISA	Enzyme linked immunosorbent assay
FADD	Fas-associated protein with death domain

FITC	Fluorescein isothiocyanate
FSC	Forward Scatter
FTIR	Fourier transform infrared spectroscopy
g	Gram
GC	Gas chromatography
GCMS	Gas chromatography – mass spectrometry
GR	General grade
H	Hydrogen
HCT-116	Human, colon tumor cell line
HL-60	Human promyelocytic leukemia
HETCOR	Heteronuclear correlation spectroscopy
HMBC	Heteronuclear multiple bond coherence
HMQC	Heteronuclear multiple quantum coherence
HPLC	High performance liquid chromatography
Hz	Hertz
IAP	Inhinitor of apoptosis
IC_{50}	Inhibition concentration of 50%
IC_{85}	Inhibition concentration of 85%
INK 4	Inhibitors of CDK4
IR	Infrared spectrophotometer
IUPAC	International Union of Pure and Applied Chemistry
J	Coupling constant
JNK	Jun N-terminal kinases

K-562	Human, erythromyeloblastoid leukemia
L-1210	Human, lymphoid leukimia
LDH	Lactate dehydrogenase
LF3	Fraction-3 for dichloromethane fraction of leaf
LF3-1	Fraction 1 derived from LF3 fraction
LL	Lower left
LNCaP	Human prostatic adenocarcinoma
LR	Lower right
m	Metre
M	Molar
M25-SF	Human, breast carcinoma cells
MCF7	Human, breast adenocarcinoma
mg	Miligram
MK-1	Human, gastric carcinoma cells
ml	Mililiter
mm	Milimeter
MPT	Mitochondrial permeability transition
MS	Mass spectroscopy
MTT	3-(4, 5-dimethylthiazol-2-yl)-2, 5-diphemyl-tetrazolium bromide
m/z	Molecular weight
NADPH	Nicotinamide adenine dinucleotide phosphate (reduced form)

NCI	National cancer institute
nm	nanometre
NMR	Nuclear magnetic resonance
OH	Hydroxyl
PBS	Phosphate buffer solution
PI	Propidium iodide
PS	Phosphatidylserine
PTFE	Polytetrafluoroethylene
Raji	Human, B lymphocyte; Burkitt's lymphoma
RF2	Fraction-2 for hexane fraction of root
RF6	Fraction-6 for hexane fraction of root
RF2-3	Fraction-3 derived from RF2 fraction
RF6-4	Fraction-4 derived from RF6 fraction
RF6-4-4	Fraction-4 derived from RF6-4 fraction
RLU	Relative luminescent unit
RNA	Ribonucleic acid
Rnase	Ribonuclease
ROS	Reactive oxygen species
rpm	Rotation per minute
RPM-I 1640	Roswell Park Memorial Institute 1640
SK-MEL-28	Malignant melanoma

Smac/DIABLO	Second mitochondria-derived activator of caspase/direct inhibitor of apoptosis-binding protein with low p*I*
SPE	Solid phase extraction
SSC	Side scatter
TK10	Human renal adenocarcinoma
TLC	Thin layer chromatography
TNF	Tumorr necrosis factor
TRAIL	TNF related apoptosis inducing ligand
U-2 OS	Human, caucasian, bone, osteosarcoma
UACC62	Human, melanoma
UL	Upper left
UR	Upper right
UV	Ultra violet
Wish	Human, epithelial cell line
Vero	African Green Monkey, kidney epithelial cells
v/v	volume/volume

CHAPTER 1

INTRODUCTION

Cancer has been reported as the second leading cause of death in Malaysia with an estimated 21000 cancer cases reported in 2006 alone (Ariffin, Zainudin & Nor Saleha, 2006; MAKNA, 2006). In 2010, it is predicted that around 1,529,560 of new cancer cases are expected globally (American Cancer Society, 2010). Existing therapies such as chemotherapy are not very specific for cancer cells and cause damage to normal tissue such as bone marrow, gut lining and hair follicles resulting in infection, diarrhea, vomiting and hair loss (Gore & Russell, 2003). This necessitates the search for more effective and specific treatment against cancer.

The use of herbal medicine to cure disease dates back many thousands of years. Even today, many conventional drugs are derived from plants (Yuan & Lin, 2000). There is a growing shift of people choosing herbal cures over conventional drugs due to the perception that herbals are safer and have reduced side effect (Ramlan, 2003). Clinical tests using herbal medicine have also shown no adverse effect on renal, hepatic, and bone marrow function (Yuan & Lin, 2000).

Other than herbal medicine properties, natural products produced by plants, fungi, bacteria, protozoans, insects and animal provide us with diverse chemical structures. This gives us an opportunity to discover bioactive chemical structure to treat disease such as cancer.

From 1981-2002, approximately 60 % of anticancer agents were derived from plant natural products (Lam, 2007) and a further 20 % were natural product mimics or synthetic compounds derived from natural products (Newman, Cragg & Snader, 2003). Therefore, natural compounds from plants not only serve as a drug, they also provide a rich source of novel structures that may be developed into novel anticancer agents.

The systemic screening of plant for cytotoxic activity started with National Cancer Institute (NCI, USA) in 1960. Under this program, NCI screened over 114000 extracts and yielded taxol and camptothecin as anticancer agents. Other notable large scale screening programmes include the work by the Council for Scientific and Industrial Research (CSIR) in South Africa that identified anticancer agents from plant natural products between 1998 – 2006 (Fouche, Cragg, Pillay, Kolesnikova, Maharaj & Senabe, 2008).

Malaysia is listed among the 12th most biodiverse countries in the world with over 15000 flowering plants and 3000 species of medicinal plants. Among the medicinal plants, only about 50 are used commercially and even less are being researched scientifically for their medicinal properties (Ramlan, 2003). One example of a local plant that is believed to possess ethnomedicine properties is *Hydrocotyle vulgaris*. This plant is commonly found in Malaysia and is traditionally used for wound after surgery and as a diuretic (Duke, 1996). In 2005, a Thailand researcher discovered a novel compound name as methyl oleanolate 3-O-(β-D-glucopyranoside)$_3$ from *Hydrocotyle vulgaris* and this compound able to inhibit the root generation of *Mimosa pigra* Linn (Chavasiri, Prukchareon, Sawasdee & Zungsontiporn, 2005). While in Denmark and India, this plant is traditionally used to treat whooping cough and leprosy (Felter & Lloyd, 1898; Burton, 2002). Apart from these reports, this herb has not been scientifically investigated for cytotoxicity.

In preliminary studies, the ethanolic extract of *Hydrocotyle vulgaris* shown cytotoxic effect against K-562, HL-60 cell line (Human promyelocytic leukemia), Raji cell line (human, B lymphocyte; Burkitt's lymphoma), and U-2 OS cell line (human, Caucasian, bone, osteosarcoma) (Wong, 2006 ; Tee, 2007). Studies on other species of *Hydrocotyle* family like *Hydrocotyle asiatica* and *Hydrocotyle sibthorpioides* Lam had shown the presence of cytotoxic compounds against

cancer (Graham, Quinn, Fabricant & Farnswort, 2000). Thus, this genus of plants may give potential lead compounds.

Therefore, the aims of this study are to isolate cytotoxic compounds from *Hydrocotyle vulgaris* using bioassay-guided isolation and characterize the pure cytotoxic compound. Besides, determinate cytotoxicity of puried compound isolated from *Hydrocotyle vulgaris* and investigated the cell killing mechanism of puried compound against K-562 cells.

CHAPTER 2

LITERATURE REVIEW

2.1   Cancer

Cancer can be described as a disease in which cells grow and spread unrestrained throughout the body, eventually causing death. Cancerous cells will invade neighboring tissues and to the other parts of the body, and thus is potentially life-threatening (Becker, Kleinsmith & Hardin, 2003). Cancer can be categorized into carcinomas, sarcomas, leukemias, lymphomas and myelomas and central nervous system cancers (NCI, 2009).

Cancer is mainly caused by mutations in the DNA. Some cancers are triggered by DNA damaging chemicals (benzene or nickel) and radiation (UV-radiation or X-rays), whereas other arise from spontaneous DNA mutations and replication errors. Mutation in certain genes such as proto-oncogenes like ras and tumour suppressor gene like p53 will influence the regulation of fundamental cellular processes like proliferation, differentiation, and apoptosis (Scholzova, Malik, Evcik & Kleibl, 2007; Kintzios & Barberaki, 2003). Certain mutations are inherited and predispose the individual to a higher risk of cancer. Some cancers

are also related to viral infection, such as the Human Papilloma Virus and Epstein-Barr virus.

Cancer development or carcinogenesis is a multistep process and these steps reflect genetic alteration that generates the progressive transformation of normal cells to highly malignant tumours. Generally, carcinogenesis can be divided into initiation, promotion and progression stages (Ito, Hasegawa, Imaida, Hirose, Asamoto & Shirai, 1995). During initiation stage, metabolism state, DNA repair efficiency and proliferation play an important role in the development of this stage. Metabolism may inactive or activate the carcinogen, resulting in the carcinogen interacting with DNA to generate DNA adducts and lesions. While an inefficient DNA repair mechanism may allow these mutations or adducts to propagate during cell division. Proliferation permanently embeds the change in the genome (Tannock, Hill, Bristow & Harrington, 2005). During promotion stage, the initiated cells show altered phenotypic expression that support rapid proliferation in a supportive environment that maintains the proliferative potential (Ito, Hasegawa, Imaida, Hirose, Asamoto & Shirai, 1995). The last stage is progression, where a variety of consequences for the tumour cell ensue. Genetic instability which occurred in this stage will lead to chromosome or gene amplification, translocation and rearrangements. For example, deletions may lead to proto-oncogene activation and tumour suppresser gene (p53) inactivation.

These alternations allow the cancer cells to acquire malignancy and survive in the human body (Ruddon, 2007).

Cancer cells generate six alterations in cell physiology to defect the regulatory circuits that govern normal cell proliferation and homeostasis. In addition, these alterations let the cancer cells obtain novel capabilities to successfully circumvent the anticancer defense mechanisms of the body. These alterations including, self-sufficiency in growth signal, insensitivity to growth-inhibitory-signal, evasion of programmed cell death (apoptosis), limitless replicative potential, sustained angiogenesis, and tissue invasion and metastasis (Hanahan & Weinberg, 2000).

2.2   Treatment of Cancer

The type of cancer treatment varies depending upon the type of cancer, the stage of cancer, symptoms and the site of origin (tissue or organ). The aim of cancer treatment is to reduce patient's symptoms and also to control disease. Presently, the three main treatments for cancer include surgery, radiotherapy and chemotherapy.

2.2.1 Radiotherapy

Radiotherapy is the use of ionizing radiation to kill or suppress the growth of cancer cells selectively, while minimizing the damage to surrounding healthy cells. This method is somewhat selective because unlike normal cells, malignant cells have defects in DNA repair and will be selectively killed by radiation (Gore & Russell, 2003).

2.2.2 Surgery

Surgery is used to remove tumours to relieve symptoms or side effects of cancer. However not all tumours can be safely removed and it is limited to non metastasized cancer. Surgery is often combined with other cancer treatments, such as chemotherapy and radiotherapy (Robert & Johnson, 2009).

2.2.3 Chemotherapy

Chemotherapy uses drugs to kill cancer cells (cytotoxic drug) or limit the growth of cancer cells (cytostatic drugs) (Gore & Russell, 2003). Chemotherapy is based on the systemic administration of anticancer drugs that travel throughout the whole body system via the blood circulatory system. Hence, they are useful

against metastasized cancer cells (Kintzios & Barberaki, 2004). Unfortunately, presently used drugs are poorly selective for cancerous cells and also rapidly damage dividing tissues such as bone marrow, gut lining and hair follicles. This can cause symptoms like hair loss and diarrhea (Gore & Russell, 2003).

Generally, chemotherapy is combined with either radiotherapy or surgery. Chemotherapy can be done before surgery to shrink the tumours making it easy to remove, or after surgery to kill the remaining cancer cells (Belkacémi, Mirimanoff & Ozsahin, 2009). Chemotherapeutic drugs are classified into nine general groups as outlined in Table 2.1.

Table 2.1: The functions and examples for the nine types of chemotherapeutic drugs (Kintzios & Barberaki, 2004).

Type of chemotherapeutic drug	Examples	Functions
Antimetabolite	5-fluorouracile, Methotrexate	Act as non-functional analogues of essential metabolites in the cell, thus blocking physiological functions
Alkylating agents	Busulfan, Cyclophosphamide, Ifosfamide	Binding with DNA through alkyl groups, and lead to damage on the DNA template and subsequent cessation of DNA synthesis
Topoisomerase inhibitors	Amsacrine	Inhibit DNA replication in rapidly dividing cells
Plant alkaloids	Vinblastine, Vincristine, Vindesine	Blocking mircotubules depolymerisation causing chromosome detachment during mitosis
Antibiotics	Plicamycin, Mitomycin, Bleomycin	Blocking protein synthesis and DNA replication.

Table 2.1 Continued

Type of chemotherapeutic drug	Examples	Functions
Anthracyclins	Doxorubicin hydrochloride, Rubidazone, Daunorubicin	Blocking protein synthesis and DNA replication
Enzymes	L-asparaginase, Tyrosine kinase inhibitor	Inhibits protein synthesis and reproduction by depriving cells of required amino acid in cell proferation
Hormones	Adrenocorticoids, Estrogens	Regulating the endocrine system hey find specific application against carcinoma of breast, prostate and endometrium
Immunomodulators	Interferons, Interleukins	Inhibiting tumuor proliferation through the stimulation of the host's immune system

2.3 Cell Cycle

The cell cycle is a highly controlled and ordered mechanism which is essential in every cell in an organism. The functions of the cell cycle are to cause replication, increase genetic information and inheritance of gene from generation to generation (Israels & Israels, 2000). In general, the cell consists of two major activities, DNA synthesis (S phase) and mitosis or cell division (M phase). These phases are separated by the 2 Gap phase (G phase) to provide the cell with a proofreading period for DNA replication and cell division. The first gap to separate the M phase from S phase is G_1 phase and the second gap separating the S phase from M phase is G_2 phase. G_0 phase called as quiescence, occurs when the cell exits from cell cycle because of the absence of mitogenic growth signals (Foster, 2008).

The G_1 phase (preparation of DNA replication) is unique because it is the only phase to detect the signal from extracellular environment and regulates the decision of the cell to either continue through the cell cycle or exit from the cell cycle and return to G_0 phase. Once the cells are committed to proliferation, they will start to syntheses proteins which are necessary to replicate their genome. Then, the cell will assemble various components like nutrients, growth factors and enzymes for DNA replication. Once it completed, the cells can enter in the S phase for DNA replication. Thereafter, the cells will go through the G_2 phase for the preparation of mitosis and allow the cells for cell division. In mitosis, the cell

separates into two daughter cells and each receives an exact copy of DNA. After mitosis the cell proceeds through another cell cycle if mitogenic growth signals are present or may exit the cell cycle and return into G_0 phase (Mendelsohn, Howley, Israel, Gray & Thompson, 2008; Maddika et al., 2007).

2.3.1 Cell Cycle Checkpoints and Regulations.

Transitions between each phase are controlled by a series of checkpoints (Figure 2.1). These checkpoints function to make sure that mitogenic growth signals are available, repair mechanisms are activated and ensure the DNA damage or DNA mutations are absent throughout the whole cell cycle (Maddika et al., 2007). There are three checkpoints present in a cell cycle. The first checkpoint, G_1 checkpoint, is a restriction checkpoint present between the G_1 phase and S phase. This checkpoint allows decision to be made on whether a cell should continue dividing or enter the quiescent phase in the present or absent of mitrogenic growth signal (Israels & Israels, 2000). The second checkpoint, G_2 checkpoint, present at the end of G_2 phase to ensure that no mutated DNA is carried through into mitosis. The last checkpoint is the mitotic checkpoint, present in prometaphase. This checkpoint monitors the formation of the mitotic spindles (Mendelsohn, Howley, Israel, Gray & Thompson, 2008).
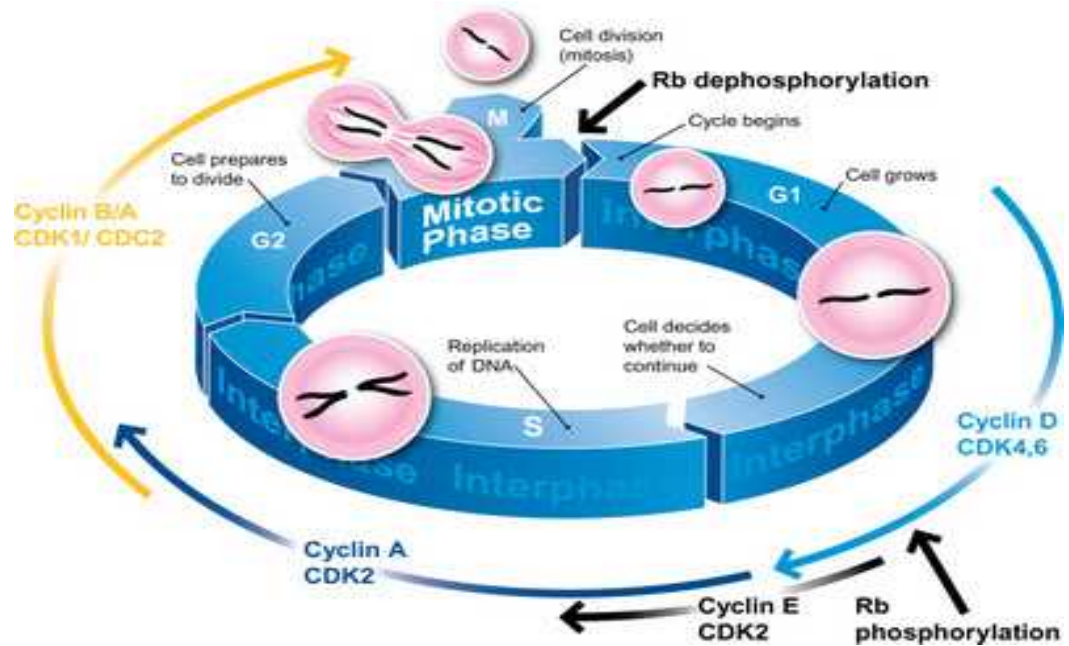
Figure 2.1: The overview of the cell cycle with present of restriction check point, G_1 check points and G_2 check point. The arrows indicate the stages in the cell cycle in which the specific CDK-cyclin pairs are believed to act (Abcam®, 2010).

These checkpoints are highly regulated via interaction between cyclin, cyclin dependent kinase (CDK) and cyclin dependent kinase inhibitor (CKI). CDKs are binary enzymes (Foster, 2008). In the monomer form, the CDK has no enzyme activity. Once the CDK binds with specific cyclins, this will induce the conformation change in a C-terminal domain of the CDK and activate the kinase function. In addition, the cyclin contains nuclear localization signals that are able to lead the cyclin: cyclin dependent kinase complex toward the nucleus and ensured DNA damage or DNA mutations are absent throughout the whole cell

cycle. Specific cyclin and cyclin dependent kinase are present in the particular phase in the cell cycle (Figure 2.1). The CDK activities are regulated by a small-polypeptide inhibitor protein cyclin dependent kinase inhibitor (CDK inhibitor) or CKI. The inhibitor directly binds to the CDK-cyclin complexes and inactive the functions of the complexes. The CKI can be classified into two major groups, they are the inhibitor of CDK4 (INK4) and Cip/Kip. The INK 4 family proteins, $p16^{Ink4a}$, $p15^{Ink4b}$, $p18^{Ink4c}$, and $p19^{Ink4d}$, bind exclusively to G_1 phase's CDKs, CDK4 and CDK6 (Malumbres & Barbacid, 2009). The INK4 inhibitors can directly bind to and inactive the functions of CDK4/6- cyclin complexes or bind to monomeric CDK4/6 and prevent the cyclins from associating with CDK4/6. The Cip/Kip family proteins that include p21, p27, and p57 can bind to a broad range of CDK-cyclin complexes except CDK2 complexes (Maddika et al., 2007).

2.3.2 Cell Cycle Analysis

Analysis of the DNA content in replicating cells can be achieved by fluorescence staining of the nuclei of the cell in suspension and analyzing the fluorescence properties of each cell by using flow cytometer. The fluorochromes will emit their fluorescence when they bind to DNA. There are several types of fluorescence staining available for analysing DNA in a population of cells, such as propidium iodide (PI), bromodeoxyuridine (BrdU) or Hoechst 33342 staining. However, the

plasma membrane of viable cells is able to eliminate most of the fluorochromes. Therefore, the plasma membrane is permeabilised with nonionic detergents, hypotonic solution or proteolytic enzymes in low pH. These techniques allow staining of DNA, for cell cycle analysis by flow cytometry. However, cell membrane component or cytoplasmic constituents may be lost. The most common solvent used for cell fixation is ethanol. 70 % ethanol is able to perforate cell membranes and not degrade the DNA, RNA and proteins in the cell (Gray & Darzynkiewicz, 1987).

Propidium iodide (PI) is a red fluorescent dye that binds double stranded DNA. The PI solution cannot differentiate between double stranded DNA and RNA. Since the PI solution will bind with double stranded RNA and emit the fluorescence, the double stranded RNA must be degraded using RNase. PI has an maximum of absorption at 536 nm and maximum of emission at 623 nm (Gray & Darzynkiewicz, 1987).

Hoechst dyes are benzimidazole derivatives that emit blue fluorescence light when excited by 350 nm UV light. The Hoechst dyes specifically bind to DNA, in particular A-T rich regions, but do not intercalate. Hoechst 33342 is the most widely used for staining viable cells by direct addition of (2.0-5.0 μg/ml) into culture medium (Gray & Darzynkiewicz, 1987).

Bromodeoxyuridine (BrdU) is a thymidine analog that will bind to DNA in place of thymidine when introduced into a cell. Fluorescein-conjugated monoclonal antibodies with specificity for BrdU are available. Once the cells have been pulsed with BrdU for a short period of time, they can then be treated to partially denature their DNA, exposing the BrdU within the double helix DNA so that is can be stained with anti-BrdU antibody. Any cells that have uptake the BrdU during the pulse will then stain fluorescein positive (Kessler, 2000).

Cells stained with a DNA fluorescent dye and analysed with flow cytometer are usually displayed as a histogram with DNA content on the x-axis. Normal eukaryotic cells in G_0 or G_1 will have one copy of DNA and will give 1X of fluorescence intensity. For replicating cells in G_2 or M phase before cytokinesis, the DNA content will have doubled and the fluorescence intensity will increase to 2X. During S phase when the cell is actively synthesizing DNA, the DNA content will vary between 1X to 2X and the resulting fluorescence intensity will also be between 1X and 2X (Givan, 2001). Thus, in a normal population of cells, the distribution of DNA content will resemble the general pattern shown in Figure 2.2.
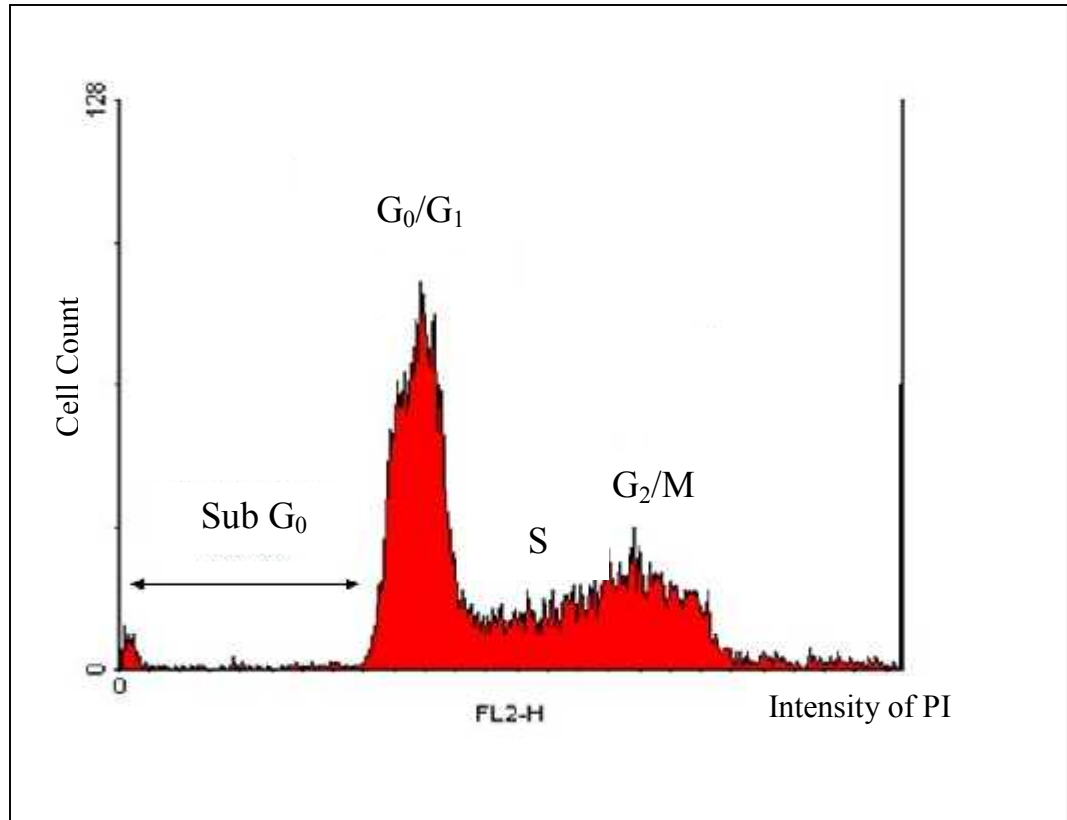
Figure 2.2: The common histogram to represent DNA content of untreated cell which stained with propidium iodide and analysis by flow cytometer. The DNA content of the untreated cell was distributed in Sub G_0, G_0/G_1, S and G_2/M phase (Medical Univercity of Vienna, 2005).

2.4 Apoptosis

Apoptosis, also known as programmed cell death, can be characterised as energy dependent biochemical mechanism. Apoptosis is a fundamental requirement for embryogenesis, organ metamorphosis, deletion of damaged cells and tissue homestasis. Cells defective in apoptosis are often the root cause of complex

diseases, such as cancer, neurodegenerative disease and autoimmune disorder (Fadeel et al., 1999). Generally apoptosis can characterised by morphological and biochemical changes. The morphological changes include cell shrinkage, chromatin condensation, nuclear fragmentation, membrane blebbing and formation of apoptotic bodies (Reed & Tomaselli, 2000) which the biochemical changes include discrete DNA fragmentation, caspases activation and the presentation of phosphotidyserine on the outer surface of the cell membrane (Tan, Ooi, Nawfal, Ahmed & Tengku, 2009).

The mechanism of apoptosis can be divided into two major pathways which are the intrinsic pathway (mitochondria pathway) and extrinsic pathway (death receptor pathway). However, there is increasing evidence for an additional pathway called the perforin/granzyme pathway which can induce apoptosis (Elmore, 2007). However, these 3 pathways are caspases dependent pathway. The activation of caspase enzymes play a central role in the apoptotic signaling network in cell death.

The term caspases is derived from cysteine-dependent aspartate-specific proteases; their catalytical activity depends on a critical cysteine-residue within a highly conserved active-site pentapeptide QACRG. The caspases specifically cleave their substrates after Asp residues (Denault & Salvesen, 2002; Richardson

& Kumar, 2002). There are 14 different caspases discovered in mammals. Normally, caspases are synthesis as inactive zymogens, called procaspases. At the N-terminal side of procaspases carries a pro domain followed by a large and small subunits which sometimes are separated by a linker peptide. Once capases are activated, the procaspases linkers are proteolytically cleaved, resulting in a small and a large subunit. In the activation of procaspases, two small and two large subunits will form a heterotetramer, resulting in an active caspase.

The caspases can be categorized into initiator (caspase-2, 8, 9, 10), effector (caspase-3, 6, 7) and inflammator (caspase-1, 4, 5). Caspases 11, 12, 13 and 14 are participants in cytokine activations (Elmore, 2007). Effector caspases only possess a short prodomain while initiator capases possess a long prodomain. Long prodomains in initiator caspases contain the death effector domain (DED) for caspases-8 and 10 or caspase recruitment domains (CARD) for caspases-9 and 2 (Gewies, 2003).

Analysis of the peptide recognition elements reveals a specific requirement for a tetrapeptide sequence N-terminus to the point of the cleavage. Because the caspases specifically cleave their substrates after Asp residues, the substrates must have the Asp at P_1 position. While liberal substitution is allowed at P_2 position and to some extent P_3, the P_4 residue varies between the caspases and this specificity

allows us to distinguish different types of caspases (Thornberry et al., 1997). The

optimal sequences for caspase enzyme specificities are shown in Table 2.2.

Table 2.2: Optimal sequences were determined for nine known human caspases (Thornberry et al., 1997).

Group	Caspase	Optimal Sequence
I	Caspase - 1	WEHD
	Caspase - 4	(W/L)EHD
	Caspase - 5	(W/L)EHD
II	Caspase - 2	DEHD
	Caspase - 3	DEVD
	Caspase - 7	DEVD
III	Caspase - 6	VEHD
	Caspase - 8	LETD
	Caspase - 9	LEHD

2.4.1 Extrinsic Pathway

The extrinsic pathway is initiated by ligand binding to transmembrane receptors. These 'death receptors' belong to the tumour necrosis factor (TNF) gene superfamily which consists 80 amino acid cytoplasmic domain. The death receptor will transmit the death signal from the cell surface to intracellular signaling pathways. Examples of ligand/receptor pairing, include FasL/FasR, TNF-α/ TNFR1, Apo3L/DR3, TRAIL R1/DR4 and TRAIL R1/DR5. Upon ligand binding, cytoplasmic adapter proteins which exhibit corresponding death domains (DD) are recruited to bind with the receptor complex (Fulda & Debatin, 2006).

The Fas ligand binding to Fas receptor results in the binding of the adapter protein FADD. FADD will have an interaction with procaspase-8 via dimerization of the death effector domain. A death-inducing signaling complex (DISC) is generated and causes the auto catalytic activation of procaspase-8 to caspase-8 which triggers the execution phase of apoptosis (Elmore, 2007; Gewirtz, Holt & Grant, 2007).

TRAIL is an unique ligand among the TNF superfamily because this ligand can bind with five different receptors. Two of the receptors, type-1 transmembrane receptor DR4 (death receptor 4/TRAIL R1) and DR5 (death receptor 5/KILLER/TRICK2) contain DD's and are pro-apoptotic. The other three

receptors lack DDs, including one that binds TRAIL very weakly at physiologic temperatures. The remaining two receptors are DcR1/TRID/TRAIL-R3 and DcR2/TRUNDD/TRAIL R4 are also called decoys receptor because these receptors are unable to transduce the death signal. Binding of TRAIL to DR4 or DR5 leads to DISC formation which then triggers activation of caspase-8/10 (Gewirtz, Holt & Grant, 2007). Once the activation of caspase-8/10, they trigger activation caspase-3/7 to induce apoptosis process.

2.4.2 Intrinsic Pathway

The intrinsic pathway involves a diverse array of non-receptor mediated stimuli that produce intracellular signals that directly targets within the cell or mitochondria. Examples of intracellular signals include DNA damage, oxidative stress, starvation (lack of glucose or L-glutamine), as well as those signals induced by chemotherapeutic drugs. All these stimuli will induce the opening of mitochondrial permeability transition (MPT) pore which allows the release of two groups of pro-apoptotic proteins from intermembrane space to cytosol. The first group of proteins are cytochrome c, Smac/DIABLO and the serine protease HtrA2/Omi. The Smac/DIABLO promotes apoptosis by antagonizing the Inhibitor of Apoptosis Protein (IAP). The cytochrome c will bind with Apaf-1 as well as procaspase-9 to form the apoptosome which is a cytosolic death signaling

protein complex (Bunz, 2001). The apoptosomes bind to procaspase-9, leading to activation of procaspase-9 and the effectors procaspases-3, 6, and 7 are proteolytically activated as a result of the activation of procaspase-9. The second group of protein includes Apoptotic Inducing Factor (AIF), endonuclease G and caspase activated DNase (CAD). The AIF is translocated into nucleus and binds to DNA. This results in chromatin condensation and DNA fragmentation into ~ 50-300 kb pieces. The endonuclease G cleaves nuclear chromatin to produce oligonucleosomal DNA fragments. Once CAD requires cleavage by caspase-3, CAD translocates to the nucleus and generates oligonucleosomal DNA fragmentation and more advanced chromatin condensation (Elmore, 2007).

The mitochondrial pathway is highly regulated by the pro-apoptotic proteins and anti-apoptotic proteins. The pro-apoptotic proteins include Bcl-10, Bax, Bid, Bad, Bim, Bik and Blk while the anti-apoptotic proteins consist of Bcl-2, Bcl-X, Bcl-XL, Bcl-XS, Bcl-w and BAG (Hector & Prehn, 2009). The balance between the level of pro- and anti-apoptotic proteins in a cell is believed to control the permeability of the mitochondrial membrane and release of mitochondrial intermembrane space protein to the cytosol. The anti-apoptotic proteins sequester pro-apoptotic proteins by binding to their BH3 domain and thereby ultimately prevent activation of Bak and Bax and consequently inhibits the mitochondrial pathway to trigger apoptosis process.

There is considerable cross-talk between the extrinsic and intrinsic pathways. For instance, caspase-8 can proteolytically activate Bid, which can then facilitate cytochrome c release (Green, 2000; Esposti, 2002). This apparently amplifies the apoptotic signal following death receptor activation and different cell types may be more reliant on this amplification pathway than others (Fulda et al., 2001). The mechanism of apoptosis induced by intrinsic pathway extrinsic pathway is shown in Figure 2.3.
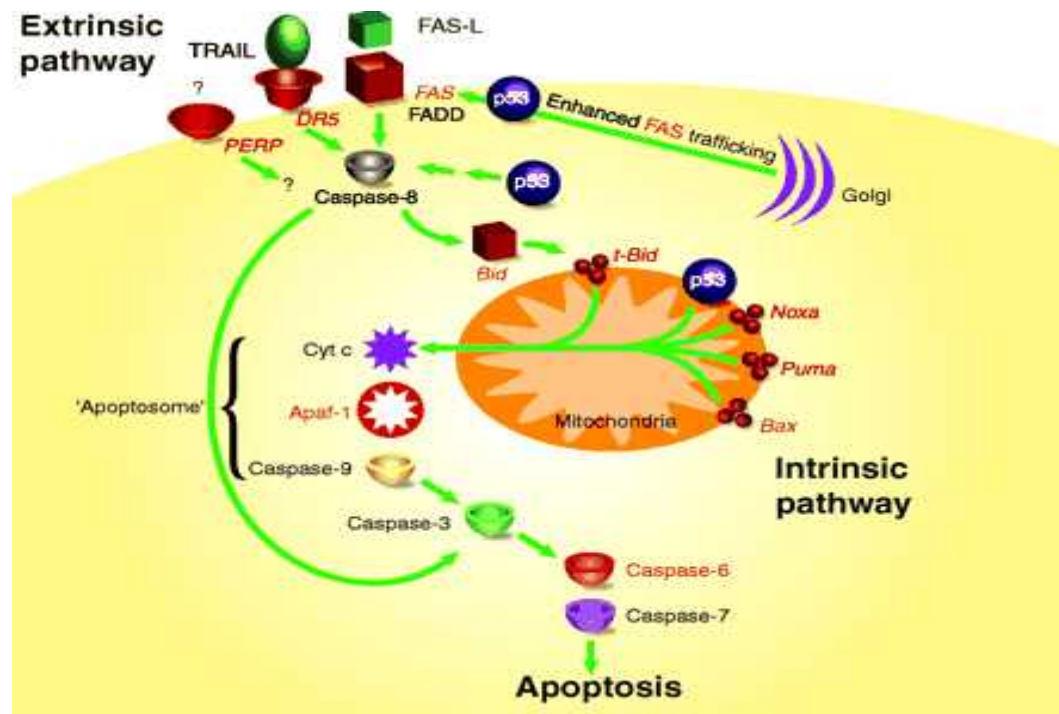
Figure 2.3: A model depicts extrinsic and intrinsic apoptotic pathways. The convergence of the two pathways through Bid is shown (Haupt, Berger, Goldberg & Haupy, 2003).

2.4.3 Detection and Quantification of Apoptosis

2.4.3.1 Annexin V-FITC/Propidium Iodide (PI) Staining

One of the early stage biochemical alternations is the loss of plasma membrane polarity and translocation of phosphatidyserine (PS) from the inner membrane to the outer membrane. Annexin V is a 35-36 kDa Ca^{2+} dependent phospholipid-binding protein that has a high affinity for PS and bind to cells with exposed PS. Annexin-V can be conjugated with a flourochrome such as FITC and when analysed microscopically or using flow cytometry, the intensity of the fluorescence signal from FITC allows to distinguish cells in early stage of apoptosis. Double staining with a DNA specific dye like propidium iodide will allow discrimination between early apoptosis cells with viable membranes and late stage apoptotic cells with leaky membranes that are also known as secondary necrotic cells (BD Bioscience, 2006).

Briefly, unstained or viable cells will not accumulate PI or show FITC fluorescence. This is because non-apoptotic cells do not expose the PS on outer layer of membrane and PI cannot penetrate membrane of the cell. Cell only stained with FITC dye are in early apoptosis. The cells at early apoptosis stage, start to translocate the PS from the inner surface of membrane to outer surface of the membrane but the membrane is still intact can still exclude PI (Prasad, 2003).

During late stage of apoptosis, cell membrane starts to breakdown and the Annexin-V-FITC will bind to PS at outer layer of membrane and also passes through the pores at the membrane and binds with the PS at the inner layer of membrane. The compromised membrane also no longer excludes PI and DNA will stain with PI. Thus, it is difficult to differential between late apoptosis and necrosis cells (Elmore, 2007). The dot pots use to quantitate early apoptotic cells, late apoptotic cell, necrotic cells and viable cells show in Figure 2.4.
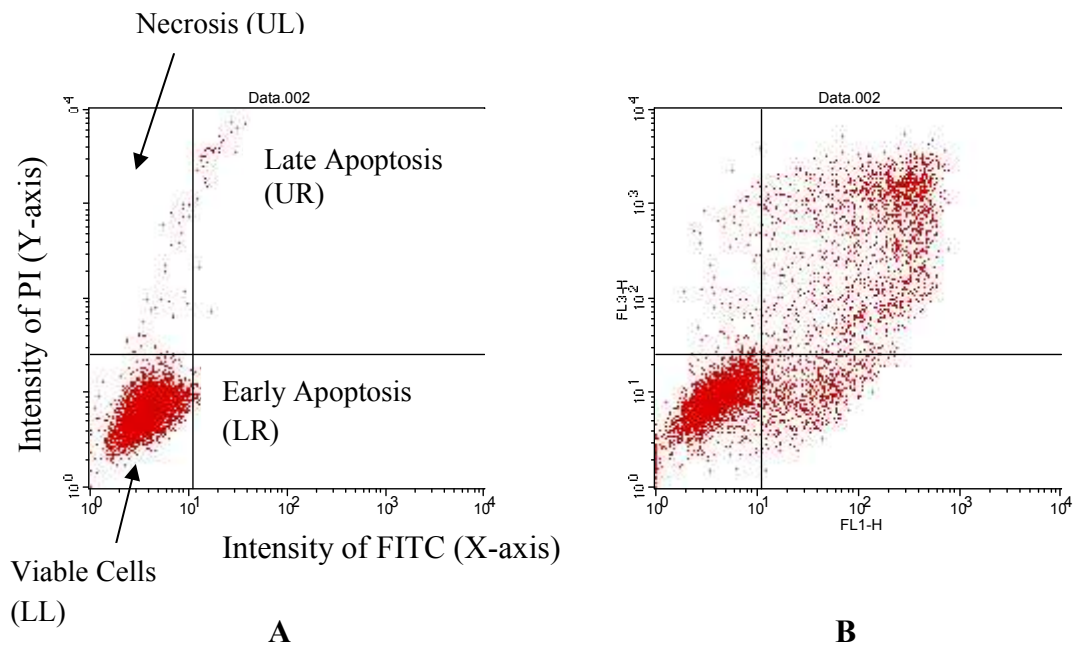
Figure 2.4: Dot plot of flow cytometry analysis of apoptosis. The FL-1 represented the PI on the Y-axis while FL-3 represented the FITC on X-axis. A: Untreated cell, B: Treated cell (Cell treatred with chemotherapy drug). Viable cell are defined by lower left quadrant (LL), necrotic cell-upper left (UL) quadrant, early apoptotic cell-lower right (LR) and late apoptotic cells- upper right (UR).

2.4.4 The Principles of Bioluminescent Caspases Assay

It is known that different caspases play important roles in the caspases dependent pathway to induce apoptosis. Quantification of specific caspases enzyme activities induced by drugs over time can provide information regarding the mechanisms employed in the activation of apoptosis in a cell.

The measurement of caspases activities using a bioluminescent marker is a more sensitive method compared with using fluorescence or colorimetric methods. The low background inherent in bioluminescence allows for a better signal-to-noise ratio and the overlapping of the excitation and emission wavelengths does not occur with bioluminescence methods (Fan & Wood, 2007). In a typical bioluminescent caspase assay, the substrate is pro-luciferin which is luciferin conjugated to the optimal sequence recognized by a specific caspase enzyme. The pro-luciferin is converted into amino-luciferin through catalytic processing by specific caspases and this compound produces a luminescent signal when combined with luciferase and ATP. The luminescent signals of the assay are dependent on the amount of caspase enzyme activity present in the cell (Cali, Niles, Valley, O'Brien, Riss & Shultz, 2008). For example, the pro-luciferin containing the DEVD sequence (DEVD-6'-aminoluciferin) is recognized and cleaved by caspase-3 or caspase-7, the amino-luciferin is released and the amino-luciferin is luminogenic substrate of luciferase. The concentration of amino-luciferin rises until the rate of the cleavage reaction matches the rate of the

luciferase reaction. The luminescent signals are proportional to the amount of caspase-3 and caspase-7 (Cali, Niles, Valley, O'Brien, Riss & Shultz, 2008). A schematic showing the cleavage of pro-luciferin by caspase-3/7 to produces a bioluminescent signal is shown in Figure 2.5.
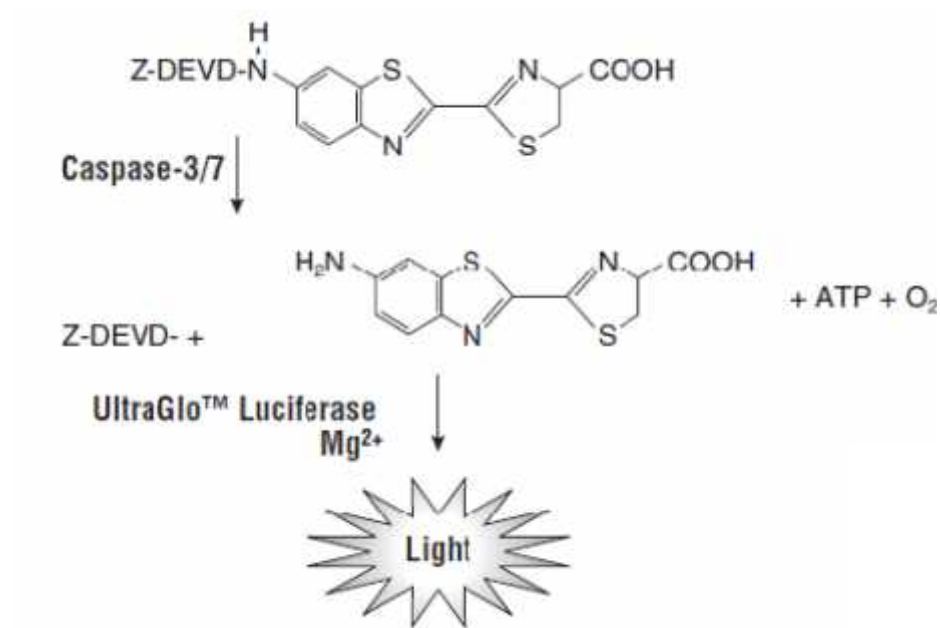
Figure 2.5: The cleavage of pro-luciferin by caspase-3/7. Caspase-3/7 cleavage of the luminogenic substrate containing the DEVD sequence. Following caspase cleavage, a substrate for luciferase (aminoluciferin) is released and results in the luciferase reaction and the production of light (Promega, 2009).

2.5 Necrosis

Necrosis is defined as uncontrolled, chaotic and disordered process of cell destruction. Necrosis is also classified as accidental or passive response to physiologic extremes, such as hyperthermia, mechanical shear force or exposure to certain toxins (Mendelsohn, Howley, Israel, Gray & Thompson, 2008). Necrosis is also a common endpoint in pathological conditions, like Human immunodeficiency virus (HIV) related infections, Alzheimers disease, ischemia or Creutzfeldt-Jakob disease (Proskuryakov, Konoplyannikov & Gabai, 2003). Morphological features of cellular necrosis include cytoplasmic swelling, plasma membrane rupture and rapid cell lysis (Figure 2.6) (Gewirtz, Holt & Grant, 2007). Permeabilisation of cells plasma membrane occurs at the early stage of necrosis and is then accompanied by cytoplasmic swelling. This action creates larger pores in the plasma membrane and allows cytosolic constituents to spill into extracellular space (Proskuryakov, Konoplyannikov & Gabai, 2003). The ruptured lysosomes release acid hydrolases, nucleases, peptidases, proteases, phosphateses, sulfatases, glycosidases and lipases. These enzymes will degrade most macromolecules, including, RNA, DNA and proteins (Mendelsohn, Howley, Israel, Gray & Thompson, 2008). During lysis various breakdown products are released into the extracellular environment which damages neighboring cells by causing inflammation.
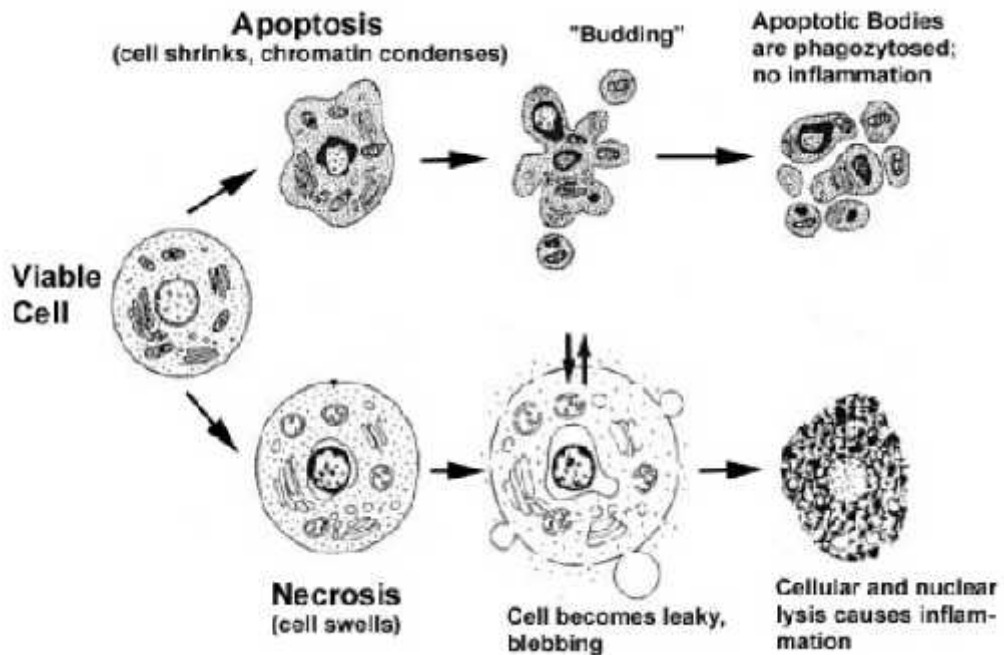
Figure 2.6: The morphology change of cell went through the apoptosis or necrosis process (Van Cruchten & Van Den Broeck, 2002).

2.6 Plant Natural Products as Source of Anticancer Agent

Plant natural products or secondary metabolites are the organic compounds synthesized by plants. Plant secondary metabolites are usually classified according to their biosynthesis pathways (Harborne, 1999). The three large families include phenolics, terpenes and alkaloid. Plant secondary metabolites contribute to plant fitness by interacting with the ecosystem. They deter predators, destroy other plants that compete for the same space and attract pollinators (Yuan & Lin, 2000). Some of these metabolites have anticancer, antibiotic, antifungal and antiviral properties (Bourgaud, Gravot, Milesi & Gontier, 2001). Due to their

31

inherent biological activities, plants that contain such secondary metabolites have been used as medicines in several countries many thousands of years ago. For examples, the first written record for the medicinal uses of plants appeared at about 2600 BC from Egyptian and Akkaidians writing, while the Chinese Materia Medica recorded more than 600 medicinal plants from 1100 BC (Mohammad, 2006). Therefore, plants potentially provide a valuable source of drug for the pharmaceutical, cosmetics, fine chemicals and nutraceutical industry (Bourgaud, Gravot, Milesi & Gontier, 2001).

The search for anticancer agents from plant natural products started in earnest in 1958 following the discovery of the vinca alkaloids (vinblastine and vincristine) (Mishra, 2011). Therefore, the United State National Cancer Institute (NCI) collected over 35,000 plant samples in temperate regions form 1960 to 1982. Under this programe, NCI yielded 114,000 extracts and discovered the anticancer agents taxol and camptothecin. More recently, the Council for Scientific and Industrial Research (CSIR) in South Africa also implemented a screening program to searching for anticancer agents from plant natural products from 1998 – 2006. This programe collected approximately 700 species of plants and yielded 7500 plant extracts. A total of 950 extracts exhibited a growth inhibition of above 75 % toward MCF7 (Human, breast adenocarcinoma), TK10 (Human renal adenocarcinoma) and UACC62 (Human, melanoma) cell lines. From this programe, five pure cytotoxic compounds are successfully isolated using the

bioassay guided isolation were solasonine, tatridin A, eucannabinolide, deacetyl-β-cyclopyrethrosin and 13-methoxy-15-oxozoapatlin (Fouche, Cragg, Pillay, Kolesnikova, Maharaj & Senabe, 2008). Researchers from the International Medical University in Malaysia isolated the bioactive compound astaxanthin, zingerone [6]-gingerol and phycocyanin from local plants such as *Elephantopus mollis, Morinda citrifolia, Pereskia bleo, Euphorbia hirta, Zinger officinale, Mangifera indica and Nephelium lappaceum* and algae (Chu & Radhakrishnan, 2008).

The new development of isolation and screening technologies has shortened the time required to isolate anticancer agents from natural sources. These include the combination of separation technologies such as high performance liquid chromatography (HPLC), solid phase extraction (SPE) with spectroscopic analysis like nuclear magnetic resonance (NMR) and mass spectrometry (MS) to isolate and elucidate pure compound from plant natural product. Based on these advance techniques, it is possible to isolate and elucidate the structure of natural product present in the crude extract in a shorter time (Lam, 2007). For screening technology, high through-put assays run in 96, 384 or 1536 well plate and equipped with automatic robotic processes allow scientists to screen biological or biochemical properties of thousands of compounds in a week. Examples of bio-assays used for high through put screening are ELISA, proliferation/cytotoxic assay, reporter assay and macromolecular binding assay (Mishra, Ganju, Sairam,

Banerjee & Sawhney, 2008). Combination of these two advance technologies allows scientists to discover more anticancer agents from plant natural products.

From 1981-2002, around 60 % anticancer agents were derived from plant natural products (Lam, 2007), for examples, cucurbitacins derived from *Helicteres angustifolia* which exhibited significant inhibitory activities against the growth of both hepatocellular carcinoma BEL-7402 cells and malignant melanoma SK-MEL-28 cell *in vitro* (Chen, Tang, Lou & Zhao, 2006). Silvestrol which is isolated from the bark of Malaysia plant, *Aglaia leptantha* Miq. induces apoptosis and cell cycle arrest in human prostatic adenocarcinoma LNCaP cell line (Kinghorn et al., 2009).

Following the identification of bioactive secondary metabolites from plants, the total synthesis, combinatorial biosynthesis and chemoenzymatic approach also be used to produce natural product mimics or synthetic compounds derived from the study of natural product for drug discovery. These advance methods can enhance the bio-active effect or reduce the toxicity against normal human cells by modifications such as removal or addition of functional groups. An example is the modification of camptothecin into 7-(acylhydrazone)-formylcamptothecin. The 7-(acylhydrazone)-formyl camptothecin was more active against topoisomerase II compared with camptothecin. The modification of podophyllotoxin to etoposide

by acetalization of the 4- and 6-hydroxy groups of the glucopyranose moiety at C-4 of C-ring at podophyllotoxin, reduced the toxicity against human body (Itokawa, Morris-Natschke, Akiyama & Lee, 2008). The chemical structure of camptothecin and podophyllotoxin and their modified derivatives are shown in Figure 2.7.

In the period of 1981-2002, approximately 20% of new chemical entities were natural product mimics or synthetic compound derived from the natural products (Newman, Cragg & Snader, 2003). Compounds isolated from plants not only serve as new drugs but also serve as a template for the synthetic chemist to create a more effective drugs against diseases like cancer (Lam, 2007). For example, nitisinone which is a modification of mesotrion isolated from the *Callistemon citrinus* Stapf (Myrtaceace) was found to be effective against a rare inherited disease, tyrosineaemia (Balunas & Kinghorn, 2005).

$R_1 = H$

$R_2 =$ ...

Camptothecin   7-(Acylhydrozono)-formylcamptothecin

$R_1 = Me, R_2 = H$

Podophyllotoxin   Etoposide
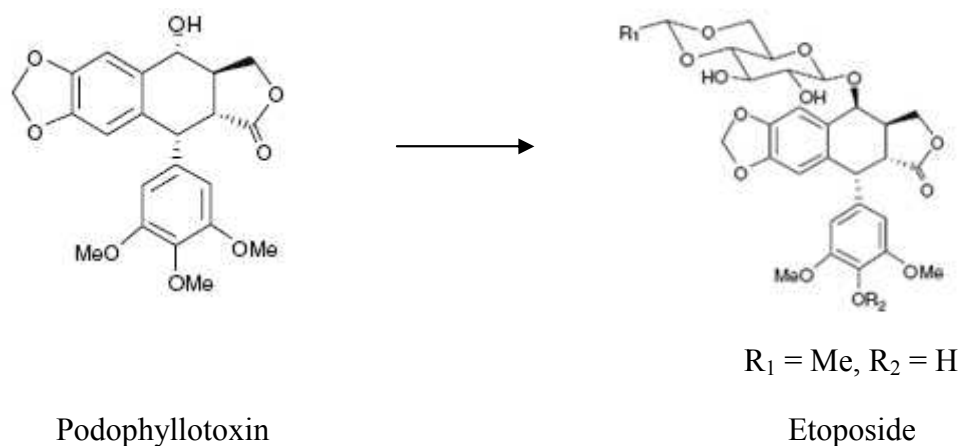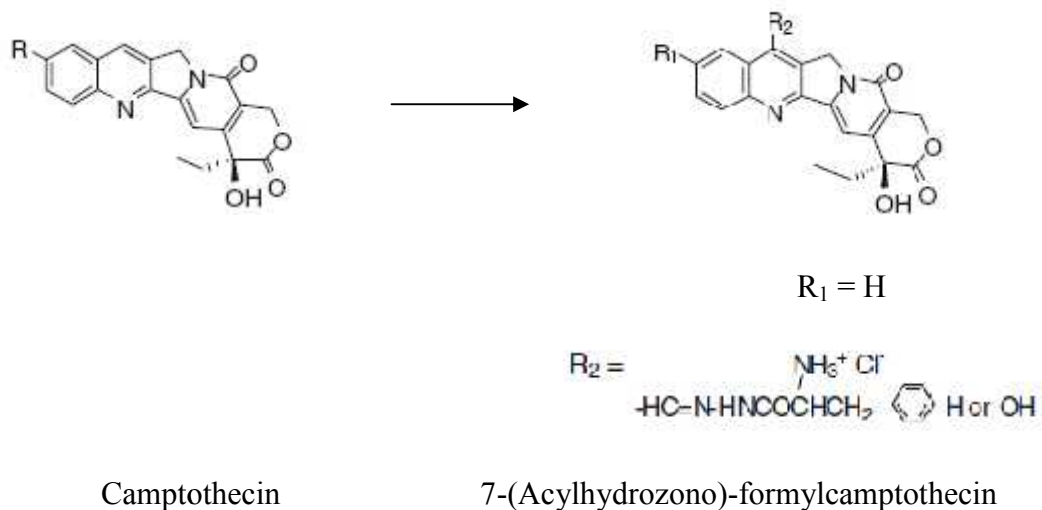
Figure 2.7: The chemical structures of the camptothecin, podophyllotoxin, 7-(Acylhydrozono)-formylcamptothecin and etoposide. 7-(Acylhydrozono)-formylcamptothecin and etoposide are the compounds which modificated from camptothecin and podophyllotoxin, respectively. Both modified compounds enhance bio-active effect and reduce the toxicity against human body (Itokawa, Morris-Natschke, Akiyama & Lee, 2008).

2.7 Bioassay-Guided-Isolation

In the process of bioassay-guided-isolation, the crude extracts of natural products are separated into many fractions. Then, bioassay of each fraction is performed to determine which of them should be subjected to further separation. Through the circle of separation and bioassay, a pure active compound may be isolated (Cheng, Wang & Wang, 2006). In the process of drug discovery, bioassay-guided-isolation has been used as a rapid and successful method to isolate pure bioactive compounds from natural products, either from plants, microorganisms or fungi. This method uses bioassay to monitor the activity of fractions generated from chromatography separation steps deployed in the isolation of bioactive compounds (Vlietinck, Pieters & Vander Berghe, 1995; Rimando, Olofsdotter, Dayan & Duke,2001).

The bioassay can be defined as the biological system to detect properties of the crude extract, chromatographic fraction, mixture or pure compounds. Bioassays include antibacterial, anti-HIV, antifungal and anticancer assays (Sarker, Latif & Gary, 2006a). The anticancer properties of the extracts can be detected using cytotoxic assays which measure the ability of drugs to kill cells. These assays are based on parameters, such as metabolic activity and cell morphology. For example, MTT (3-(4, 5-dimethylthiazol-2-yl)-2, 5-diphenyltetrazolium bromide) assay to measure mitochondrial activity, lactate dehydrogenase leakage assay to investigate membrane integrity, neutral (3-amino-m-dimethylamino-2-

methylphenazine hydrochloride) red assay to measure the viable cell after exposure to toxicant, ATP measurement and macromolecular synthesis and glutathione depletion (Weyermann, Lochmann & Zimmer, 2005). Bioassay can be done by using either *in vivo* (clinical trial, whole animal experiment), *ex in vivo* (isolated organ or tissue), or *in vitro* (cell culture) systems. *In vivo* studies are more related to clinical applicability and also provide the toxicity data of the compound against humans or animals. However *in vitro* bioassays can quickly identify the bioactivities of the extract or compounds in a short term (Sarker, Latif & Gary, 2006b).

The purification or separation of compounds in this process is done by using chromatography techniques, such as gravity column chromatography, thin layer chromatography, and high performance liquid chromatography (HPLC). The purified compound can be characterized by spectroscopic methods like fourier transform infrared spectroscopy, mass spectrometry and nuclear magnetic resonance spectrometry (Pieters & Vlietinck, 2005).

2.8 Chromatography Technique

Chromatography is the most widely used separation technique in chemical laboratories, where it is used for isolation, analysis and purification. This technique was developed by a Russian botanist, Mikhail Tswett in 1906. He separated different colour constituents of crushed leaf extract by passing it through a column containing calcium carbonate, alumina and sucrose. Therefore he named the method from the Greek words *chroma* meaning "colour" and *graphein* meaning "to write" (Skoog, Holler & Nieman, 2004). Chromatography is a physical method of separation in which the components to be separated are distributed between 2 phases, is stationary phase and mobile phase (Ahuja, 2003). Common stationary phases are silica, alumina or C-18 powder, while the mobile phase can be liquid or gas. The mobile phase will carry the analyte across the stationary phase. The analytes ideally equilibrate or differentially partition between the 2 phases, resulting in different migration rate through the system. Two major implementations of chromatography are gas chromatography and liquid chromatography (Villas-BOAS, Roessner, Hansen, Smedsgaard & Nielsen, 2007).

2.8.1 Gas Chromatography

Gas chromatography is a technique to separate volatile compounds by converting the compounds into the gas form based on their boiling points or polarity difference. The mixture of compounds can then be separated by the affinity of interaction with the stationary phase in the capillary column of gas chromatography. Gas chromatography is very sensitive and provides qualitative and quantitative data in a single operation (Harborne, 1998).

2.8.2 Liquid Chromatography

Liquid chromatography uses liquid as a mobile phase, commonly an organic solvent. The stationary phase can consist of liquid absorbed onto a solid support, an organic species spreads over a solid support, a solid or a resin. The examples of liquid chromatography are thin layer chromatography (TLC), gravity column chromatography and high performance chromatography (HPLC).

2.8.2.1 Priciples of Thin Layer Chromatography

Thin layer chromatography (TLC) is a rapid, sensitive and easy technique to analyse the contents of a mixture and purify small quantities of organic compounds. The migrations of compounds on TLC are governed by competitive interaction affinity between the compounds to the stationary phase and the mobile phase to stationary phase. The TLC plate consists of a thin layer of sorbents (stationary phase) coated on a support material, like plastic, glass or aluminum. Common stationary phase sorbents are silica gel and alumina (Cannell, 1998).

Less common type of sorbents include celite, calcium hydroxide, ion exchange resin, magnesium phosphate, polyamide, and sephadex. The mobile phase are composed a mixture of solvents. Mixture of solvents provide solvent straight to separate individual compound from the extract, when the compounds migrate at the TLC plate. The separation process of TLC can be done in the chamber with a suitable solvent system (Harborne, 1998).

2.8.2.2 Principle of Gravity Column Chromatography

Gravity column chromatography is commonly used for large scale separation and purification. The column dimension and also stationary phase can be selected to fit the sample to fractioned. The most common stationary phase for gravity column chromatography is silica gel. Silica gel is a typical polar sorbent, chemically represented by $SiO_2 \cdot H_2O$ and weakly acidic on their surface. Silica gels preferentially adsorb strongly basic substances. Silica gel can also be manufactured to be very small which gives very small pore sizes and this offers a large surface area in range of 5-800m^2/g. Based on these physical properties of silica gel, a wide range of chemical compounds can be separated (Sarker, Latif & Gary, 2006b). Other than that, alumina polystyrene, sephadex and polyacrylamide can also be used as stationary phases.

The stationary phase can be introduced into the column in slurry form (in solvent) or dry form. The sample is applied on the top of the stationary phase. Fractions eluted from the column are collected based on the volume or visible bands separated on the column. The purity of the fractions can be determined by using TLC and HPLC (Cannell, 1998).

2.8.2.3 Principle of High Performance Liquid Chromatography

High performance liquid chromatography (HPLC) is a technique to separate components of a mixture by using a variety of chemical interaction between the substance being analyzed and the stationary phase. HPLC is very sensitive and is able to provide qualitative and quantitative data in a single run. HPLC is also suitable to analyse nonvolatile compounds and thermally fragile ones (Skoog, Holler and Nieman, 2004b). Normally, the mobile phase is loaded into the column by using high pressure pump to obtain a satisfactory flow rate. The selectivity of HPLC depends on different types of stationary phase and mobile phase used (Rouessac & Rouessac, 2000).

2.9 Structure Elucidation

Structure elucidation of unknown compounds can be achieved by spectroscopic methods. These spectroscopic methods include Fourier transform infrared spectroscopy, mass spectrometry and nuclear magnetic resonance spectrometry (Sarker, Latif & Gary, 2006a).

2.9.1 Nuclear Magnetic Resonance Spectrometry

In the last four decades, the development of nuclear magnetic resonance (NMR) spectrometry has had profound effects on the development of organic, inorganic and biochemical analyse, especially in structure elucidation. NMR spectrometry is a technique to determine the structure of organic compounds by measuring the number of different types of proton and carbons present in the molecules and relationship among each other. NMR is very sensitive and requires only up to 5 milligram of material for analysing. Now, NMR can be categorized into 2 major group: one dimension NMR (example: ^{1}H and ^{13}C NMR) and two dimensional NMR (example: heteronuclear correlation spectroscopy (HETCOR), homonuclear shift correlation spectroscopy (COSY), heteronuclear multiple quantum coherence (HMQC) and heteronuclear multiple bond coherence (HMBC) (Sarker, Latif & Gary, 2006a).

According to the spectrum from proton ^{1}H NMR spectrum, four important types of information can be interpreted. These include the number of different signals that indicate different types of protons are present in the pure compound, the chemical shift of each signal indicates the electronic environment, the intensity or integration of each signal indicates the number of protons for each signal and the splitting of each signal indicates the number of adjacent protons. While there are three important types of information obtained from ^{13}C NMR spectrum, like the number of different signals indicates different types of carbons are present in the

compound, the chemical shift of each signal indicates the electronic environment and using DEPT, each signal is identified as CH_3, CH_2, CH, or C. Typical chemical shift of protons and carbons are listed in Appendix A and Appendix B.

Information obtained from an NMR spectrum may not be able to unambiguously confirm the structure of a compound because some of the functional groups cannot be differentiated in the spectrum. Fourier transform infrared spectroscopy (FTIR) can be used to identify the functional groups present in the compound. Fourier Transform Infrared Spectroscopy is one kind of infrared spectroscopy to detect the functional group and create the finger printing of the compounds (Shriner, Hermann, Morrill, Curtin & Fuson, 2004).

2.9.2 Mass Spectroscopy

The molecular weight and the mass fragmentation pattern obtained from mass spectroscopy (MS) is also an important part for elucidating a structure of a compound. MS can analysis vary types of compounds and provides information about the elemental composition of sample or matter, the structure of inorganic, organic and biological molecules, the qualitative and quantitative composition of complex structure and composition of solid surface and isotopic ratio of atom in sample in homogeneities (Skoog, Holler & Nieman, 2004a).

2.10 *Hydrocotyle vulgaris*

Hydrocotyle vulgaris (Figure 2.8) classified as plantae kingdom and apiales order. *Hydrocotyle vulgaris* also belongs to the Araliaceae family (Umbelliferea) and is commonly referred as Mash Pennywort. *H. vulgaris* is a hardy variety from North Africa and Europe and can grow up to 0.1m-0.5m in height. It flowers from June and August and the seeds ripen from July to October. The flowers are hermaphrodite (have both male and female organs). *H. vulgaris* will grow in full shade in a moist to wet soil mix. *H. vulgaris* is propagated from division of the creeping stem and from seed (Plant for a Future, 2000).

Figure 2.8: *Hydrocotyle vulgaris*.

In Malaysia, the traditional usages of *H.vulgaris* are treating wounds caused by surgery and as a diuretic. While in India, *H.vulgaris* was used as a herb to treat leprosy since 1985 (Felter & Lloyd, 1898). In Denmark, the root of *H. vulgaris* is traditionally used to treat whooping cough (Burton, 2002). Besides that, this plant has been used as sunburn remedy and shown to have anti-exudative activity (Watts, 2007).

One novel triterpenoid glycoside, methyl oleanolate 3-O-(β-D-glucopyranoside)$_3$ was isolated from the chloroform from of *H. vulgaris*. This compound possessed the highest root inhibitory activity against seedling of *Mimosa pigra* Linn (Chavasiri, Prukchareon, Sawasdee, Zungsontiporn, 2005). Preliminary studies showed that the alcoholic extracts of *H. vulgaris* possessed cytotoxic activity against HL-60, Raji, K-562 and U2-OS cell line (Tee, 2008; Wong, 2006).

CHAPTER 3

MATERIALS AND METHODS

3.1 Indentification and Preparation of Dry Plant Materials

This plant (Figure 3.1) was identified as *Hydrocotyle vulgaris* by Prof. Dr. Ong Hean Chooi from the Institute of Bioscience, Universiti Malaya. Fresh *Hydrocotyle vulgaris* was collected from Johor Bahru, Malaysia. The plants were separated into leaf, stem and root and washed with tap water to remove the dust and dirt on the surface of the plants. The plants were dried at room temperature for 4-5 days. The total weight of dry *Hydrocotyle vulgaris* was 2518.6g. The weight of dry leaf, stem and root of *Hydrocotyle vulgaris* was measured and recorded as 1024.3g, 525.6g and 968.7g.

Figure 3.1: The plant of *Hydrocotyle vulgaris*.

3.2 Extraction of Crude Extract from dried leaves, stem and root of *Hydrocotyle vulgaris*

The dried leaves, stems and roots of *Hydrocotyle vulgaris* were ground into powder using a blender and the ground leaves were sequentially extracted by hexane, dichloromethane and methanol (Merck, Germany). For the leaves samples, the ground leaves were soaked in hexane with occasional shaking for 3 days. The hexane extract were filtered through a cotton plug and evaporate under vacuum at 35º C using a rotary evaporator (BUCHI, Rotavapor R2000) to obtain the hexane fraction. After soaking three times with hexane, the ground leaves were air dried to remove all the hexane residues and continued soaking in dichloromethane solvent. These processes again were repeated for dichloromethane and methanol. The whole processes were repeated for stem and root parts of *Hydrocotyle vulgaris*. The weight of each type of crude extract were measured and recorded. These fractions were used for cytotoxicity test at 50 μg/ml in the MTT assay.

3.3 Gravity Column Chromatography of Active Extracts from Leaves and Roots

The dichloromethane extract of leaves and hexane extract of roots were the most cytotoxic based on MTT assay and were selected for further isolation. These extracts were subjected to column chromatography (6 cm diameter X 100 cm height) using Silica gel 60 (Merck 230-400 MESH ASTM, Germany) which was packed in a glass column. First, the column was plugged at the bottom with a cotton plug to prevent the loss of absorbent material. Silica gel was made into slurry with hexane and poured into the column and allowed to settle (approximately 15 cm in height). Approximately 3 column volumes of hexane were eluted through the column to ensure proper packing. The column was left for overnight.

The ratio of extract to silica gel used was 1:15. The 4 g of dried extract was first dissolved in 100 ml chloroform (Merck, Germany) and adsorbed onto a 60 g of silica gel and dried to become powder in the fume hood. Then, 50 ml of hexane was added to this powder to make slurry which was layered onto the top of the column. After that, the first eluting solvent was slowly added to the top of the column. The column was eluted by a stepwise gradient solvent system where the polarity of the solvent system was increased by mixing a higher percentage of ethyl acetate (Merck, Germany), for each 300 ml of eluting solvent. Table 3.1 and Table 3.2 represented the solvent systems and the volumes used in the gravity

Table 3.1: Different compositions and volume of solvent systems were applied in the gravity column chromatography for separating the dichloromethane fraction of leaves.

Hexane (%) (v/v)	Ethyl Acetate (%) (v/v)	Total volume (ml)
100	0	300
98	2	300
96	4	300
94	6	300
92	8	300
90	10	300
85	15	300
80	20	300
75	25	300
70	30	300
65	35	300
60	40	300
55	45	300
50	50	300
45	55	300
40	60	300
35	65	300
30	70	300
25	75	300
20	80	300
15	85	300
10	90	300
5	95	300
0	100	300

Table 3.2: Different compositions and volume of solvent systems were applied in the first time gravity column chromatography for separating the hexane fraction of roots.

Hexane (%) (v/v)	Ethyl Acetate (%) (v/v)	Total volume (ml)
90	10	300
85	15	300
80	20	300
75	25	300
70	30	300
65	35	300
50	50	300
40	60	300
20	80	300
0	100	300

column chromatography for isolating bioactive compounds from dichloromethane extract of leaves and hexane extract of roots. Fractions were collected in 40 ml volumes and analysed on TLC. Fractions with similar TLC profile were pooled and the pooled fractions were then tested for cytotoxicity at 50 µg/ml.

The dichloromethane extract of leaves were chromatographed only once to obtain fractions for testing. The hexane extract of roots was subjected to gravity column chromatography and subsequent pooled fractions. Fraction RF2 and RF6 were subjected to a second gravity column chromatography by using hexane and acetone as a solvent system. Table 3.3 and Table 3.4 show the solvent system and volumes used in the gravity column chromatography for purifying the pooled fractions RF2 and RF6.

Table 3.3: Different compositions and volume of solvent systems were applied in the gravity column chromatography for separating active sub-fraction RF2 from hexane fraction of roots.

Hexane (%) (v/v)	Acetone (%) (v/v)	Total volume (ml)
95	5	200
93	7	200
90	10	200
85	15	200
80	20	200
75	25	200
70	30	200
65	35	200
60	40	200
55	45	200
50	50	200
40	60	200
30	70	200
20	80	200
10	90	200
0	100	200

Table 3.4: Different compositions and volume of solvent systems were applied in the gravity column chromatography for separating active sub-fraction RF6 from hexane fraction of roots.

Hexane (%) (v/v)	Acetone (%) (v/v)	Total volume (ml)
98	2	150
96	4	150
94	6	150
92	8	150
90	10	150
88	12	150
86	14	150
84	16	150
82	18	150
80	20	150
75	25	150
70	30	150
65	35	150
60	40	150
50	50	150
40	60	150
20	80	150
0	100	150

3.4 Purification of Cytotoxic Compounds

Active fractions of dichloromethane extract of leaves (LF3) and hexane extract of roots (RF2-3 and RF6-4) were analysed on HPLC to determine the purity of the fraction. Briefly, the fraction LF3 was dissolved with acetonitrile HPLC grade (Merck, Germany), filtered through a 0.2 μm PTFE membrane (Sartorius Stedium, Germany) and injected into HPLC (Shimadzu, Japan) equipped with an analytical column (100 mm X 4.6 mm RC18, Chromolith ® Performance, Merck, Germany). The polarity of the solvent system was decreased by mixing a progressively higher percentage of acetonitrile in water. The condition and solvent used for analysis the active fraction LF3, RF2-3 and RF6-4 are shown in Table 3.5.

For the active fraction LF3, RF2-3 and RF6-4 were further purified by semi-preparative HPLC. The active fractions LF3, RF2-3 and RF6-4 were further subjected to semi-preparative HPLC using a semi-prep column (100 mm X 10 mm RC18, monolithic, Phenomenex, USA) and sub fractions were collected based on the peaks eluting from the column. Fractions were dissolved in HPLC grade methanol and filtered through a 0.2 μm PTFE membrane and injected into HPLC. The polarity of the solvent system was decreased by mixing a progressively percentage of methanol in water. The sub-fractions collected from purification of active fraction LF3, RF2-3 and RF6-4 by semi-preparative HPLC were tested again MTT assay to determine its IC_{50} value. The conditions and

solvents used for separation of fractions are summarized in Table 3.5.   The

summary of purification for partial pure cytotoxic compound from hexane

fraction of root and pure cytotoxic compound from dichloromethane fraction of

leaves are shown at flow chart in Figure 3.2 and Figure 3.3, respectively.

Table 3.5: The condition to analyses the purity of fraction LF3, RF2-3 and RF6-4 by using analytical column and the condition for purifying fraction LF3, RF2-3 and RF6-4 by using semi-prep column.

Fraction for isolation	Column	Flow rate	Time (Min)	Water (%) (v/v)	Acetonitrile (%) (v/v)	Methanol (%) (v/v)
LF3	Analytical	1 ml/min	0.01	50	50	0
			5.00	25	75	0
			11.00	15	85	0
			15.00	5	95	0
			20.00	0	100	0
			25.00	0	100	0
	Semi-prep	4.75 ml /min	0.01	50	50	0
			5.00	25	75	0
			11.00	15	85	0
			15.00	5	95	0
			20.00	0	100	0
			25.00	0	100	0
RF2-3	Analytical	1 ml/min	0.01	50	0	50
			4.00	30	0	70
			15.00	0	0	100
			20.00	0	0	100
	Semi-prep	4.75 ml/min	0.01	50	0	50
			4.00	30	0	70
			15.00	0	0	100
			20.00	0	0	100
RF6-4	Analytical	1 ml/min	0.01	70	0	30
			5.00	50	0	50
			15.00	0	0	100
			20.00	0	0	100
	Semi-prep	4.75 ml /min	0.01	70	0	30
			5.00	50	0	50
			15.00	0	0	100
			20.00	0	0	100

Hexane Fraction
of roots

Column chromatography
Hexane: Ethyl acetate

| RF1 (No Bioactive) | RF3 (No Bioactive) | RF5 (No Bioactive) | RF7 (No Bioactive) | RF9 (No Bioactive) | RF11 (No Bioactive) |

| RF2 (Bioactive) | RF4 (No Bioactive) | RF6 (Bioactive) | RF8 (No Bioactive) | RF10 (No Bioactive) | RF12 (No Bioactive) |

**Column chromatography
Hexane: Acetone**

| RF6-1 (No Bioactive) | RF6-3 (No Bioactive) | RF6-5 (No Bioactive) | RF6-7 (No bioactive) | RF6-9 (No Bioactive) |

| RF6-2 (Bioactive) | RF6-4 (Bioactive) | RF6-6 (No Bioactive) | RF6-8 (No Bioactive) | RF6-10 (No Bioactive) |

**RF2 Fraction
Column chromatography
Hexane: Acetone**

**HPLC
Solvent system: Methanol + water**

| RF6-4-1 (No Bioative) | RF6-4-3 (No Bioactive) | RF6-4-5 (Bioactive) | RF6-4-7 (Bioactive) | RF6-4-9 (No Bioactive) |

RF6-4-8 (No Bioactive)

| RF6-4-2 (No Bioactive) | RF6-4-4 (No Bioactive) | RF6-4-6 (Partial pure bioactive) |

C1 compound

| RF2-1 (No Bioactive) | RF2-3 (Bioactive) | RF2-5 (No Bioactive) | RF2-7 (No Bioactive) | RF2-9 (No Bioactive) | RF2-11 (No Bioactive) |

| RF2-2 (No Bioactive) | RF2-4 (No Bioactive) | RF2-6 (Bioactive) | RF2-8 (Bioactive) | RF2-10 (No Bioactive) | RF2-12 (No Bioactive) |

**HPLC
Solvent system: Methanol + water**

| RF2-3-1 (No Bioactive) | RF2-3-2 (No Bioactive) | RF2-3-3 (Bioactive) | RF2-3-4 (No Bioactive) | RF2-3-5 (No Bioactive) |

Figure 3.2: Flow chart showing the technique used and the yield of extract sequential soaking, gravity column chromatography and preparative-HPLC. Pure C1 compound obtained for the root of *Hydrocotyle vulgaris*. Viab: Viability of K – 562 cells.

Dichloromethane fraction
(Active fraction)

Gravity column (Hexane: Ethyl Acetate)

Fractions yielded by gravity column was pooled into 11 sub-fractions
based on the similar TLC profile

LF1	LF3	LF5	LF7	LF9	LF11
(No Bioactive)	(Bioactive)	(No Bioactive)	(No Bioactive)	(No Bioactive)	(No Bioactive)

LF2	LF4	LF6	LF8	LF10
(No Bioactive)	(No Bioactive)	(No Bioactive)	(No Bioactive)	(No Bioactive)

Semi-prep HPLC: Acetonitrile: water

L1 compound

LF3-1
Bioactive pure compound
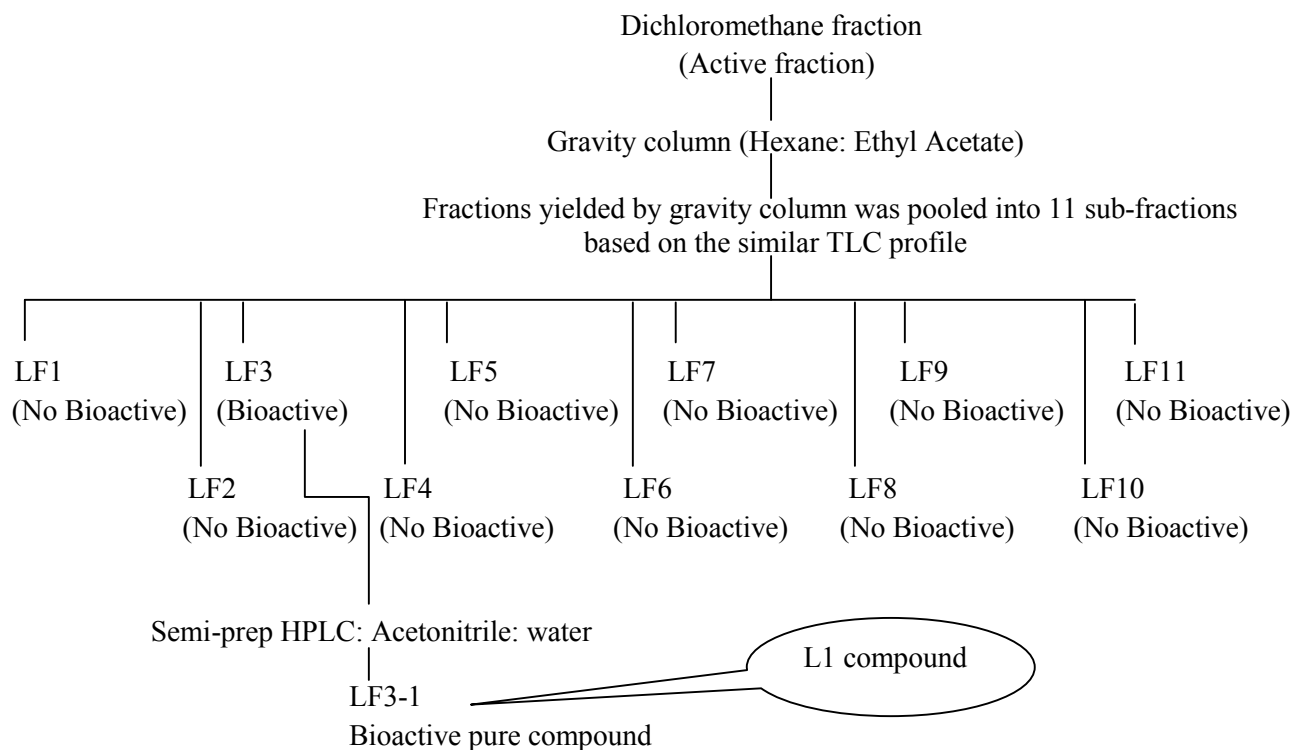
Figure 3.3: Flow chart showing the chromatography technique used in isolation process of dichloromethane of leaves, viability of K-562 cells after treated with particular fraction and the yield of extract sequential soaking, gravity column chromatography and prep-HPLC. L1 compound obtained for the leaf of *Hydrocotyle vulgaris*. Viability: Viability of K-562 cells.

3.5 Structure Elucidation

3.5.1 Determination of Molecular Weight by Gas Chromatography-Mass Spectrometry (GCMS)

The bio-active purified compounds isolated from fraction LF3 and RF6-4 by using HPLC were analysed on GCMS to obtain the molecular weight and compare the percentage of similarity with existing compounds in the library to aid in structure elucidation. Firstly the compounds were dissolved in the HPLC grade acetonitrile and diluted to 5 ppm as a final concentration. The sample was filtered through a 0.2 μm PTFE membrane and 1 μl of compounds was injected into the gas chromatography mass spectrometer machine (GCMS-QP2010 Plus Shimadzu, Japan) equipped with capillary column (0.25 μm X 0.25 mm X 30 m, BPX-5 SGE forte, Australia). The compound was analysed in the GC system with temperature adjustment from low temperature to high temperature. The initial temperature for the analysis was 80 ºC and temperature was increased up to 310 ºC within 37 minutes. The single compound will pass into the ion source of the mass spectrometry and the molecular weight of fragment for the compound was scanned by the detector from 40 m/z to 550 m/z. Then the molecular weight of the pure compound was determined. All the data were analysed by GCMS Postrun analysis program (Lab Solution GCMS Solution).

3.5.2 Determination of Functional Group by Fourier Transform Infrared Spectrophotometer (FTIR)

A small amount of bio-active pure compound isolated from fraction LF3 was dissolved in HPLC grade methanol (Merck, Germany). Then, the sample was subjected into the FTIR (IR Prestige-21 Model, Shimadzu. Japan). The FTIR spectrum was generated and analysed by the IRsolution software. The wavenumbers present at the FTIR spectrum represent the functional groups of the bio-active pure compound.

3.5.3 Nuclear Magnetic Resonance Spectroscopy (NMR)

Approximately 25 mg of bio-active pure compound isolated from fraction LF3 was dissolved in 3 ml of deuterochloroform (CD_2Cl_3) and filtered through a 0.2 μm PTFE membrane. The deuterochloform contained the bio-active pure compound was transferred into a round bottom NMR tube 178 mm long and 4.2 mm diameter (Norell, USA). The sample was subjected to analysis on a 400 MHz NMR (Model ECX400, JOEL. Japan) to obtain 1D and 2D ^{1}H NMR and ^{13}C NMR spectrums.

3.5.4 Determination of Angle of Rotation by Polarimeter.

The bio-active pure compound was isolated from fraction LF3 was analyzed under the polarimeter (Automatic polarimeter AP-300 ATAGO, Japan) to determine the angle of rotation. The bio-active pure compound was dissolved in 6 ml general grade chloroform with 42.0 µg/ml concentration. After that, the sample was transferred into polarimeter cell with 100 mm long and 10 mm diameter. Then the polarimeter cell which contained the sample was analyzed under sodium light at 589 nm in the polarimeter. The angle of rotation of the sample was displayed in positive optical rotation or negative optical rotation.

3.6 Maintenance and Storage of Cell Lines

The K-562 cell is a human erythroleukimia cell line established from the pleural effusion of a 53 years old woman with chronic myeloid leukemia (CML). Cell line was purchased from ATCC and maintained in Roswell Park Memorial Institute 1640 medium (RPM-I 1640) supplemented with 10 % (v/v) Fetal Bovine Serum (IDNA, South America). The cells were sub-cultured every 2-3 days or when the culture reached approximately 75-85 % confluence as observed with the light microscope (Nikon Eclipse TS1000, Japan). The cell lines were routinely observed under the microscope for contamination.

For cryopreservation, approximately 8 ml of a confluent K-562 suspension was transferred from culture flask into a centrifuge tube and spun at 1500 rpm for 5 minutes. The supernatant was discarded and the cell pellet was resuspended in 1 ml of RPMI-1640 medium, transferred into cryopreservation vials and supplemented with 5 % (v/v) of DMSO (Fisher Scientific, UK) as a cryoprotectant. Cells were stored at – 86 º C for one day and then transferred into the liquid nitrogen tank.

To revive frozen stocks of K-562, vials were transferred out from liquid nitrogen tank and rapidly thawed in a 37 º C water bath or between the palms of hands. The thawed cells were transferred into 100 mm culture dish (Greiner bio-one, USA) which contained 10ml RPMI-1640 medium supplemented with 10 % (v/v) of Fetal Bovine Serum. The cells were incubated in a humidified incubator (NUAIRE, USA) at 37 º C under 5 % CO_2. The following day, fresh RPM-I 1640 medium was added to replace the DMSO containing medium.

3.6.1 Preparation of Culture Medium

The culture medium was prepared by dissolving 10.4 g of RPMI-1640 powder (Sigma Aldrich, USA) and 2.0 g of sodium bicarbonate (Goodrich Enterprise, USA) in 1 L of deionized water. After that, the pH of medium was adjusted to pH

7.2-7.4 by adding 2 M acid hydrochloric. The medium was filter-sterilized through a 0.2 μm cellulose acetate membrane (Sartorius Stedim, Germany) filtration unit into a sterile 1 L Schott bottle and kept at 4 ºC.

3.7 Cytotoxic Assay

3.7.1 (3-(4, 5-dimethylthiazol-2-yl)-2, 5-diphenyltetrazolium bromide) MTT Assay

The MTT assay is a standard colorimetric assay for measuring cellular proliferation. The MTT pre-screening assay was carried out in sterile 96 well flat-bottom plates (Orange Scientific, Belgium). 10 mg of extract of each fraction was measured into a microcentrifuge tube (Eppendorf, USA) and diluted with 0.5 ml of dimethyl suphoxide (DMSO) to prepare 20 mg/ml of extract. This concentration of extract was diluted with medium for further use in the following manner. 5 μl of extract (20 mg/ml) was mixed in 955 μl of RPM-I 1640 medium in a sterile microcentrifuge tube to make a sub-stock of 100 μg/ml. 100 μl of sub-stock was transferred into sterile 96 well flat-bottom plate and mixed together with 100 μl of K-562 cells (7.5 X 10^4 cells/ml) to give a final concentration of 50 μg/ml of extract concentration and final volume of 200 μl in each well. Each sample was tested in triplicate. A sample layout of a 96 well plate used is shown

65

in Figure 3.4. A blank control (RPM-I 1640 medium only) and untreated cell control (100 µl K-562 cells + 100 µl of RPM-I 1640 medium) was included in every plate. Then the plate was incubated in 5 % CO_2 humidified incubator for 72 hours.

After 72 hours incubation, 20 µl of MTT solution (5 mg/ml) was added into all the wells and the plate was incubated further for another 3 hours in 5 % CO_2 humidified incubator. Then, the plate was spun at 1500 rpm for 5 minutes. Approximately 75 % (120 µl) of supernatant in each well was carefully removed. Then, 150 µl of DMSO was added to each well to solubilize the purple formazan crystals. The absorbance of each well was determined using a mircoplate reader (Bio-rad, Model 680 with Mircoplate Manager Software) at 550 nm and cell viability was calculated using the equation shown in Appendix C. The cell viabilities were calculated from an average of three independent experiments.
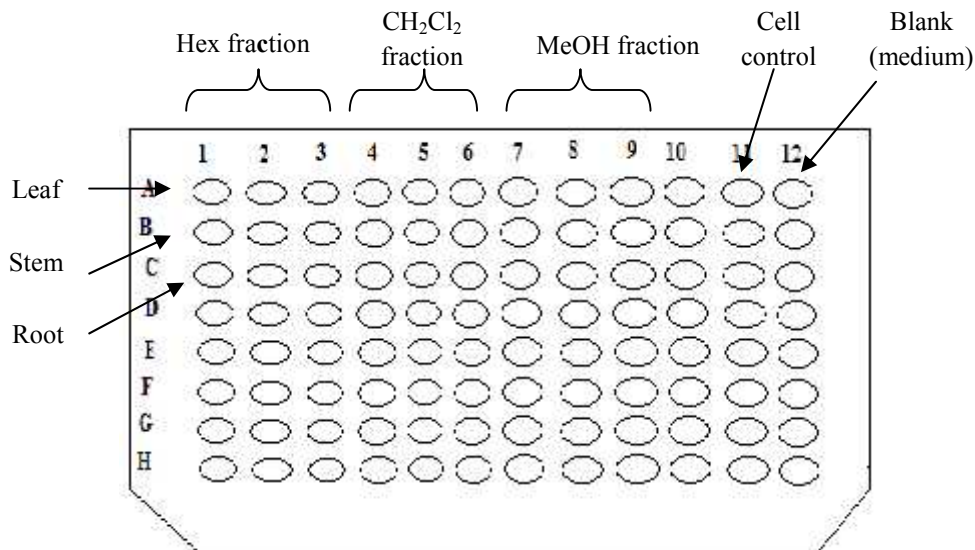
Figure 3.4: A sample layout of 96 well microtiter plate used for the cytotoxic pre-screening dilution of the plants extracts. Wells A11- C11 containing cells only as control. Wells A12-C12 containing medium as blank. Row A1-A9, B1-B9, and C1-C9 containing 100 µL of plant extract and 100 µL of cell with $7.5X\ 10^4$ cell/ml per well. Hex = hexane, CH_2Cl_2 = dichloromethane, MeOH = methanol.

3.7.2 Determination of Inhibition Concentration (IC) Value for Panaxynol, C1, Cisplatin and Doxorubicin Against K-562.

Panaxynol (pure bioactive compound which isolated from fraction LF-3) and C1 (partial pure compound which isolated from fraction RF-6-4) separated on the HPLC were serially diluted to determine the cytotoxic effectiveness against K-562 cells line at different concentration and compared with effectiveness of commercial drugs like cisplatin (Calbiochem, USA) and doxorubicin

(Calbiochem, USA). MTT assay was performed as decribed in section 3.2. For panaxynol, a sub stock of 40 µg/ml was prepared by diluting 4 µl (10 mg/ml) in 996 µl of medium. For C1, a sub stock of 60 µg/ml was prepared by diluting 3 µl (20 mg/ml) in 997 µl of medium. For cisplatin and doxorubicin, a sub-stock of 20 µg/ml and 2 µg/ml was prepared by diluting 20 µl (1 mg/ml) in 980 µl and 2.0 µl (1 mg/ml) in 998 µl of medium, respectively. Then a serial dilution of panaxynol, C1, cisplatin and doxorubicin were carried out according to the diagram shown in Figure 3.5 to obtain eight different concentrations. Commercial drugs were serially diluted in the same manner. Then, 100 µl of each concentration was pipptted in triplicate into 96 well flat bottom plate that containing 100 µl of K-562 cells suspension at the concentration of 7.5 X 10^4 cell/ml (Figure 3.6). The final volume in each well was 200 µl with the concentration of drug in each well halved due to the dilution with cells.

X µl of fresh medium was added

X µl mother stock was added

X mg/ml of compound (mother stock)

500µl   500µl   500µl   500µl   500µl   500µl   500µl

Y µg/ml   Y/2 µg/ml   Y/4 µg/ml   Y/8µg/ml   Y/16 µg/ml   Y/32µg/ml   Y/64µg/ml   Y/128 µg/ml

500µl of fresh medium was added
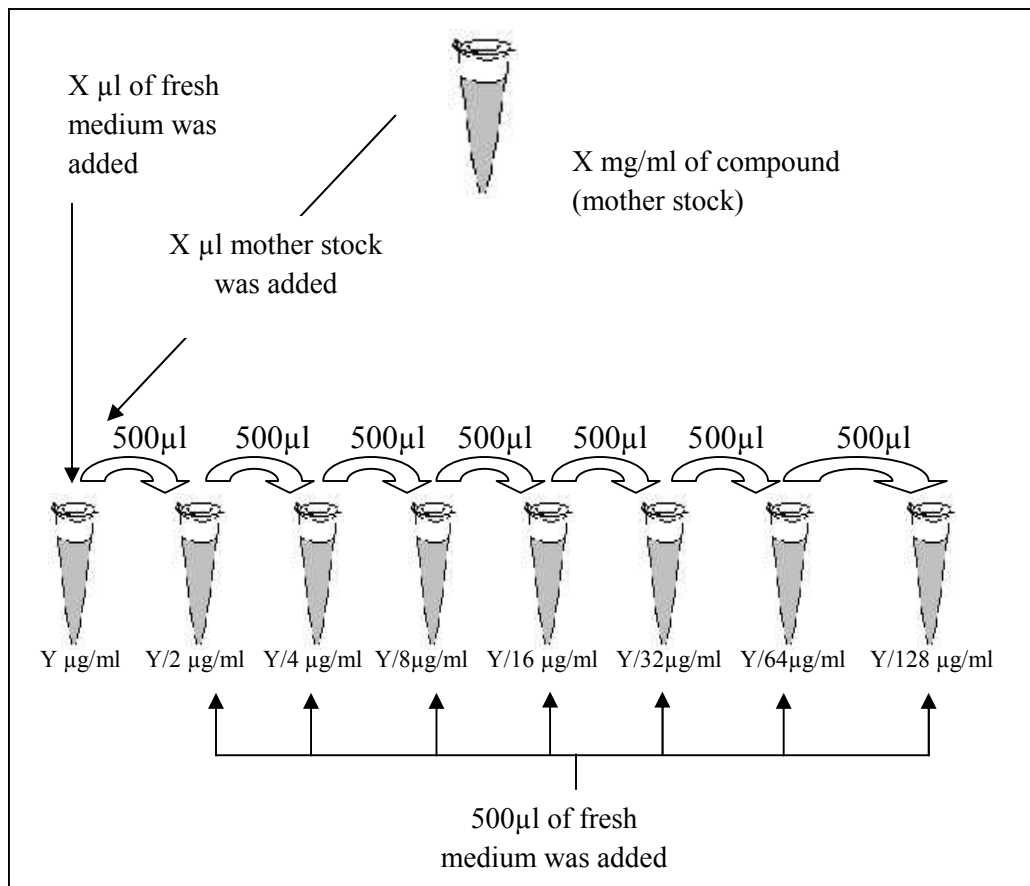
Figure 3.5: The serial dilution process of the studied compound to obtain eight different concentrations.
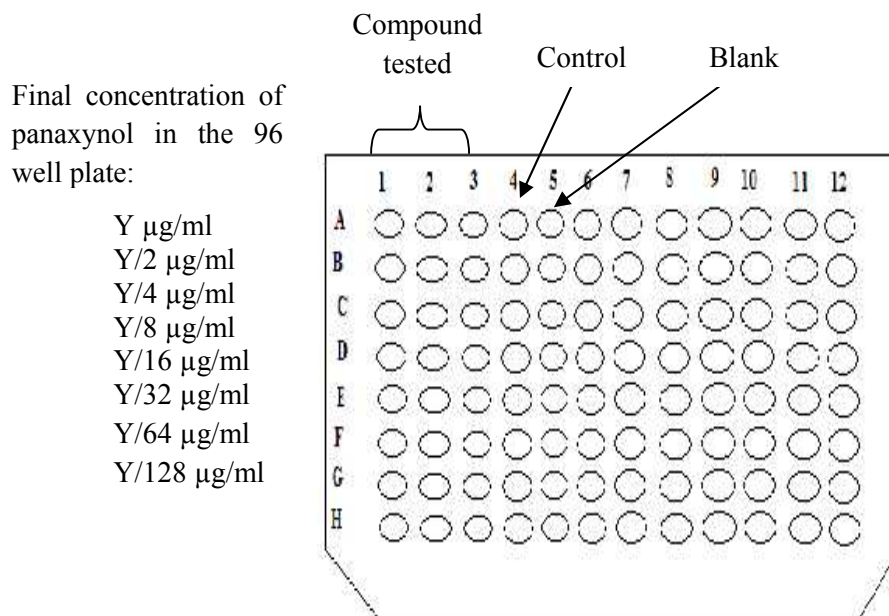
Figure 3.6: A sample layout of 96 well plate used for the cytotoxic pre-screening dilution of the compounds with different comcentration. Wells A4-C4 contain untreated cells (control). Wells A5-C5 containing 200 μl medium (blank). Rows 1, 2, 3 and 4 containing 100 μl of different concentrations of the studied compounds and 100 μl of cell with 7.5×10^4 cell/ml per well.

3.8 Cell Cycle Analysis

In the process of cell cycle analysis, 3 ml cell suspension containing approximately 1.0×10^5 K-562 cells was transferred into 60mm culture dish (TPP, Switzerland). 1.02 μl and 1.8 μl of panaxynol (pure compound isolated from fraction LF-3) was transferred from mother stock (41 nM) to each 60mm culture dish with 2998.98 μl and 2998.2 μl medium respectively to give IC_{50} (13.9

μM) and IC_{85} concentrations (24.6 μM). These dishes were incubated in the 5 %
CO_2 incubator for 12, 24, 48 and 72 hours. Each concentration of panaxynol and
time points were tested for cell cycle analysis in duplicate and the experiment was
repeated three times. For the positive control, 29 μl of cisplatin was transferred
from mother stock (3.33 mM) to each 60 mm culture dish to give IC_{85} (32.19 μM)
concentration and incubated in the 5 % CO_2 incubator for 12, 24, 48 and 72 hours.
For the negative comtrol (cells only), 1×10^5 of K-562 cells were transferred into
60 mm culture dish with 3 ml medium and incubated in the 5 % CO_2 incubator for
12, 24, 48 and 72 hours.

At each time point stated above, the dish was resuspended gently and the
supernatant containing cells were completely transferred into a 15 ml tube and
centrifuge at 1500 rpm for 5 minutes. The supernatant was discarded and pellet
was resuspended in 300 μl PBS and 300 μl of this suspension was transferred into
a microcentrifuge tube and 700 μl ice cold absolute ethanol (Merck, Germany)
was added dropwise while gently vortexing the tube. These tubes were kept in the
-20 ºC freezer for at least 2 hours.

Then, the absolute ethanol was removed by brief centrifugation and the cell pellet
was washed twice with ice cold PBS. After the second wash, the pellet was
resuspended in 500 μl PBS and 5 μl of Rnase (10 mg/ml) (Invitrogen, USA) and

left at room temperature for 10 minutes. For DNA staining, 2 µl of PI solution (1mg/ml) (Sigma, USA) was then added and incubated for another 5 minutes in the dark. Cells were analysed within an hour on a FACS Calibur flow cytometer (Beckton Dickinson, US) with a laser emission at 488 nm and the PI fluorescence detected with FL2 in linear mode. A dot plot with Forward Scatter (FSC) on x-axis and Side Scatter (SSC) on the y-axis was constructed and then a gate was drawn in the centre. Next, a histogram was set up with FL2 on x-axis and cell population on y-axis to analyse gated populations of living cells. Then, the gated cells were displayed on fluorescent histogram to determine the percentage of cells in G1, S and G2/M phases (Figure 3.7). A total of 10000 events were analysed by flow cytometer. In flow cytometry analysis of cell cycle, three independent experiments were done and the results were averaged.
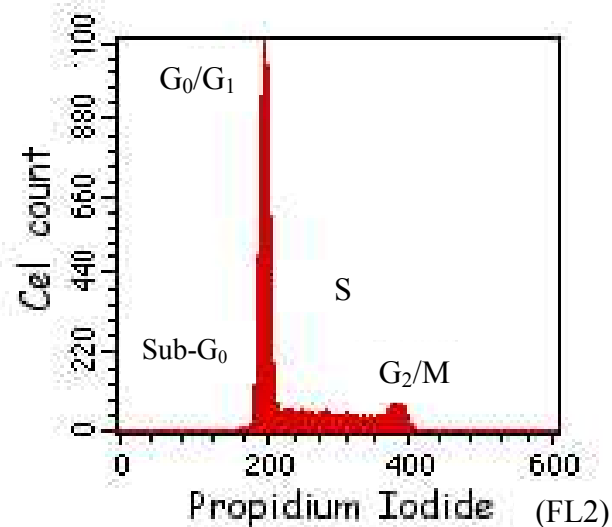

Figure 3.7: The common histogram to represent DNA content of negative control (cells only) which is analysed by flow cytometer. The DNA content of the negative control (cells only) is distributed in Sub G_0, G_0/G_1, S and G_2/M phase. Y-axis represented cell population and X-axis represented PI intensity.

72

3.9 Apoptosis Assay

An early event of apoptosis is membrane blebbing and subsequent exposure of phosphatidylserine (PS) on the outer surface of plasma membrane. Annexin V has high affinity to bind with PS and when conjugated with FITC dye, allows the detection of apoptotic cells and non apoptotic cells by using the flow cytometer. Double staining with PI able to distinguish apoptotic cell (PI negative and FITC positive) and necrotic cell (PI positive and FITC negative).

K-562 cells were treated with panaxynol (pure compound isolated from fraction LF-3) at IC_{50} (13.9 µM) and IC_{85} (24.6 µM) concentration and cisplatin at IC_{85} (32.19 µM) concentration. Control consisted of untreated K-562 cells (cells only) and treated K-562 cells were incubated for 4, 8, 12, 16, 24, 48 and 72 hours in 5 % CO_2 incubator and freshly harvested for analysis. The incubated cells were harvested at the particular incubation time and the resulting cell pellet was washed twice with ice cold PBS and resuspended in 100 µl of 1X binding buffer. The binding buffer contains 0.1 M HEPES (4-(2-hydroxyethyl)-1-piperazineethanesulfonic acid), 1.4 M of NaCl and 25 mM of $CaCl_2$. 100 µl of cell suspension ($\sim 1 \times 10^5$ cells) was transferred to a 5 ml polystyrene round-bottom tube (Beckton Dickinson, USA) and mixed with 5 µl Annexin-V FITC and 2 µl PI solution (10 mg/ml). The tube was incubated for 15 minutes in the dark. 400 µl of 1 X binding buffer was then added and the sample analysed on a FACS Calibur flow cytometer (Beckton Dickinson, USA) equipped with a 488

laser. Fluorescence was detected on FL1 (FITC) and FL3 (PI) in log mode. A dot plot with Forward Scatter (FSC) on x-axis and Side Scatter (SSC) on the y-axis was constructed and then a gate was drawn in the centre. Another dot plot was set up with FL1 on x-axis and FL3 on y-axis to analyse gated populations of living cells (Figure 3.8). In order to get an accurate result, the photomultiplier tube's setting was optimised before the analysis of cells. For example, in the analysis of control sample, the voltage gained on FSC and SSC were adjusted to shift the signal from living cells to fall within the gate. Then, the voltage gained for FL1 and FL3 were adjusted to shift the fluorescence of living cells which are negative for annexin V-FITC staining and PI staining to appear in the lower left quadrant. A total of 10000 events were analysed by flow cytometer. In flow cytometry analysis of apoptosis, three independent experiments were done and the results were averaged.
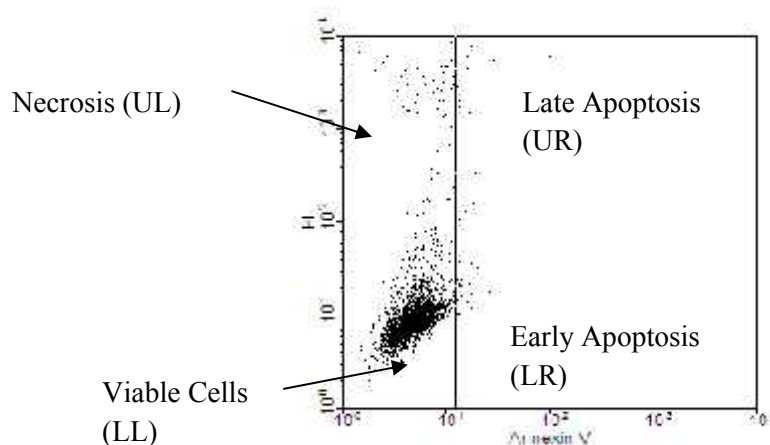

Figure 3.8: Dot plot of flow cytometry analysis of apoptosis. The FL-1 represented the intensity of PI on the Y-axis while FL-3 represented the intensity of FITC on X-axis. Viable cells are located at lower left quadrant (LL), necrotic cells are located at upper left (UL) quadrant, early apoptotic cells are located at lower right (LR) and late apoptotic cells are located at upper right (UR).

3.10 Determination of Caspase-3/7, 8 and 9 Activities

The unique peptide recognition sequence of the caspase family can be utilized to determine specific caspase activity. The luminogenic substrates with tetrapeptide sequence DEVD, LETD or LEHD are specifically cleaved by caspase-3/7, caspase-8 and caspase-9, repectively. These substrates when cleaved by the particular caspase enzyme would release amino luciferin which would be catalysed by luciferase and ATP to generate a luminescent signal. The luminescent signal is proportional to the amount of caspase activity. The caspase-glo caspase ® 3/7, 8 and 9 assay kit was purchased from Promega, USA and used according to the manufactures protocol.

Approximately 1 X 10^5 K-562 cell suspension were cultured in 60 mm culture dish and treated with IC_{85} concentration of panaxynol (pure compound isolated from fraction LF-3) (24.6 μM) and cisplatin (32.19 μM) for 4, 8, 12, 16, 24 hours. Controls are consisting of untreated cells (cells only). At each time point, untreated K-562 cells and treated K-562 cells were harvested freshly. The dish was resuspended gently and supernatant containing cells were completely removed into a 15 ml tube and centrifuged at 1500 rpm for 5 minutes. The supernatant was discarded and pellet was resuspended in 500 μl RPM-I medium. Then 100 μl RPM-I medium containing around 20000 cells were transferred into a white colour, flat solid bottom 96 well plate (Grenier bio-one, USA). Each of the sample was tested in three individual experiment. 100 μl buffer containing the

substrate was added into each well and was incubated for 30 minutes in dark condition. The luminescent signal was measured by a microplate luminometer (TECAN model, DKSH, USA). The amount of caspase activity for a cell was calculated using the equation shown in Appendix D. The amounts of caspase activity per cell were calculated from an average of three independent experiments. A sample layout of a 96 well plate used is shown in Figure 3.9. A blank control (RPM-I medium only) was plated into A10 to C10. The Untreated K-562 cells and K-562 cells treated with IC_{85} concentration of panaxynol and cisplatin in different time points were plated into 96 well plate according to the layout shown at Figure 3.9.
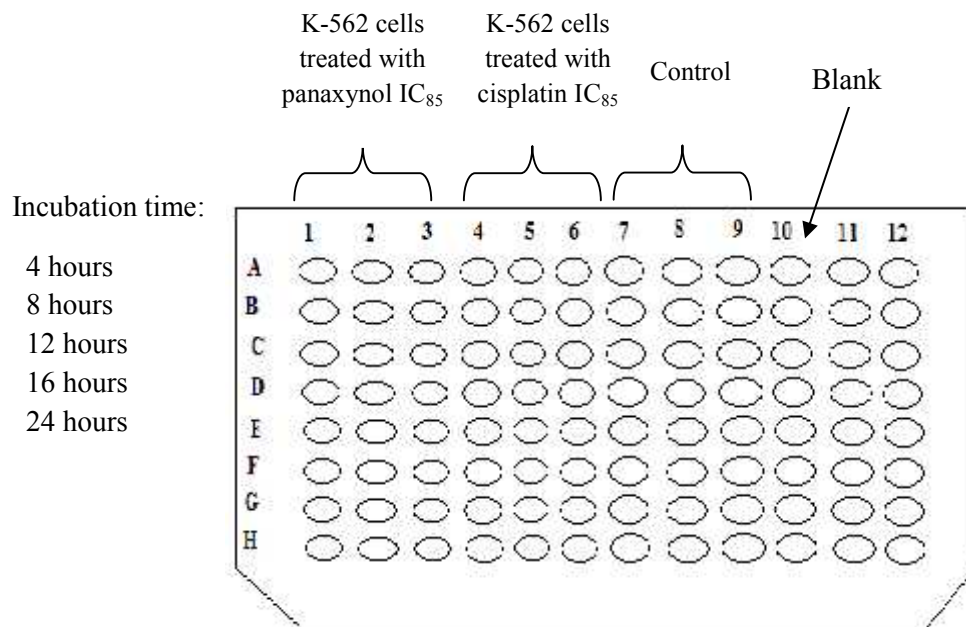

Figure 3.9: A sample layout of 96 well plate used for bioluminescent detection of enzyme activities of caspase-3/7, 8 and 9. Wells A10 –C10 containing 100 µl of RPM-I medium (Blank). The K-562 treated with IC_{85} concentration of panaxynol and cisplatin and untreated K-562 cells in different incubation time were pippetted in rows 1-3, 4-6 and 7- 9, respectively.

CHAPTER 4

RESULTS

4.1 Plant Collection and MTT Pre-Screening

Hydrocotyle vulgaris was chosen in this study because an earlier study reported on the cytotoxicity of the ethanolic extracts of the leaves of the plant on HL-60, Raji and U2-OS cell lines (Wong, 2006). Thus, this study focused on the isolation of the cytotoxic compounds from this plant species. The measured dry weight of the leaf, stem and root of *Hydrocotyle vulgaris* is shown in Table 4.1. The measured dry weight of plant materials are needed for the calculation of yield for bioactive fraction and bioactive pure compound. Following sequential exhaustive extraction, the cytotoxicity of the hexane, dichloromethane and methanol extracts of leaf, stem and root samples of *Hydrocotyle vulgaris* were tested against K-562 cells using a MTT assay. The yield of each fraction obtained and the cytotoxicity of each fraction from dry leaf, stem and root samples are summarized in Table 4.2. The highest cytotoxicity was obtained for the dichloromethane fraction of leaves, hexane fraction of stems and roots. These fractions were chosen for further bioassay-guided-isolation.

Table 4.1: Dry weight for leaves, stems roots of *Hydrocotyle vulgaris*.

Plant Species	Part of plant	Weight (g)
Hydrocotyle vulgaris	Leaves	1024.25
	Stem	525.581
	Root	968.733
	Total	2518.834

Table 4.2: Average cell viability of K-562 with ± standard deviation in three individual experiment carried out in triplicate with 50 µg/ml fraction of leaf of *Hydrocotyle vulgaris* and the yield of fraction.

Parts of plant	Fraction of plant	Average cell viability (%)	*Yield (%)
Leaf	Hexane	33.41 ± 4.46	3.68
	Dichloromethane	13.73 ± 4.60	2.48
	Methanol	79.46 ± 2.62	4.89
Stem	Hexane	2.49 ± 2.07	0.57
	Dichloromethane	32.43 ± 6.07	0.87
	Methanol	79.31 ± 2.55	7.15
Root	Hexane	1.97 ± 0.81	1.01
	Dichloromethane	42.89 ± 6.43	0.69
	Methanol	89.68 ± 7.64	8.20

* Yield (%) ➔ (weight of crude extract (g) / weight of dry plant material (g)) X 100 %

4.2 Bioassay-Guided-Isolation of the Dichloromethane Fraction of Leaves

Gravity column chromatography of the dichloromethane fraction of leaves produced 97 fractions. The 97 small fractions were pooled into 11 fractions based on similarity of TLC profiles of each fraction. Cytotoxicity of these 11 fractions against K-562 cells was determined by using MTT assay and the results are shown in Table 4.3. Only fraction LF3 killed more than 95 % of cells at 50 μg/ml. The HPLC profile of LF3 is showing one major and 2-3 minor peaks (Figure 4.1). Fraction LF3 was fractionated further using semi-preparative HPLC to collect the major peak eluting between 10.5-11 minutes. Analysis of the collected fraction (LF3-1) on analytical HPLC showed an estimated purity of 96.4 % detected at 254 nm (Figure 4.2). Gas chromatography analysis on LF3-1 showed only a single peak present in the chromatography with approximately 99 % purity (Figure 4.3). A total of 44.5 mg of LF3-1 was extracted giving a yield of 0.004 % from dry weight of leaves. MTT cytotoxicity assay of LF3-1 showed that this compound decreased cell viability to 2.99 ± 0.13 % at 50 μg/ml. The fraction LF3-1 concluded as a pure bioactive compound and named it as L1. A flow chat of the separation scheme for the dichloromethane fraction of leaves is shown in Figure 4.4.

Table 4.3 Cytotoxicity of fractions from dichloromethane extract of *Hydrocotyle vulgaris* leaves. K-562 cells were treated with 50 µg/ml of sample for 72 hours and MTT assay used to determine cell viability. Results are an average of three individual experiment.

Sub-fraction	Average cell viability (%)	Weight of fraction (g)	*Yield (%)
LF1	88.57 ± 1.48	3.18	0.31
LF2	84.77 ± 6.73	0.51	0.05
LF3	1.90 ± 0.19	1.02	0.10
LF4	22.60 ± 6.12	0.82	0.08
LF5	91.14 ± 6.48	1.54	0.15
LF6	64.52 ± 6.45	2.88	0.28
LF7	55.39 ± 2.38	1.95	0.19
LF8	44.38 ± 5.15	1.13	0.11
LF9	63.12 ± 1.92	0.51	0.05
LF10	40.99 ± 5.92	5.33	0.52
LF11	49.28 ± 6.74	3.89	0.38

* Yield (%) ➜ (weight of crude extract (g) / weight of dry plant material (g)) X

100 %
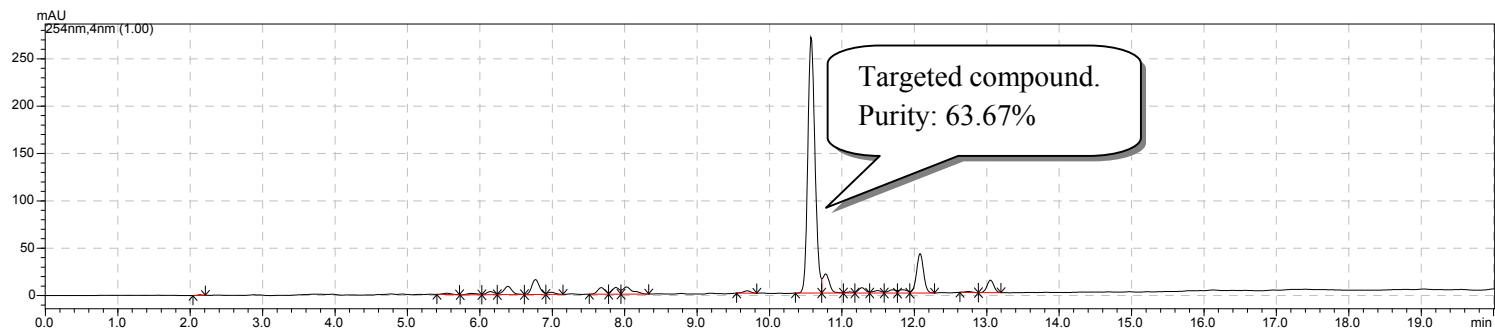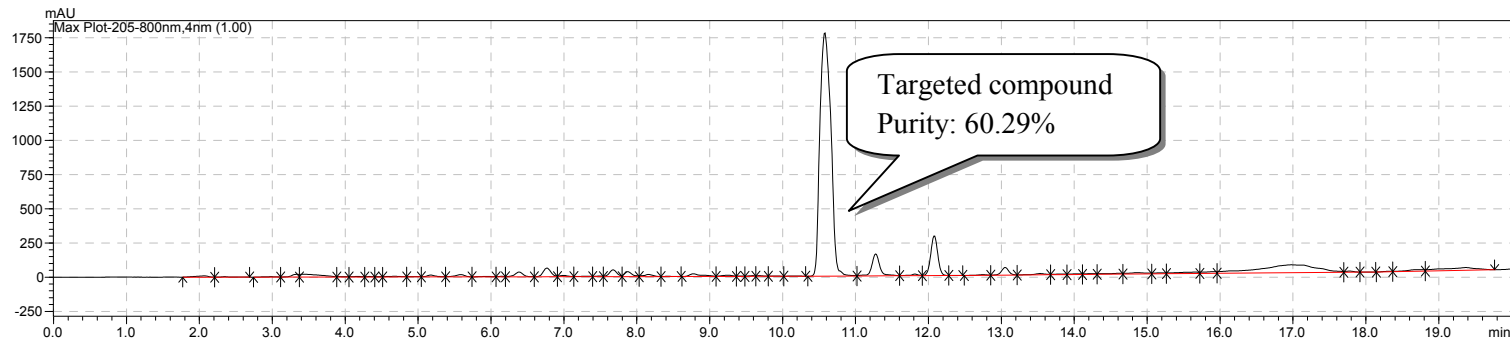
Figure 4.1: HPLC profile of fraction LF3 for leaves of *Hydrocotyle vulgaris*. HPLC column used for this analysis is 100 mm X 4.6mm RC18, (Chromolith ® Preformance) and the fraction LF3 detected under (A) 254 nm wavelength and (B) maximum spectrum 205-800 nm. Flow rate is 1ml/minutes.
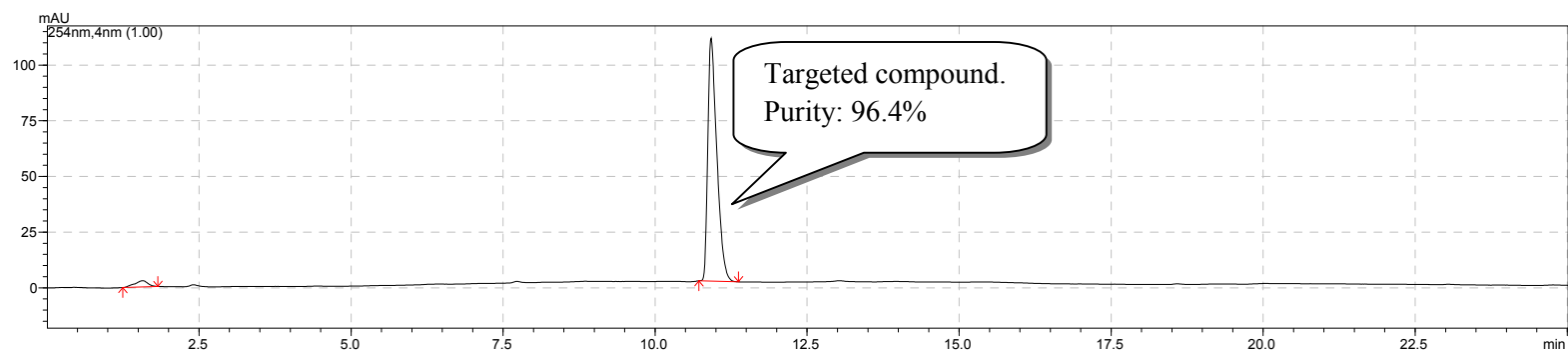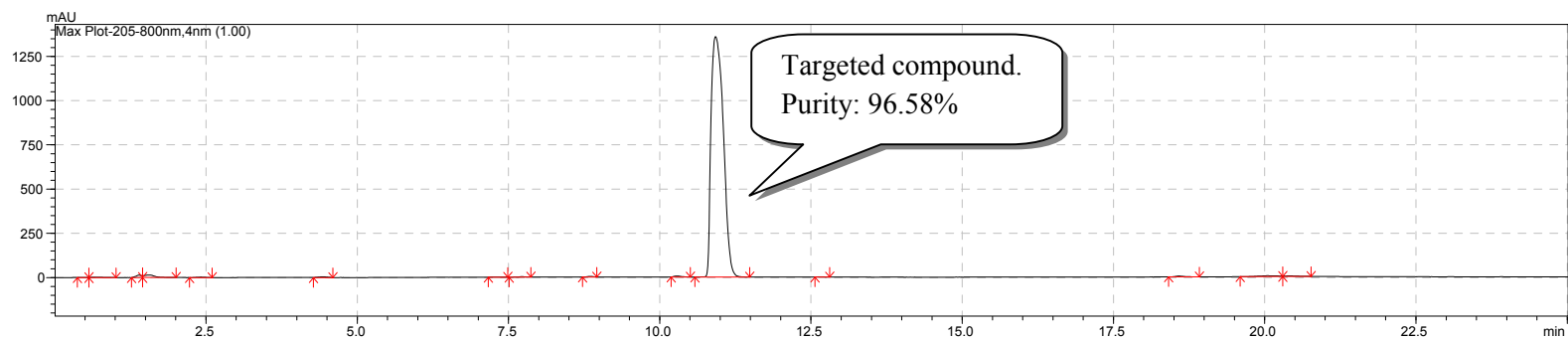
Figure 4.2: HPLC profile of fraction LF3-1 for leaf extracts of *Hydrocotyle vulgaris*. HPLC column used for this analysis is 100 mm X 4.6mm RC18, Chromolith ® Preformance and under (A) 254 nm wavelength and (B) Maximum spectrum 205-800nm. The solvent system used for analysis is gradient 50%-100% of acetone nitrile: water over 25 minutes with 1 ml/minutes flow rate.
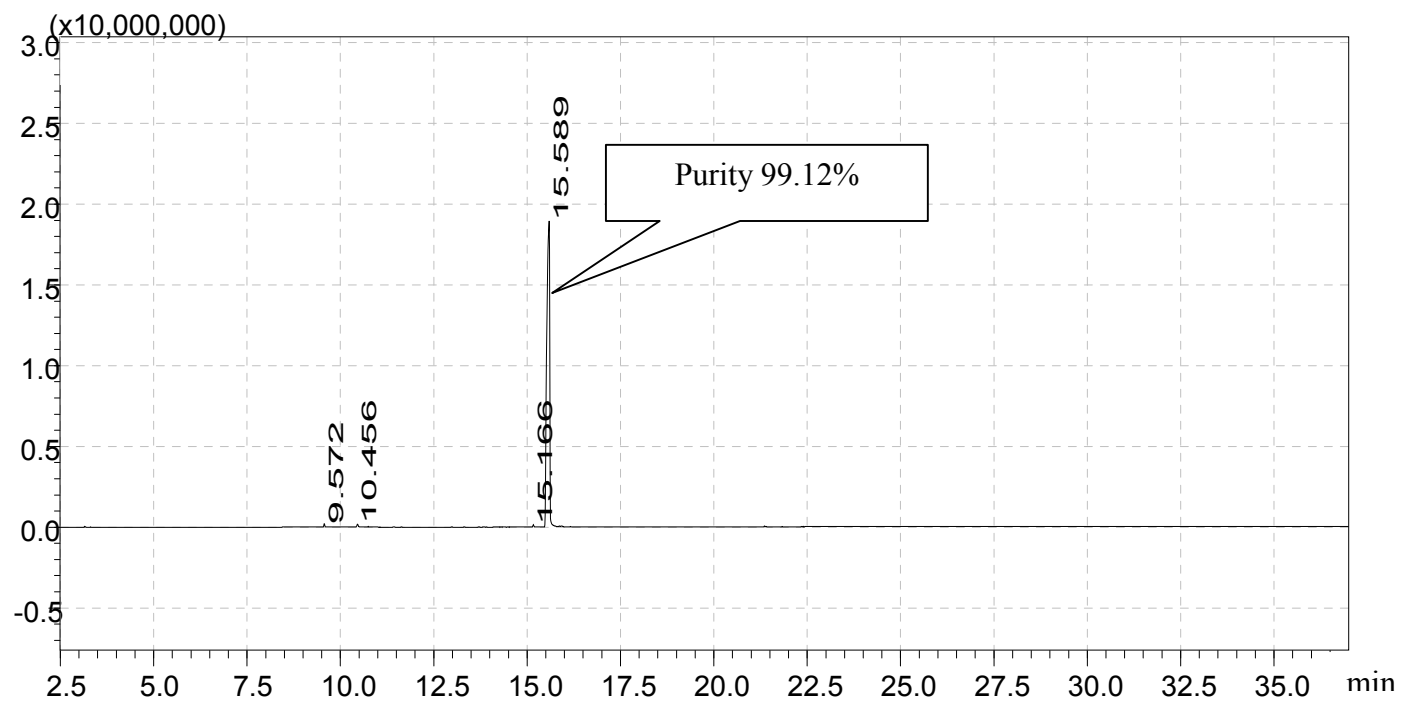
Figure 4.3: GC profile of fraction LF3-1 for *Hydrocotyle vulgaris*. The GC column used for analysis is capillary column 0.25µm X 0.25mm X 30m, BPX-5 SGE forte. The retention time of the peaks is represented at the profile.

Dried *Hydrocotyle vulgaris*'s leaf

(1024.25g)

Sequential Soaking

Hexane fraction
Yield: 3.86%
% viability: 33.41± 4.46

Dichloromethane fraction
Yield: 2.48%
% viability: 13.73 ± 4.60

Methanol fraction
Yield: 4.89%
% viability: 79.46 ± 4.89

Gravity column (Hexane: Ethyl Acetate)

LF1
Yield: 0.31%
% viability: 88.57±1.48

LF3
Yield: 0.10%
% viability: 1.90±0.19

LF5
Yield: 0.15%
% viability: 91.14±6.48

LF7
Yield: 0.19%
% viability: 55.39±2.38

LF9
Yield: 0.05%
% viability: 63.12±1.92

LF11
Yield: 0.38
% viability: 49.28±6.74

LF2
Yield: 0.05%
% viability: 84.77±6.73

LF4
Yield: 0.08%
% viability: 22.60±6.12

LF6
Yield: 0.28%
% viability: 64.52±6.45

LF8
Yield: 0.11%
% viability: 44.38±5.15

LF10
Yield: 0.52%
% viability:40.99±5.92

Semi-prep HPLC: Acetonitrile: water

L1 compound

LF3-1
Yield: 0.004%
% viability: 2.15± 1.31

Figure 4.4: Flow chart showing the chromatography technique used in isolation process of dichloromethane of leaves, viability of K-562 cells after treated with particular fraction and the yield of extract sequential soaking, gravity column chromatography and prep-HPLC. L1 compound obtained for the leaf of *Hydrocotyle vulgaris*. Viability: Viability of K-562 cells.

4.3 Bioassay-Guided Isolation of the Hexane Fraction of Root

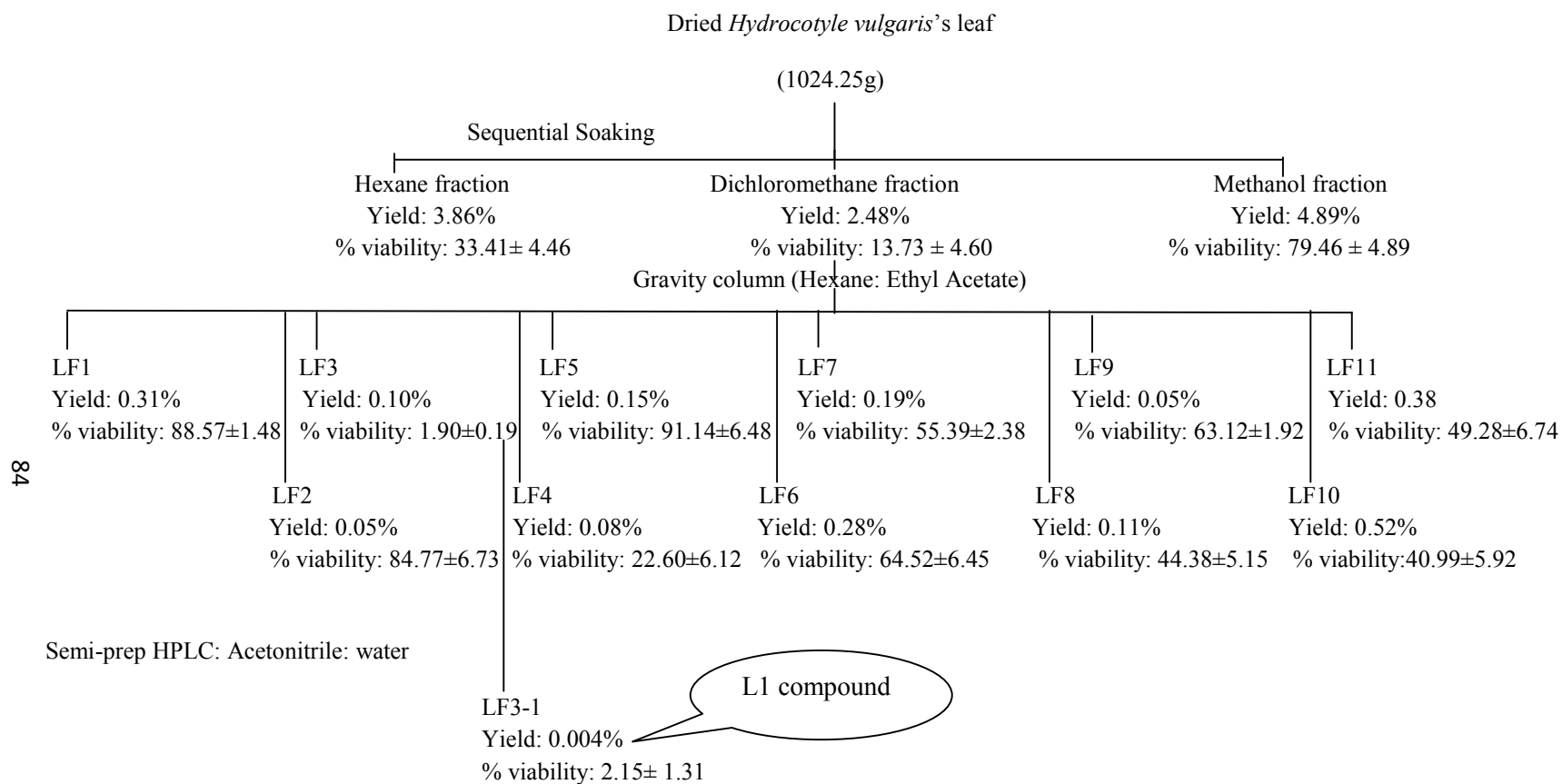Gravity column chromatography of the root hexane fraction produced 60 fractions. The 60 small fractions were pooled into 12 fractions based on similarity of TLC profile of each fraction. Cytotoxicity of these 12 fractions against K-562 cells was determined by using MTT assay and the results are shown in Table 4.4. The fraction RF2 and RF6 killed more than 95 % of cells at 50 µg/ml. The RF2 and RF6 were further purified by gravity column chromatography again. RF2 was yielded another 85 small fractions. The 85 small fractions were pooled into 12 fractions based on similarity of TLC profile of each fraction (RF2-1 to RF2-12). Thought chromatography RF6 was further separated into another 51 small fractions. The 51 small fractions were pooled into 10 fraction based on similarity of TLC profile of each fraction (RF6-1 to RF6-10). Cytotoxicity of these fractions against K-562 cells was determined by using MTT assay and the results are shown in Table 4.5.

Fractions RF2-3 and RF6-4 killed more than 92 % of cells at 50 µg/ml. The HPLC profile of RF2-3 is showing five major peaks (Figure 4.5). Fraction RF2-3 was fractionated further using the semi preparative-HPLC into five individual sub-fractions (RF2-3-1 to RF2-3-5). While HPLC profile of RF6-4 shown 2 major peaks and 7 minor peaks shown in Figure 4.6. Fraction RF6-4 was fractionated further using the preparative-HPLC into 9 sub-fractions (RF6-4-1 to RF6-4-9). The cytotoxicity of those sub fractions against K-562 cells was determined by

Table 4.4 Cytotoxicity of column chromatography fractions from hexane extract of *Hydrocotyle vulgaris* roots. K-562 cells were treated with 50 µg/ml of sample for 72 hours and MTT assay used to determine cell viability. Results are an average of three individual experiment.

Sub-fraction	Average cell viability (%)	Weight of fraction (g)	*Yield (%)
RF1	149.67 ± 3.65	0.58	0.06
RF2	4.71 ± 0.59	1.16	0.12
RF3	74.78 ± 2.64	1.06	0.11
RF4	31.83 ± 9.53	0.97	0.10
RF5	82.77 ± 2.50	0.10	0.01
RF6	4.36 ± 2.47	0.68	0.07
RF7	78.16 ± 5.66	0.29	0.03
RF8	45.96 ± 6.59	0.39	0.04
RF9	77.69 ± 4.49	0.10	0.01
RF10	27.32 ± 5.18	0.19	0.02
RF11	46.77 ± 5.61	0.78	0.08
RF12	75.83 ± 5.44	1.55	0.16

* Yield (%) ➜ (weight of crude extract (g) / weight of dry plant material (g)) X 100%

Table 4.5 Cytotoxicity of sub-fractions from fraction RF2 and RF6 of *Hydrocotyle vulgaris* roots. K-562 cells were treated with 50 µg/ml of sample for 72 hours and MTT assay used to determine cell viability. Results are an average of three individual experiment.

Fraction	Sub- fraction	Average cell viability (%)	Weight of fraction (g)	*Yield (%)
RF2	RF2-1	76.71 ± 5.60	0.058	0.006
	RF2-2	15.59 ± 2.52	0.019	0.002
	RF2-3	4.03 ± 3.21	0.194	0.020
	RF2-4	109.28 ± 4.14	0.107	0.011
	RF2-5	28.67 ± 9.00	0.174	0.018
	RF2-6	9.63 ± 0.05	0.029	0.003
	RF2-7	54.89 ± 6.50	0.087	0.009
	RF2-8	5.64 ± 2.48	0.039	0.004
	RF2-9	106.56 ± 6.52	0.087	0.009
	RF2-10	108.46 ± 9.75	0.155	0.016
	RF2-11	98.45 ± 8.84	0.077	0.008
	RF2-12	105.01 ± 8.96	0.077	0.008
RF6	RF6-1	106.72 ± 2.57	0.136	0.014
	RF6-2	8.38 ± 2.64	0.005	5.16×10^{-4}
	RF6-3	28.75 ± 4.86	0.049	0.005
	RF6-4	7.99 ± 2.13	0.145	0.015
	RF6-5	28.59 ± 8.57	0.007	7.23×10^{-4}
	RF6-6	47.21 ± 5.89	0.019	0.002
	RF6-7	87.38 ± 7.06	0.068	0.007
	RF6-8	70.27 ± 9.82	0.077	0.008
	RF6-9	80.30 ± 5.23	0.029	0.003
	RF6-10	99.82 ± 5.33	0.097	0.010

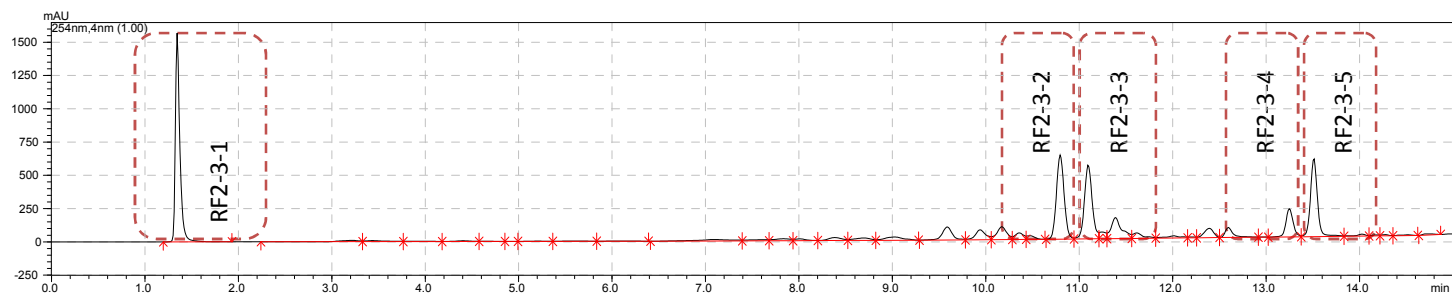* Yield (%) ➔ (weight of crude extract (g) / weight of dry plant material (g)) X 100%

Figure 4.5: HPLC profile of fraction RF2-3. Solvent system used for analysis was gradient 50%-100% methanol: water over 15 minutes with flow rate 1ml/minutes by analytical column HPLC (100 mm X 4.6mm RC18, Chromolith ® Preformance). (A) 254 nm wavelength and (B) Maximum spectrum 205-800 nm. Fraction RF2-3 of root was separated by preparative column HPLC (100 mm X 10 mm RC18, monolithic, Phenomenex) into 5 individual fractions with flow rate 4.75 ml/minutes.
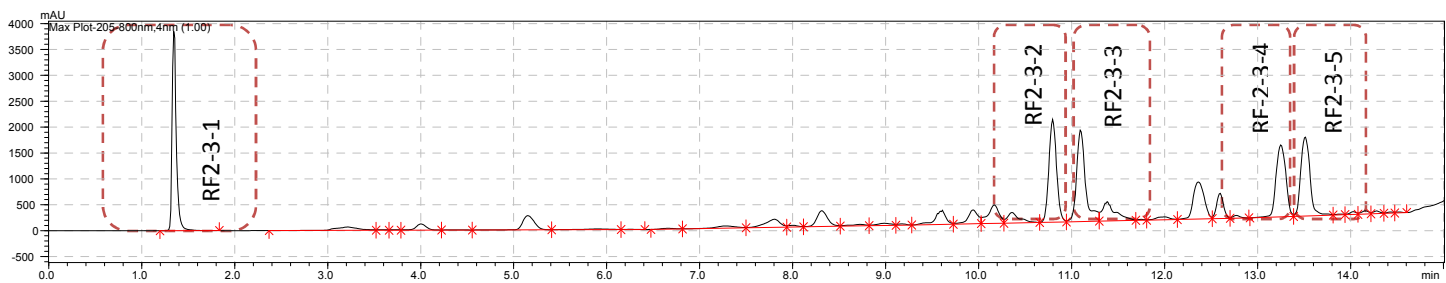
Figure 4.6: HPLC profile of fraction RF6-4. Solvent system used for analysis was gradient 30%-100% methanol: water over 15 minutes with flow rate 1ml/minutes by analytical column HPLC (100 mm X 4.6mm RC18, Chromolith ® Preformance). (A) 254 nm wavelength and (B) Maximum spectrum 205-800 nm. Fraction RF6-4 of root was separated by preparative column HPLC (100 mm X 10mm RC18, monolithic, Phenomenex) into 9 individual fractions with flow rate 4.75 ml/minutes.
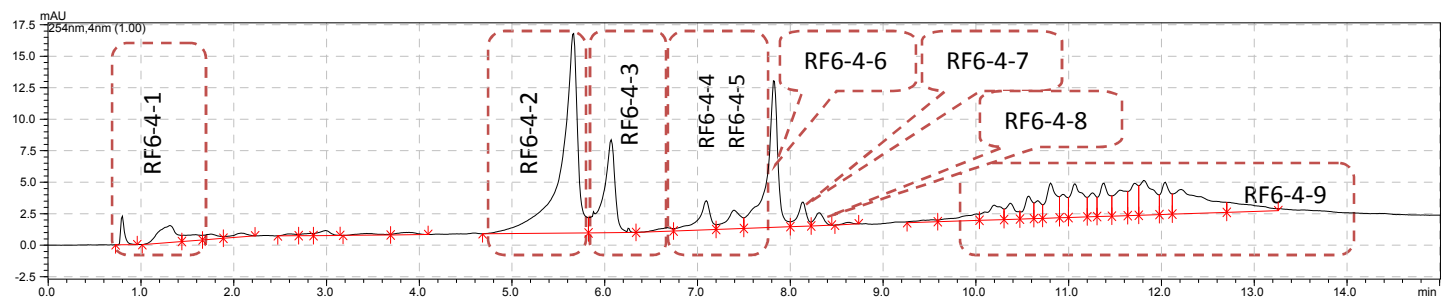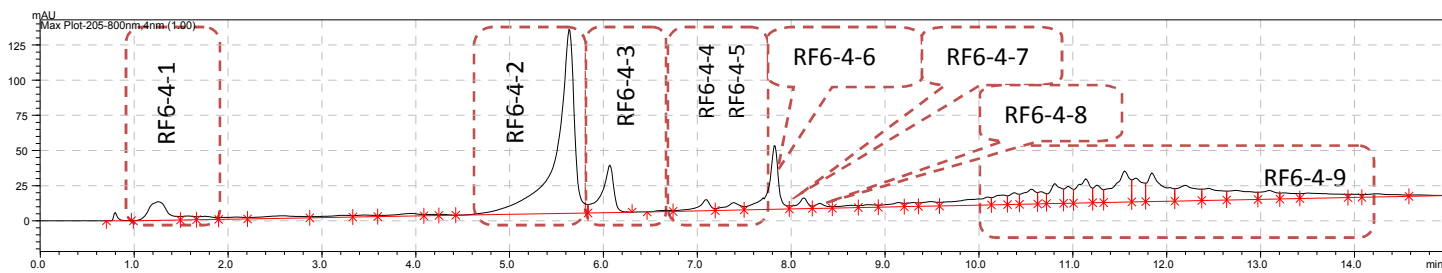
using MTT assay and the results shown at Table 4.6. In the purification of fraction RF2-3 and RF6-4 by using semi preparative-HPLC, only one partial pure cytotoxic compound was successfully isolated from the fraction RF6-4 and named as C1 (RF6-4-6). The HPLC profile and GC profile of C1 compound showing a single peak is presented in Figure 4.7 and Figure 4.8. Based on the minute amount of C1 compound (4mg), further structure elucidation like ^{1}H NMR, ^{13}C NMR and FTIR cannot be done. A flow chart of the separation scheme for the hexane fraction of the root is shown in Figure 4.9.

Table 4.6 Cytotoxicity of sub-fractions from RF2-3 and RF6-4 of *Hydrocotyle vulgaris* roots. K-562 cells were treated with 50 µg/ml of sample for 72 hours and MTT assay used to determine cell viability. Results are an average of three individual experiment.

Fraction	Fraction	Sub- fraction	Average cell viability (%)	Weight of fraction (g)	*Yield (%)
RF2	RF2-3	RF2-3-1	137.16 ± 3.22	0.003	3.14×10^{-4}
		RF2-3-2	102.98 ± 8.20	0.003	2.95×10^{-4}
		RF2-3-3	4.59 ± 2.23	0.003	3.05×10^{-4}
		RF2-3-4	43.59 ± 9.07	0.003	3.43×10^{-4}
		RF2-3-5	72.78 ± 0.99	0.003	3.38×10^{-4}
RF6	RF6-4	RF6-4-1	106.38 ± 3.32	0.001	1.05×10^{-4}
		RF6-4-2	60.70 ± 4.24	0.005	5.35×10^{-4}
		RF6-4-3	27.17 ± 0.76	0.002	1.97×10^{-4}
		RF6-4-4	17.35 ± 3.37	0.001	1.02×10^{-4}
		RF6-4-5	2.02 ± 2.09	0.001	1.03×10^{-4}
		RF6-4-6	2.02 ± 0.66	0.004	4.13×10^{-4}
		RF6-4-7	3.37 ± 1.07	0.001	1.10×10^{-4}
		RF6-4-8	75.53 ± 8.20	0.001	1.15×10^{-4}
		RF6-4-9	83.75 ± 6.19	0.005	5.16×10^{-4}

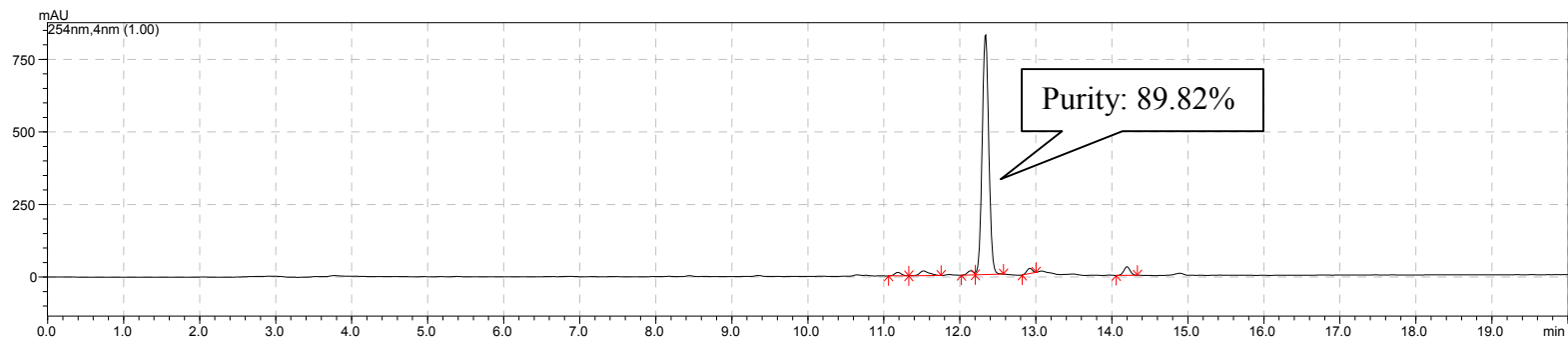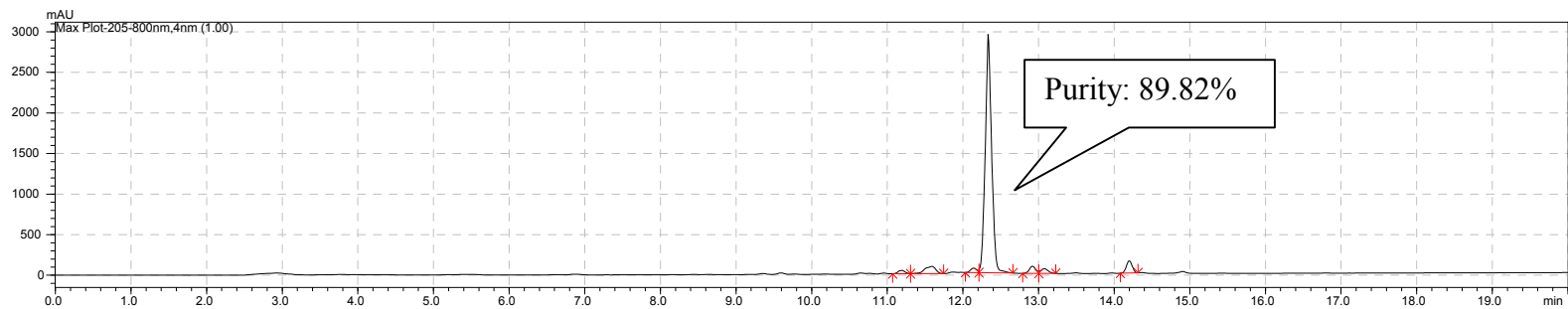* Yield (%) ➔ (weight of crude extract (g) / weight of dry plant material (g)) X 100%

Figure 4.7: HPLC profile of RF6-4-6 for root of *Hydrocotyle vulgaris*. HPLC column used for this analysis is 100 mm X 4.6 mm RC18, Chromolith ® Preformance and under (A) 254 nm wavelength and (B) Maximum spectrum 205-800 nm. The solvent system used for analysis was gradient 40%-100% of methanol: water over 20 minutes with flow rate of 1ml/minutes.
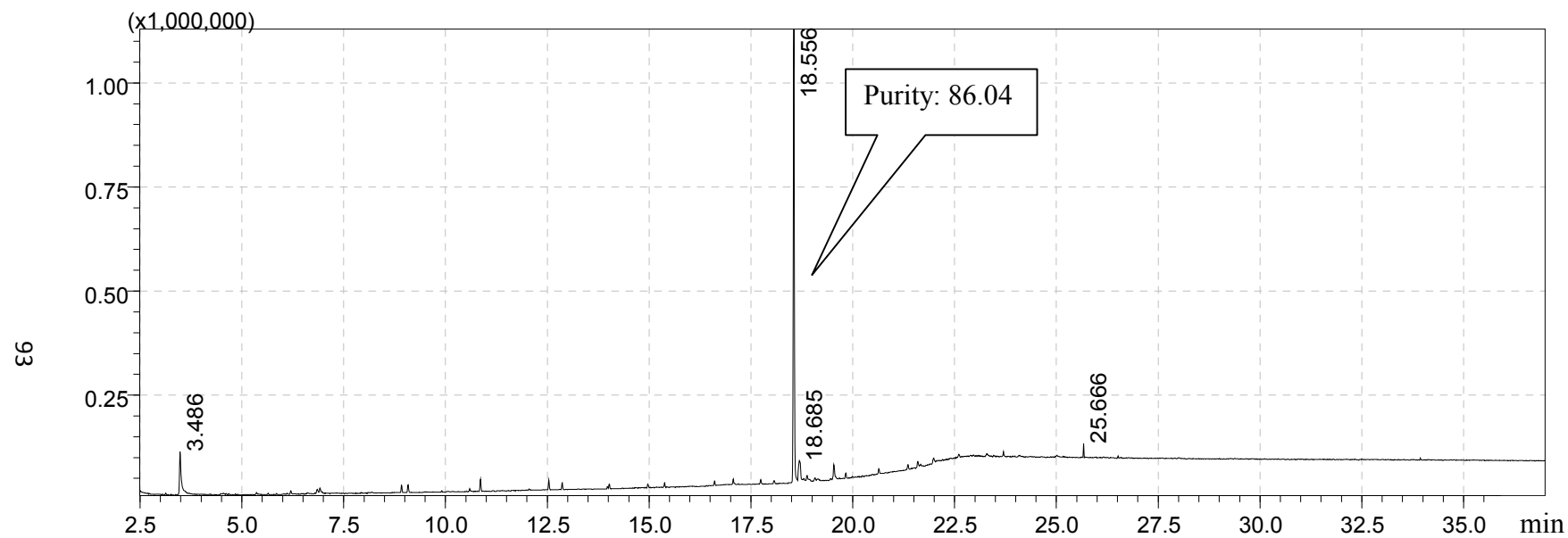
Figure 4.8: The GC profile of the fraction RF6-4-6 for root of *Hydrocotyle vulgaris*. The GC column used for analysis is capillary column 0.25 µm X 0.25 mm X 30 m, BPX-5 SGE forte. The retention time of the peaks are represented at the profile.

Dry root of *Hydrocotyle vulgaris*
(Weight: 968.773g)

Sequential soaking

Hexane fraction
Yield: 1.01%
% viab: 1.97 ± 0.81

Dichloromethane fraction
Yield: 0.69%
% viab: 42.89 ± 6.43

Methanol fraction
Yield: 8.202%
% viab: 89.68 ± 8.20

Column chromatography
Hexane: Ethyl acetate

RF1
Yield: 0.062%
% viab: 149.67±3.65

RF3
Yield: 0.109%
% viab: 74.78±2.64

RF5
Yield: 0.010%
% viab: 82.77±2.50

RF7
Yield: 0.028%
% viab: 78.16±5.66

RF9
Yield: 0.007%
% viab: 77.69±4.49

RF11
Yield: 0.081%
% viab: 46.77±5.61

RF2
Yield: 0.122%
% viab: 4.71±0.59

RF4
Yield: 0.097%
% viab: 31.83±9.53

RF6
Yield: 0.074%
% viab: 4.36±2.47

RF8
Yield: 0.04%
% viab: 45.96±6.59

RF10
Yield: 0.021%
% viab: 27.32±5.18

RF12
Yield: 0.160%
% viab: 75.83±5.44

Column chromatography
Hexane: Acetone

RF6-1
Yield: 0.014%
% viab: 106.72 ± 2.57

RF6-3
Yield: 0.005%
% viab: 28.75 ± 4.86

RF6-5
Yield: 7.23×10^{-4}%
% viab: 28.59 ± 8.57

RF6-7
Yield: 0.007%
% viab: 87.38 ± 7.06

RF6-9
Yield: 0.003%
% viab: 80.30 ± 5.23

RF6-2
Yield: 5.16×10^{-4} %
% viab: 8.38 ± 2.64

RF6-4
Yield: 0.015%
% viab: 7.99 ± 2.13

RF6-6
Yield: 0.002%
% viab: 47.21 ± 5.89

RF6-8
Yield: 0.008%
% viab: 70.27 ± 9.82

RF6-10
Yield: 0.010%
%viab: 99.82 ± 5.33

RF2 Fraction

HPLC
Solvent system: Methanol + water

RF6-4-1
Yield: 1.05×10^{-4}%
% viab: 106.38±3.32

RF6-4-3
Yield: 1.97×10^{-4}%
% viab: 27.17 ± 0.76

RF6-4-5
Yield: 1.03×10^{-4}%
% viab: 2.02±2.09

RF6-4-7
Yield: 1.10×10^{-4}%
% viab: 3.37±1.07

RF6-4-9
Yield: 5.16×10^{-4}%
% viab: 83.75 ± 6.19

RF6-4-2
Yield: 4.35×10^{-4}%
% viab:60.70±4.24

RF6-4-4
Yield: 1.02×10^{-4}%
% viab: 17.35±3.37

RF6-4-6
Yield: 2.06×10^{-4}%
% viab: 2.20±0.66

RF6-4-8
Yield: 1.15×10^{-4}%
% viab: 75.53 ± 8.20

C1 compound

RF2-1
Yield: 0.006%
% viab: 76.71±5.60

RF2-3
Yield: 0.020%
% viab: 4.03±3.21

RF2-5
Yield: 0.018%
% viab: 28.67±9.00

RF2-7
Yield: 0.009%
% viab: 54.89±6.50

RF2-9
Yield: 0.009%
% viab: 106.56±6.52

RF2-11
Yield: 0.008%
% viab: 98.45±8.84

RF2-2
Yield: 0.002%
% viab: 15.59±2.52

RF2-4
Yield: 0.011%
% viab: 109.28±4.14

RF2-6
Yield: 0.003%
% viab: 9.63±0.05

RF2-8
Yield: 0.004%
% viab: 5.64±2.48

RF2-10
Yield: 0.016%
% viab: 108.46±10.75

RF2-12
Yield: 0.008%
% viab: 105.01±8.96

HPLC
Solvent system: Methanol + water

RF2-3-1
Yield: 3.14×10^{-4}%
% viab: 137.16±3.22

RF2-3-2
Yield: 2.95×10^{-4}%
% viab: 102.98±8.20

RF2-3-3
Yield: 3.05×10^{-4}%
% viab: 4.59±2.23

RF2-3-4
Yield: 3.43×10^{-4}%
% viab: 43.59±9.07

RF2-3-5
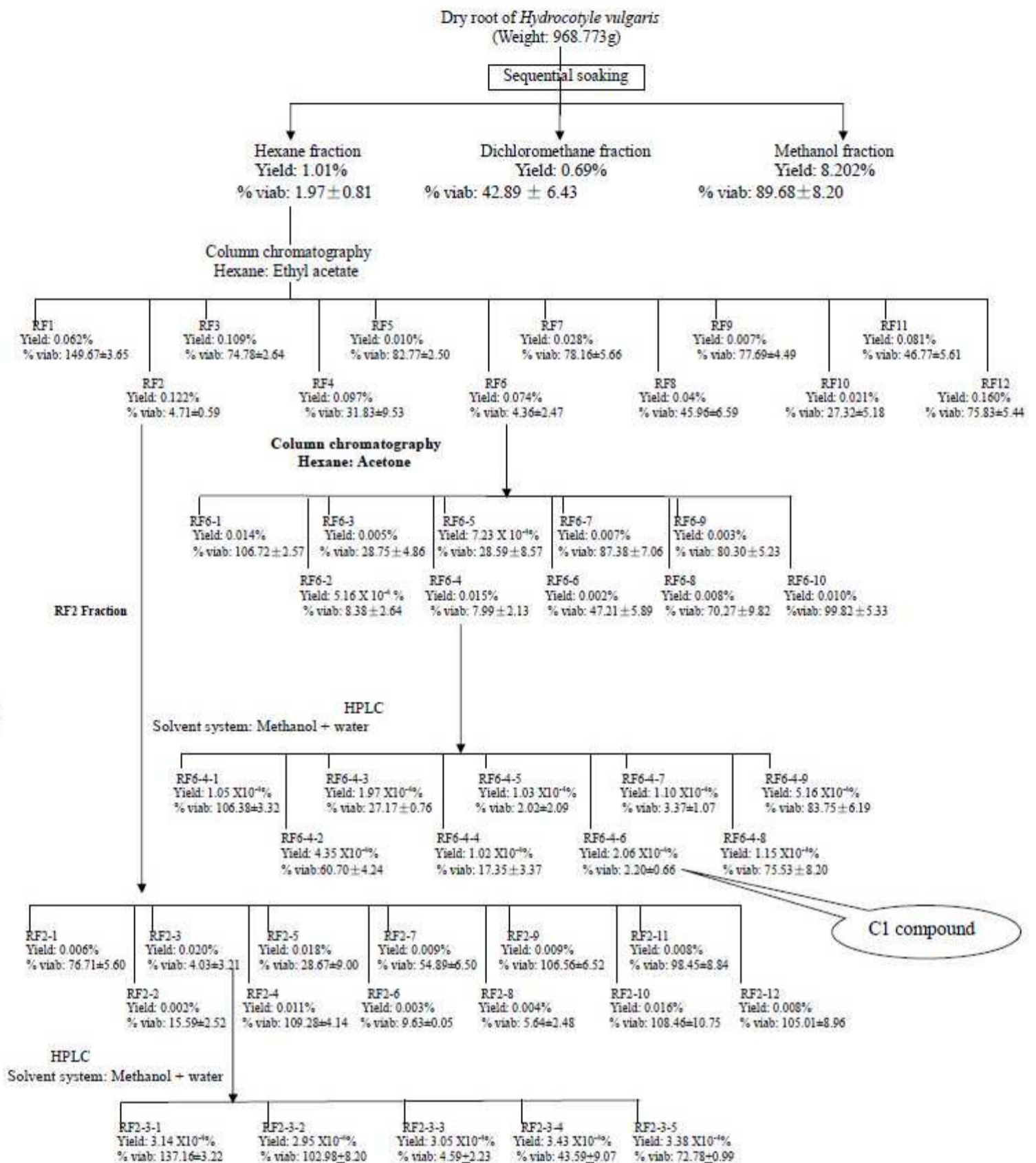Yield: 3.38×10^{-4}%
% viab: 72.78±0.99

Figure 4.9: Flow chart showing the technique used and the yield of extract sequential soaking, gravity column chromatography and preparative-HPLC. Pure C1 compound obtained for the root of *Hydrocotyle vulgaris*. Viab: Viability of K-562 cells.

4.4 Structure Elucidation of L1

4.4.1 FTIR Spectrum and MS Spectrum of L1

Compound L1 is light yellow in colour and exists as an oil with positive optical rotation $[\alpha]_D$ +31.0 °, c 0.42, CHC1$_3$. The molecular weight of L1 is 244 m/z with a molecular formula of $C_{17}H_{24}O$. MS fragmentation pattern is shown in Figure 4.10. The fragmentation pattern of L1 compound compared with the database in the library of GC software and has 95 % similarity with falcarinol (Figure 4.10) The UV spectrum measured in 99.8% methanol has one major peak at 198 nm and three minor peaks at 230, 242 and 256 nm (Figure 4.11). The FTIR spectrum shown in Figure 4.12 indicates the presence of six different types of stretching and bending patterns corresponding to the following functional groups. 1) O-H stretching, 2) C-H stretching, 3) C≡C stretching, 4) C=O stretching, 5) C=C stretching and 6) C-H bending functional group. The O-H stretching, C≡C stretching, C=O stretching, and C=C stretching occurred at 3354.21cm^{-1}, 2256.71 cm^{-1}, 1710.86 cm^{-1} and 1641.42 cm^{-1}, respectively. The C-H stretching (Alkyl type) appeared at 2954.95 cm^{-1}, 2924.09 cm^{-1}, and 2854.65 cm^{-1}, while the C-H stretching (-CH$_2$ & -CH type) presented at 3088.03 cm^{-1} , 3072.6 cm^{-1} , and 3020.53 cm^{-1}. The peaks assigned as C-H bending (RC≡CH, HC≡CH type) occurred at 1328.95 cm^{-1}, 1284.59 cm^{-1}, 1261.45 cm^{-1}, and 1224.8 cm^{-1}. The C-H bending (CH$_3$ type) appeared at 1413.82 cm^{-1} and 1377.17 cm^{-1}. While the C-H

bending with CH_2 type shown at 1462.04 cm^{-1}. Table 4.7 summarizes these functional groups and its wave number.
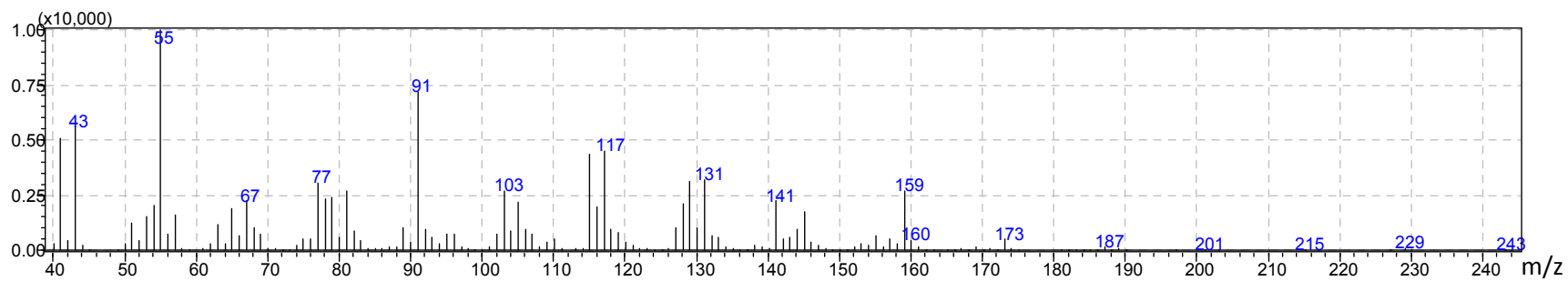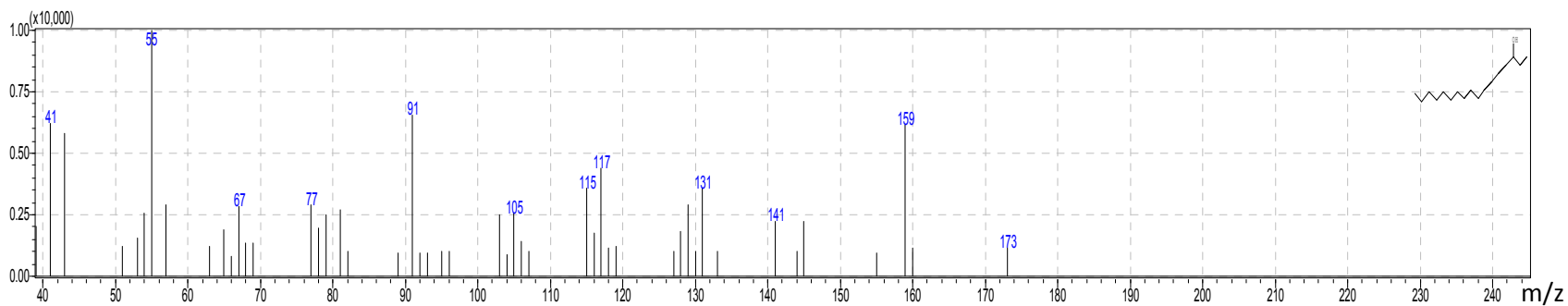
A

B

Figure 4.10 The MS spectrum shows the fragmentation pattern of L1 after bombarded with a beam of electron from electron ionization and the molecular weight. The molecular of fragment of L1 was scanned by the detector from 40 m/z to 550 m/z under scan mode. The spectrum A = L1 and B = falcarinol. The structure similarity between L1 and Falcarinol is 95%.

Figure 4.11: The UV visible spectrum of L1 was measured in 99.8% methanol has one major peak at 198 nm and three minor peaks at 230, 242 and 256 nm.
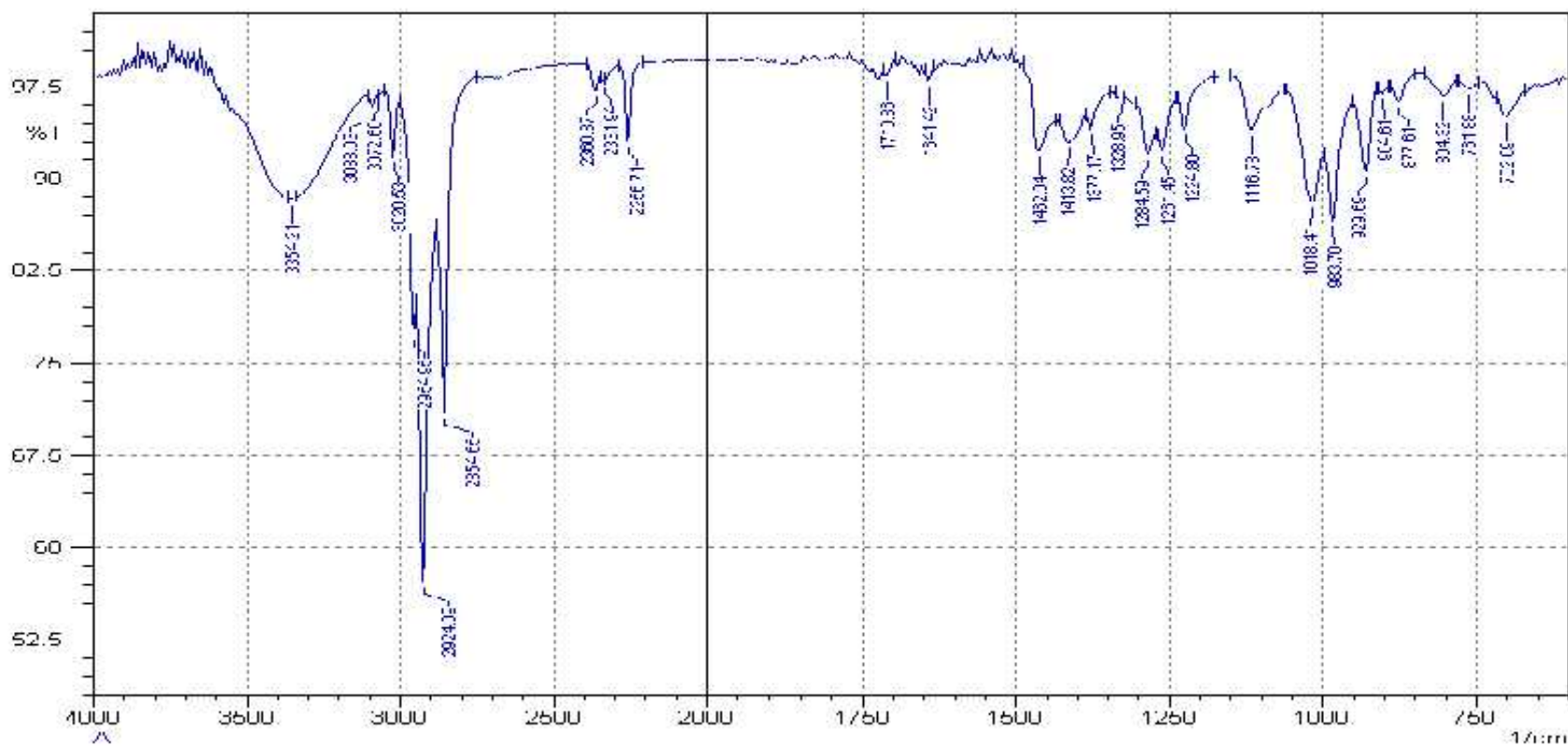
Figure 4.12: The FTIR spectrum shown wavenumber of functional group which applied at L1. L1 was dissolved by 99.8% methanol and analysis under FITR (IR Prestige-21 Model, Shimadzu. Japan). The IR spectrum of L1 was generated and analysed by the IRsolution software.

Table 4.7: Funtional groups present in the FTIR of compound L1

Bond	Compound Type	Frequency from spectrum (cm^{-1})
O – H stretching	Alcohols, phenols	3354.21
C – H stretching	-CH_2 & -CH (cyclic)	3088.03 , 3072.6 , 3020.53
	Alkyl CH_3-	2954.95, 2924.09, 2854.65
$C \equiv C$ stretching	$C \equiv C$ unsymmetrical	2256.71
C=O stretching	aliphatic	1710.86
C=C stretching	$RCH = CH_2$	1641.42
C-H bending	CH_2	1462.04
	CH_3	1413.82, 1377.17
	$RC \equiv CH$, $HC \equiv CH$	1328.95, 1284.59, 1261.45, 1224.8

4.4.2 Nuclear Magnetic Spectrum of L1

The ^{1}H NMR spectrum of L1 (Figure 4.13) shows one hydroxyl group (OH) at δ 4.90, which was assigned to the C-3 position. The two doublet signals with δ 5.25 (2H, J =10.4 Hz) and δ 5.48 (2H, J = 17.08 Hz) were assigned to the ethylene group at C-1 position. The H with the higher couple constant value (J = 17.08 Hz) was assigned the trans position, while the H with the lower couple constant value (J = 10.4 Hz) was assigned the cis position. The doublet signal at δ 3.03 (3H, J = 6.72 Hz) corresponded to the methyl group at position C-8. The methane hydrogen at C-2 position was assigned as doublet of a doublet at δ 5.93 (2H, J = 17.08, 9.76 and 5.48 Hz) and characteristic of methane hydrogen was deshielded by the anisotropy of the adjacent double bond. The multiplet with chemical shift from 1.26 – 1.35 was assigned to the 4 methylene groups from C-12 to C-16 position. A triplet and quintet signals at δ 0.87 (3H, J = 7.32) and δ 2.00 (2H, J = 7.32) was assigned to methyl group at C-17 and methylene group at C-11 position respectively. The last two double triplet signals at δ 5.38 (1H, J = 11.0, 6.72 Hz) and δ 5.51 (1H, J = 11.0, 7.0 Hz) were assigned to the ethylene group at C-9 and C-10 position.
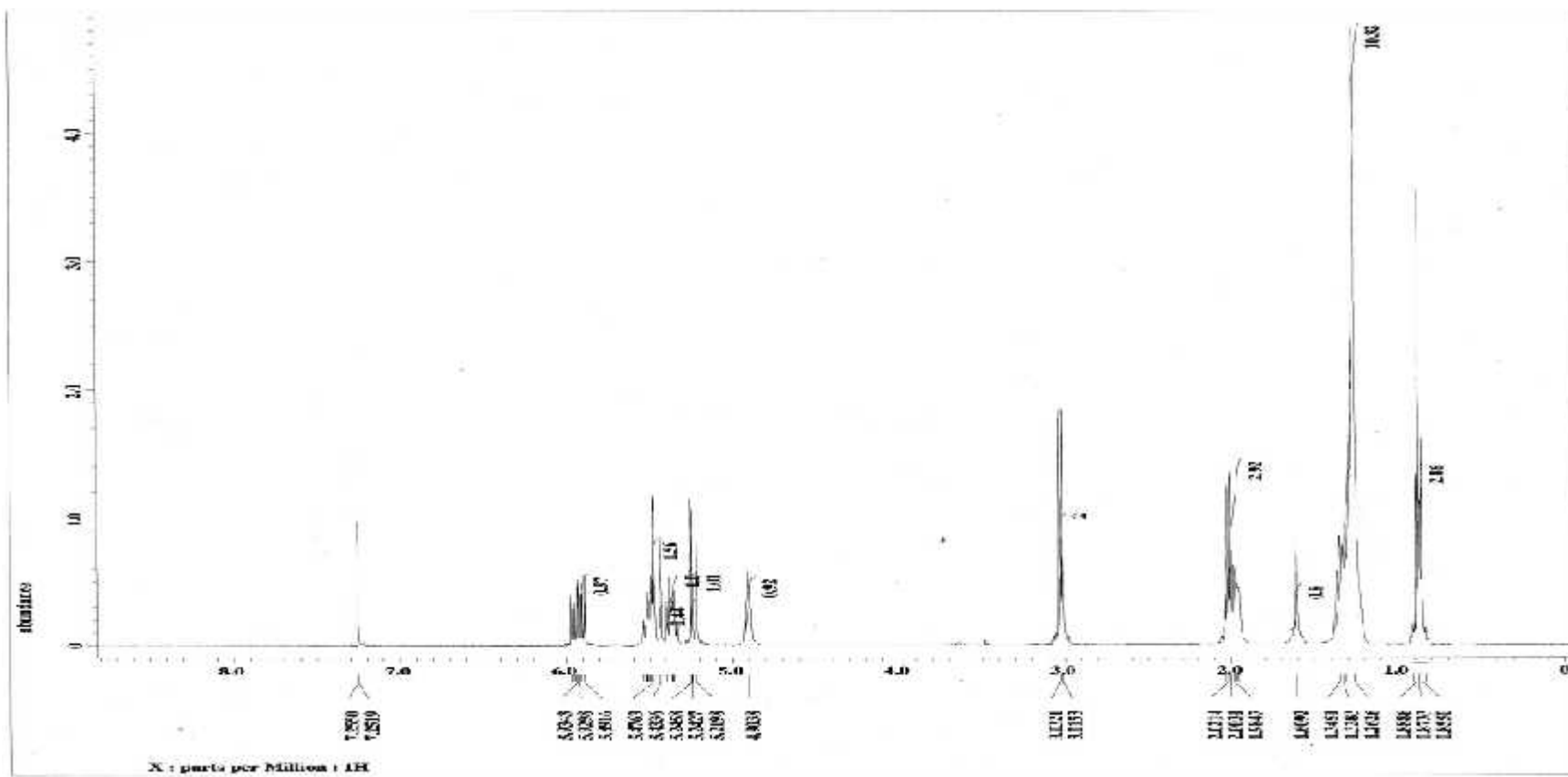
Figure 4.13: The ^{1}H NMR spectrum of L1 in deuterochloroform (400 MHz).

The ^{13}C NMR spectrum of L1 (Figure 4.14) showing 5 signals at δ 29.32, δ 29.27, δ 29.25, δ 31.9 and δ 22.8 were assigned to methylene group from C-12 to C-16 position. Another two signals appeared at δ 27.3 and δ 17.8 were assigned to methylene group located at C-11 and methyl group located at C-8 position respectively. Two ethylene groups at C-9 and C-10 gave the signal at δ 122 and δ 133.2. Three ethyne groups occurred at δ 74.3, δ 71.4 and δ 80.4 were assigned to C-4, C-5 and C-7 position, respectively. The signal with δ 14.2 assigned to methyl group at C-17 position. The vinyl group and the methylene group located at C-1 and C-2 position with δ 117.2 and δ 136.2, respectively. The methanol group at δ 63.6 was allocated to C-3.

The HMQC spectrum of L1 (Figure 4.16) shows ^{1}H NMR spectrum on the top and ^{13}C NMR spectrum along the right side. The H-1a (δ 5.25) and H-1b (δ5.48) had HMBC correlate with C-3 (δ63.6), while the H-8 (δ 3.03) had high HMBC correlation with C-5 (δ 71.4), C-6 (δ 64.1), C-7 (δ 80.4), C-9 (δ 122) and C-10 (δ 133.2). The high HMBC correlation occurred in between H-11 (δ 2.0), C-9 (δ 122), C-10 (δ 133.2) and C-122 (29.3). The H-12 -16 (δ 1.25 − 1.33) had HMBC correlated with C-12 -14 (δ 29.3), C-15 (δ 31.9) and C-17 (δ 14.2). Besides, the H-17 correlated with C-15 (δ 31.9) and C-16 (δ 22.8). The summary of data from 1D and 2D NMR spectrums of L1 compound are shown at Table 4.8.
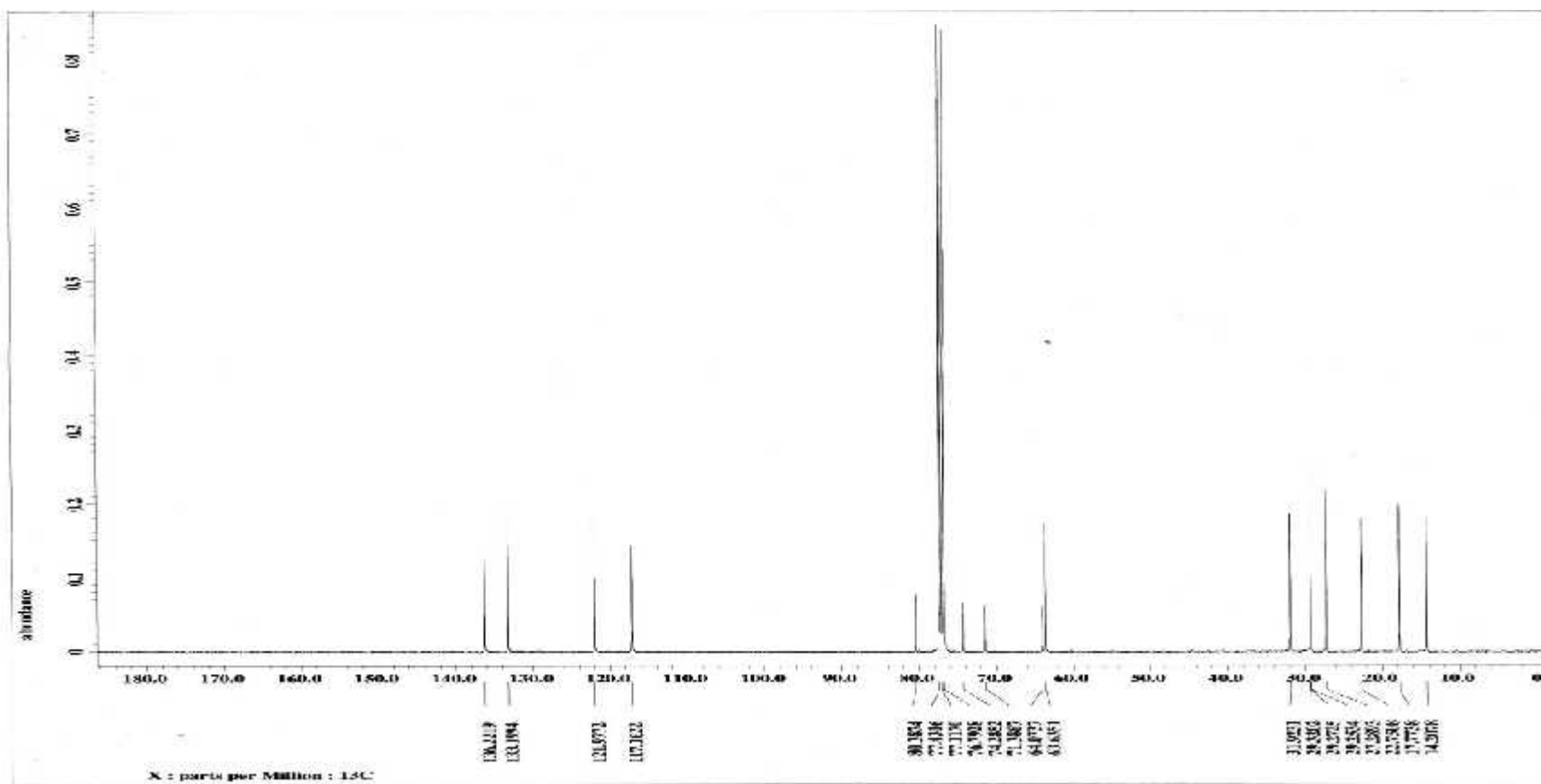
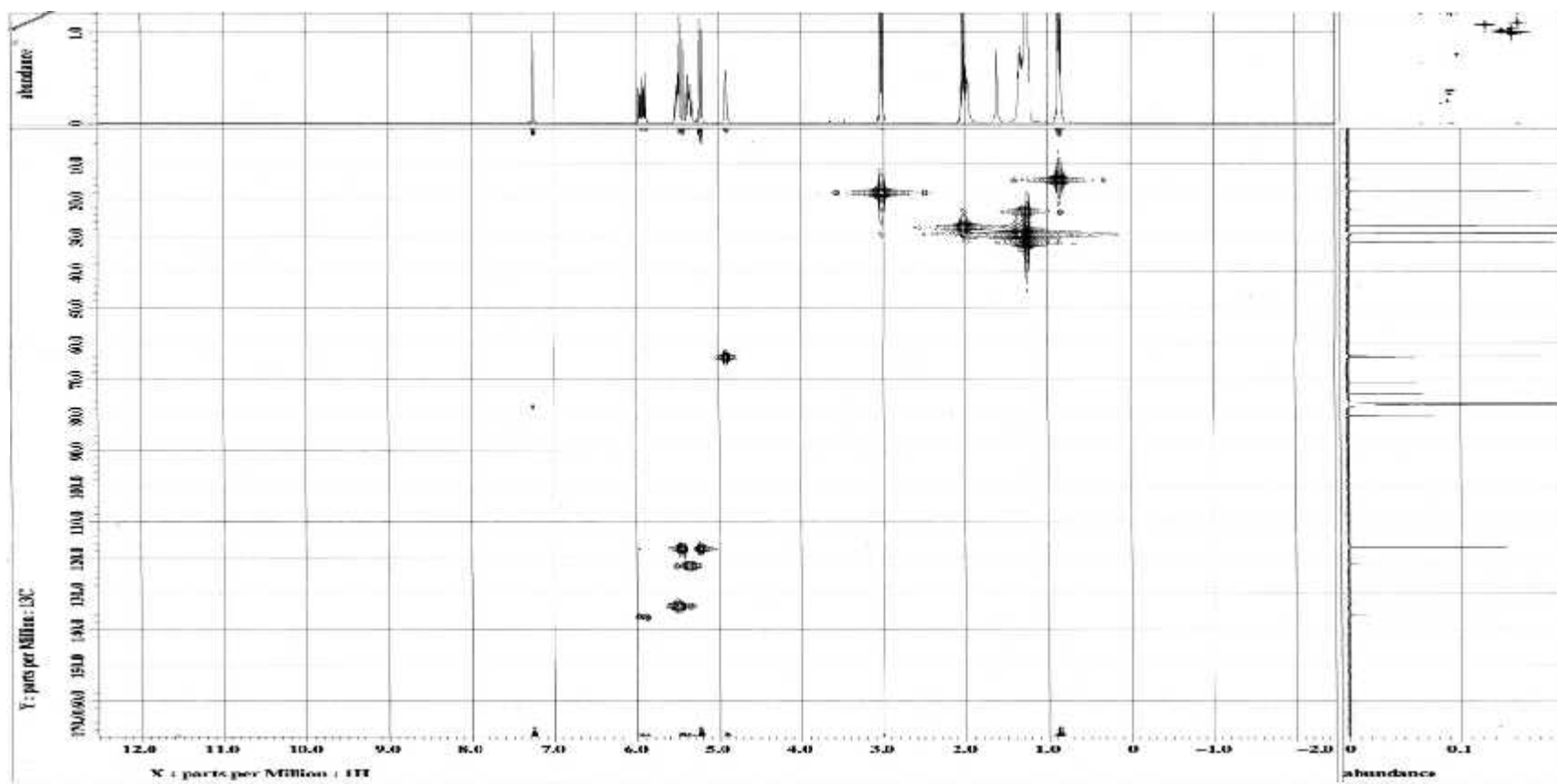Figure 4.14: The ^{13}C NMR of L1 in deuterochloroform (400 MHz).

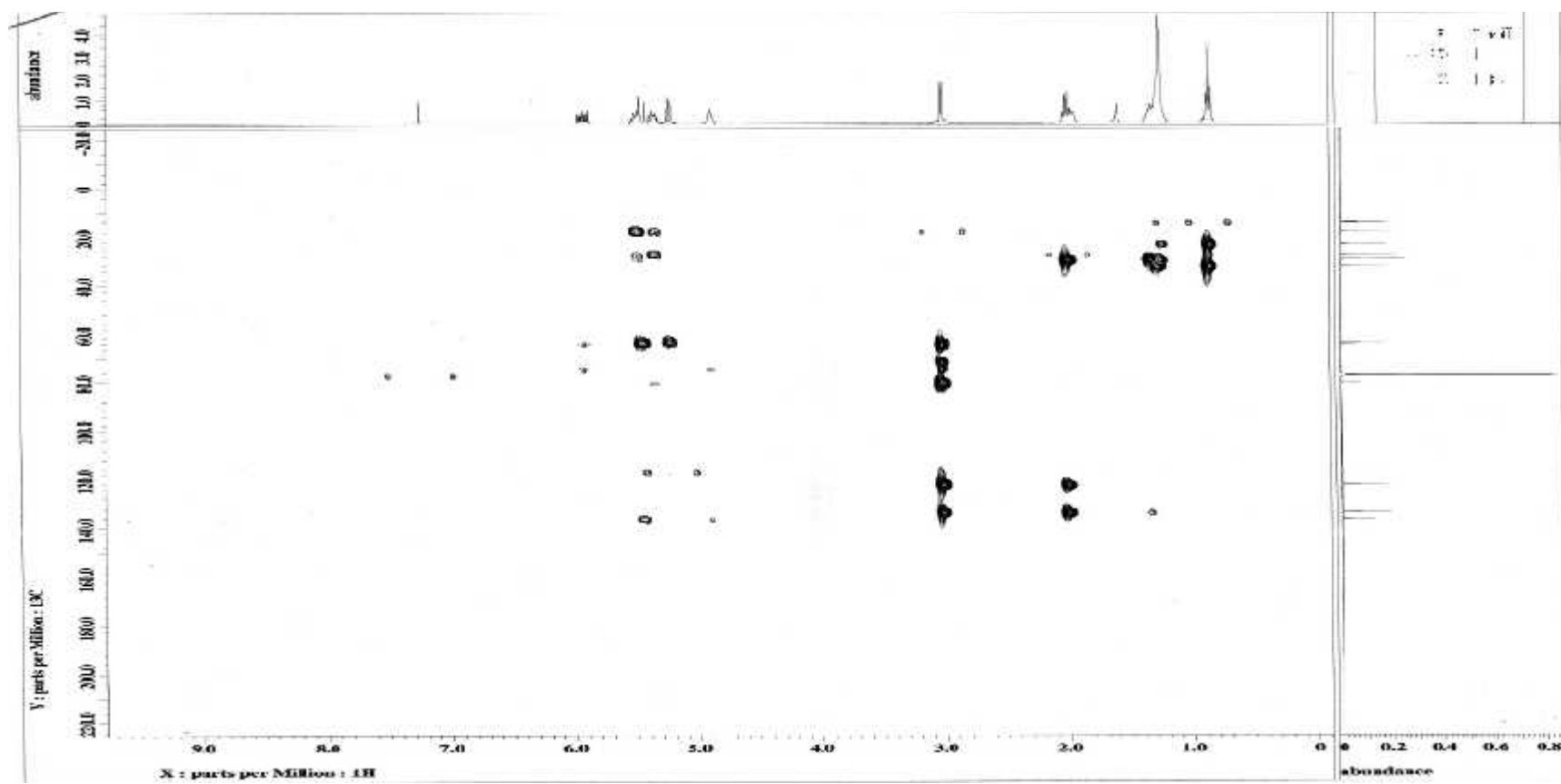Figure 4.15: The HMBC spectrum of L1 in deuterochloroform (400 MHz).

Figure 4.16: The HMQC spectrum of L1 in deuterochloroform (400 MHz).

Table 4.8: Proton chemical shift, carbon chemical shift, HMQC interaction and HMBC interaction of L1 compound.

Position	Carbon Character	^{13}C NMR (400Mhz)	^{1}H NMR(400Mhz)	HMBC
1	$H_2C=$	117.2	1a. 5.25 d (1H) J= 10.4 1b. 5.48 d (1H) J= 17.08	C - 3
2	CH=	136.2	5.93 ddd (1H) J=17.08 ,9.76,5.48	
3	-CH, OH	63.6	4.90 (1H)	
4	-C≡C-	74.3		
5	-C≡C-	71.4		
6	-CH	64.1		
7	-C≡C-	80.4		
8	$-CH_2C≡$	17.8	3.03 d (2H) J= 6.72	C – 5, C – 6, C – 7, C – 9, C - 10
9	CH= CH	122	5.38 dt (1H) J= 11.0, 6.72	
10	CH= CH	133.2	5.51 dt (1H) J= 11.0, 7.0	
11	CH_2	27.3	2.00 q (2H) J= 7.32	C – 9 , C – 10, C - 12
12	CH_2	29.3	1.26 - 1.35 m (10 H)	C-11
13	CH_2	29.3	1.26 - 1.35 m (10 H)	C-12
14	CH_2	29.3	1.26 - 1.35 m (10 H)	C-13
15	CH_2	31.9	1.26 - 1.35 m (10 H)	C-14, C-17
16	CH_2	22.8	1.26 - 1.35 m (10 H)	C-15, C-17
17	$H-CH_3$	14.2	0.87 t (3H) J=7.32	C – 15, C – 16

Combining the FTIR, MS, NMR spectrum data above and compared of the ^{1}H NMR (Table 4.9) and [13] C NMR data (Table 4.10) with the literature values of panaxynol (Yang et. al., 2008). The L1 compound still cannot assigned as falcarinol or panaxynol. Besause both of the compounds are enantiomer of each other and possessed same ^{1}H NMR, ^{13}C NMR and 2D NMR spectrum. Zhang and his team mates (1999) able to distinguish between two compounds based on their optical rotation. The falcarinol possessed negative optical rotation, while panaxynol possessed positive optical rotation. The L1 compound possessed positive optical rotation. So, the L1 compound declared as panaxynol ((3S)-heptadeca-1,9(Z)-diene-4,6-diyne-3-ol).   The numbering follows the IUPAC convention. Protons are numbered starting from the first carbon at the left hand side. The structure of panaxynol is shown in Figure 4.17.

Table 4.9: Proton chemical shift and couple constant of L1 compared with Panaxynol obtained from literature values.

Position	Proton Character	Yang, et. al. (2008) in 500Mhz	L1 compound in 400Mhz
1a	Vinyl $CH_2=$	5.24 d (1H) J= 10.1	5.25 d (1H) J=10.4
1b	-CH=CH-	5.46 d (1H) J= 17.1	5.48 d (1H) J=17.08
2	Vinyl , $CH_2=CH_2$	5.94 ddd (1H) J= 17.1, 10.1, 5.1	5.93 ddd (1H) J=17.08 ,9.76,5.48
3	CHOH	4.91 t (1H) J= 5.1	4.90 (1H)
8	$\equiv CCH_2$-CH=	3.03 d (2H) J= 6.9	3.03 d (2H) J= 6.72
9	-CH=CH-	5.37 dt (1H) J= 10.6, 6.9	5.38 dt (1H) J= 11.0, 6.72
10	-CH=CH-	5.51 dt (1H) J= 10.6, 7.1	5.51 dt (1H) J= 11.0, 7.0
11	=CH-CH_2-	2.02 q (1H) J= 7.1	2.00 q (2H) J= 7.32
12-16	CH_2	1.25-1.33 m (10H)	1.26 - 1.35 m (10 H)
17	CH_3	0.88 t (3H) J= 7.0	0.87 t (3H) J=7.32

Table 4.10: Carbon chemical shift of L1 compared with Panaxynol obtained from literature values.

Position	Carbon Character	Yang, et. al. (2008) in 500Mhz	L1compound in (400Mhz)
1	$H_2C=$	117.2	117.2
2	$CH=$	136.4	136.2
3	$-CH, OH$	63.7	63.6
4	$-C≡C-$	74.5	74.3
5	$-C≡C-$	71.5	71.4
6	$-CH$	64.2	64.1
7	$-C≡C-$	80.5	80.4
8	$-CH_2C≡$	17.9	17.8
9	$CH= CH$	122.1	122
10	$CH= CH$	133.3	133.2
11	CH_2	27.4	27.3
12	CH_2	29.4	29.3
13	CH_2	29.4	29.3
14	CH_2	29.3	29.3
15	CH_2	32.0	31.9
16	CH_2	22.8	22.8
17	$H-CH_3$	14.3	14.2
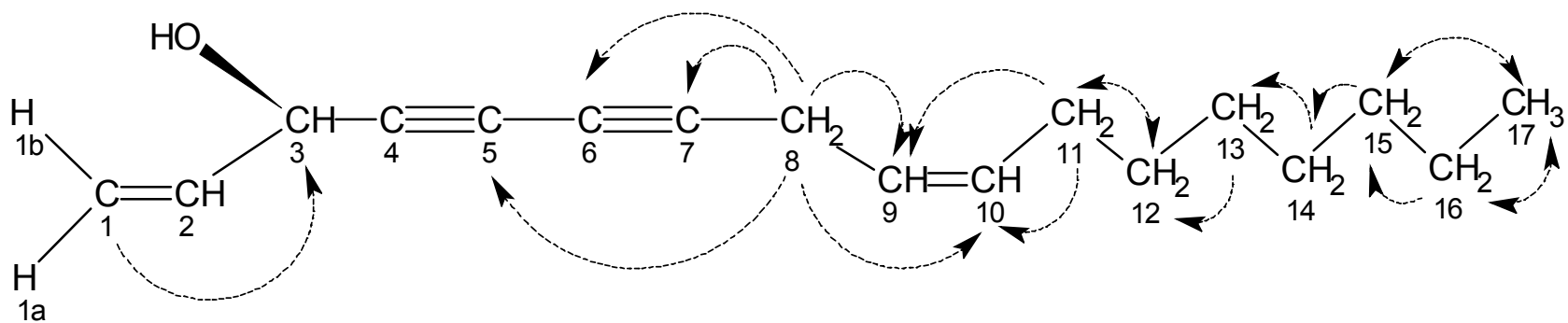
Figure 4.17: Molecular structure of L1 showing the numbering of the carbon. The HMBC correlations are shown by arrow. The L1 is postulated to be Panaxynol ((3S)-heptadeca-1,9(Z)-diene-4,6-diyne-3-ol).

4.5 Structure Elucidation of C1

Compound C1 is dark brown in colour and exists as an amorphous form. The molecular weight of C1 is 244 m/z. MS fragmentation pattern is shown in Figure 4.19. The fragmentation pattern of C1 compared with the database in the library of GC software and has 79 % similarity with octanoic acid. The UV spectrum measured in 99.8 % purity of methanol has one major peak at 203 nm and four minor peaks at 241, 254, 268 and 284nm (Figure 4.18). The minute amount of C1 compound did not allow further analysis on FTIR and ^{1}H and ^{13}C NMR.
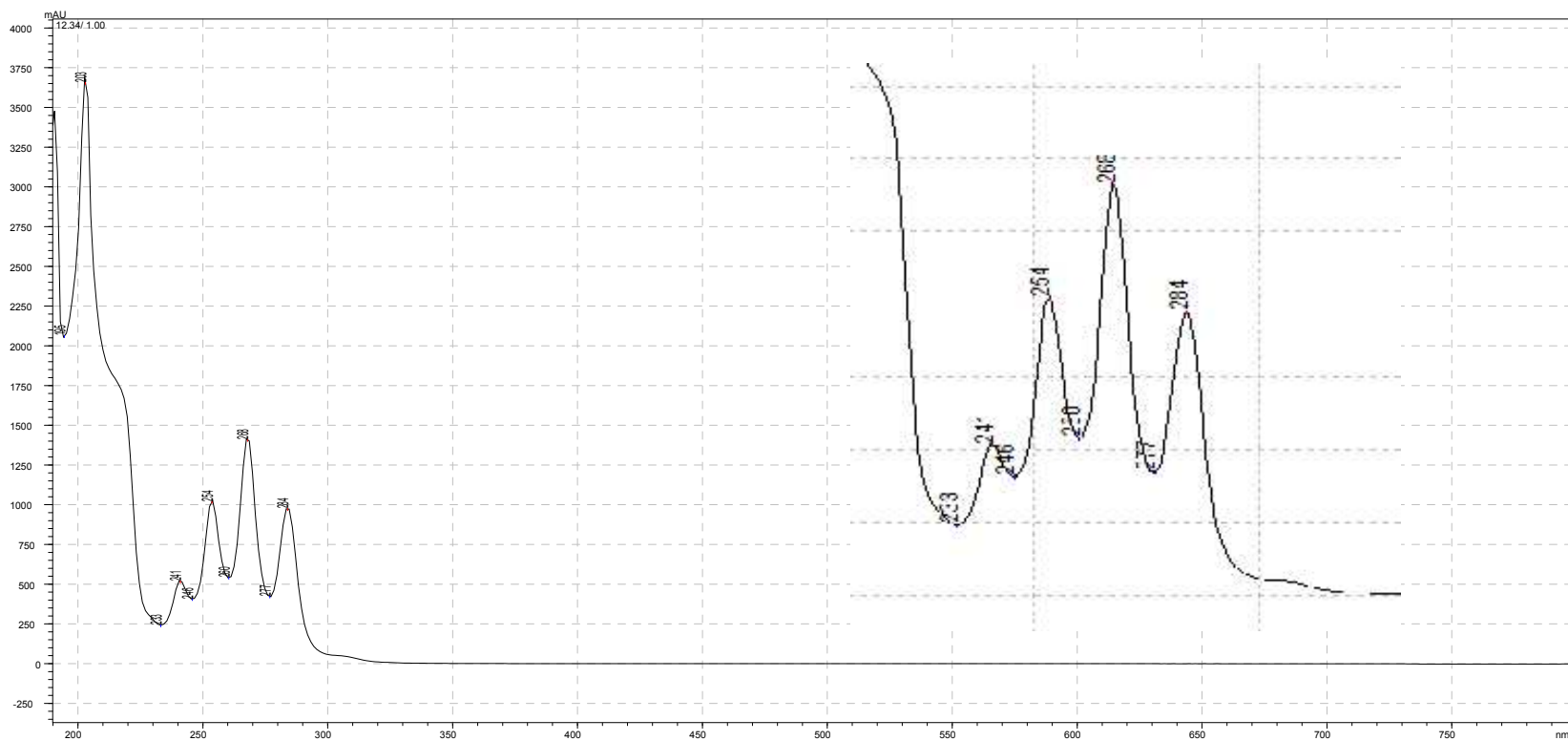
Figure 4.18: The UV visible spectrum of C1 was measured in 99.8% methanol and has one major peak at 203nm and four minor peaks at 241, 254, 268 and 284 nm.
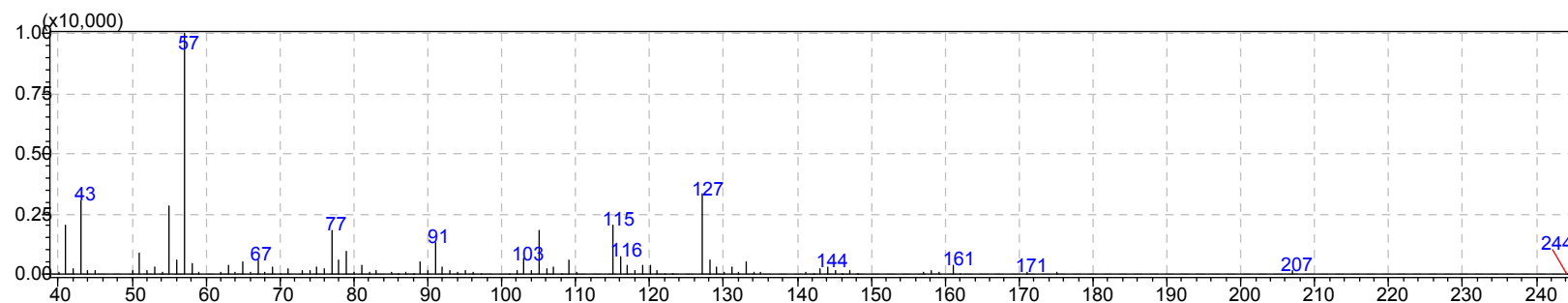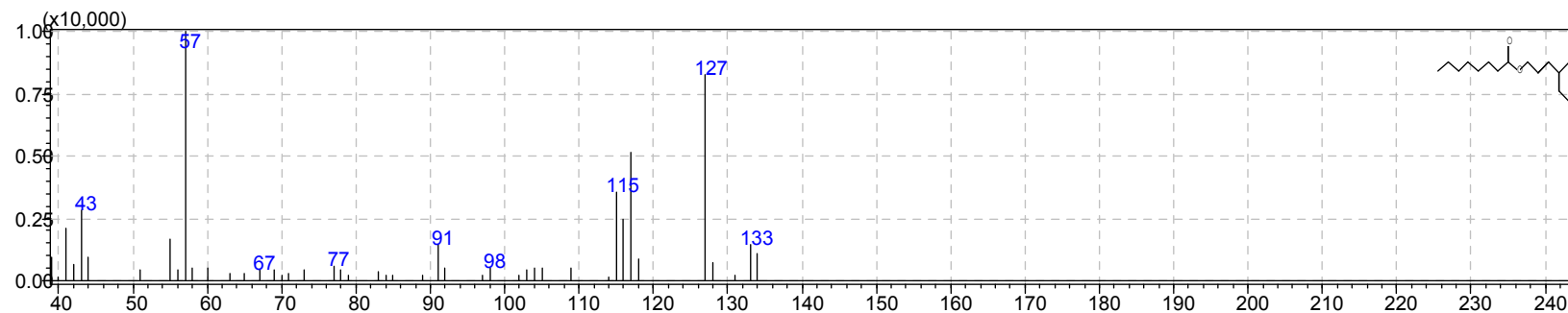
Figure 4.19: The MS spectrum shows the fragmentation pattern of C1 after bombarded with a beam of electron from electron ionization and the molecular weight. The molecular of fragment of C1 was scanned by the detector from 40 m/z to 550 m/z under scan mode. The spectrum A = C1 and B = octanoic acid. The structure similarity between C1 and octanoic acid is 79%.

4.6 Cytotoxicity of L1 (Panaxynol) and C1

The cytotoxic effect of L1 (panaxynol) and C1 against K-562 cell lines was determined using the MTT assay and the IC_{50} value was obtained. The IC_{50} values were compared with cisplatin and doxorubicin. The IC_{50} values of L1 (panaxynol), C1, cisplatin and doxorubicin against the K-562 were 13.9 μM, 34.22 μM, 14.13 μM and 0.19 μM, repectively. The cell killing curves of L1 (panaxynol), C1, cisplatin and doxorubicin are shown in Figures 4.20, 4.21, 4.22, 4.23. Based on the IC_{50} values of these drugs, the cytotoxic effect of doxorubicin against K-562 cell was much higher compared with L1 (panaxynol), C1 and cisplatin. The cytotoxic effect of L1 (panaxynol) was higher than cisplatin. The cytotoxicity of L1 (panaxynol), C1, cisplatin and doxorubicin are reflected in the changes in morphology of K-562 cells, like membrane damage, apoptotic cells and necrotic cells as seen in Figure 4.24 - Figure 4.27. For all the treatments, increasing concentration of drugs led to an increase number of death cells, debris and decreased the number of viable cells.
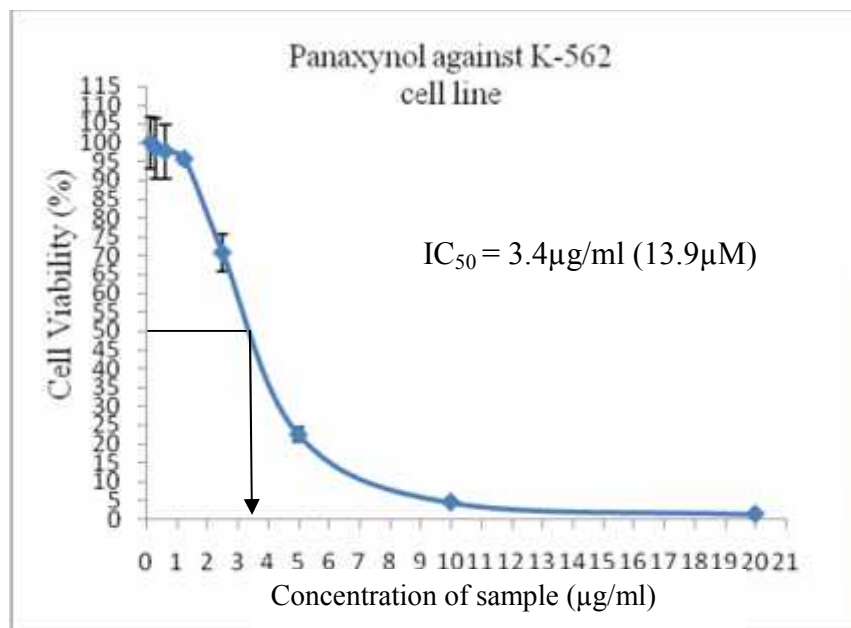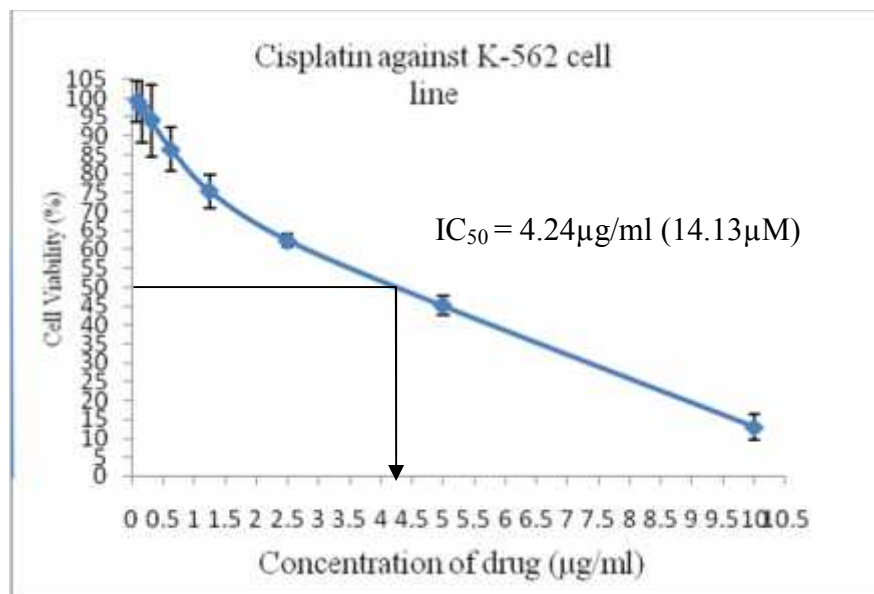
Figure 4.20: Cell killing curve of panaxynol. Cytotoxicity was determined using MTT assay after 72 hours incubation with 8 concentrations of panaxynol. Data points represent the mean of 3 individual experiment. The IC_{50} value was determined directly from the graph.
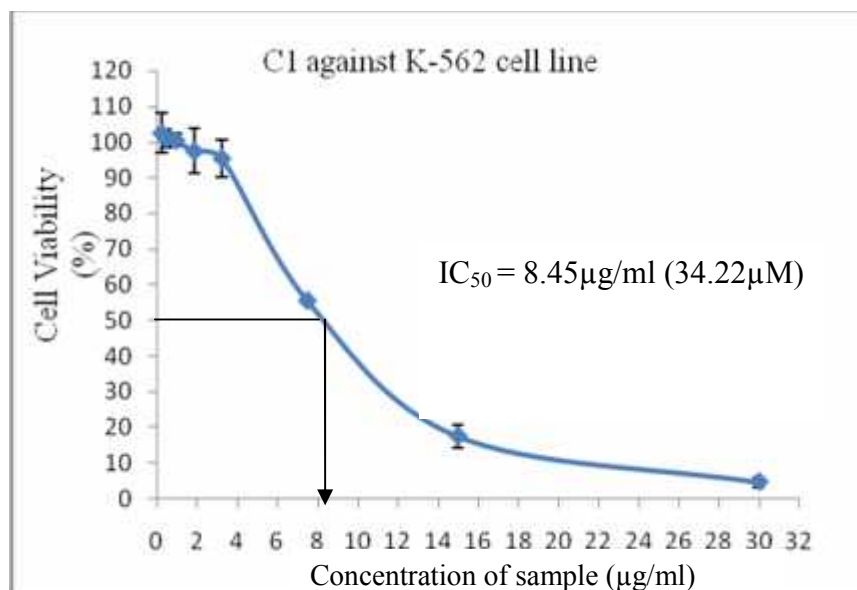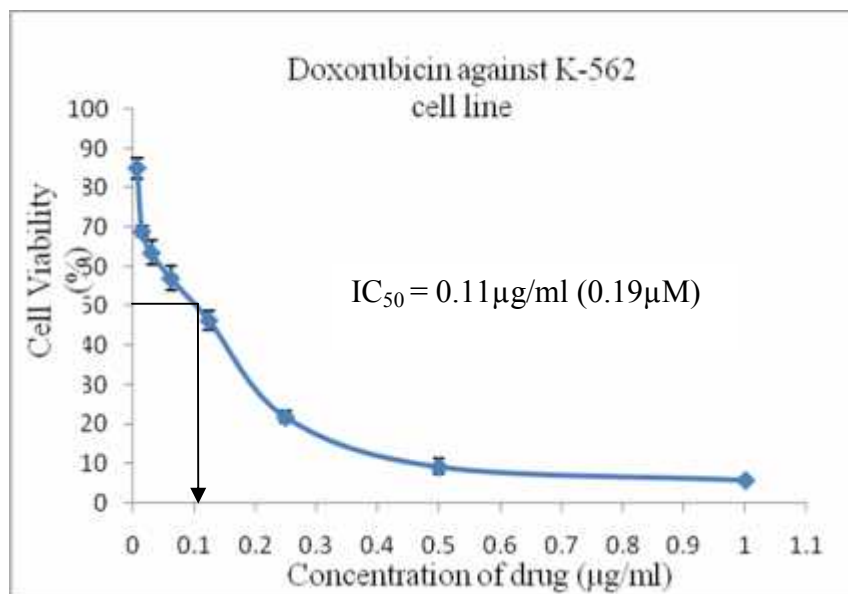

Figure 4.21: Cell killing curve of C1 compound. Cytotoxicity was determined using MTT assay after 72 hours incubation with 8 concentrations of C1 compound. Data points represent the mean of 3 individual experiment. The IC_{50} value was determined directly from the graph.

Figure 4.22: Cell killing curve of cisplatin. Cytotoxicity was determined using MTT assay after 72 hours incubation with 8 concentrations of cisplatin. Data points represent the mean of 3 individual experiment. The IC_{50} value was determined directly from the graph.
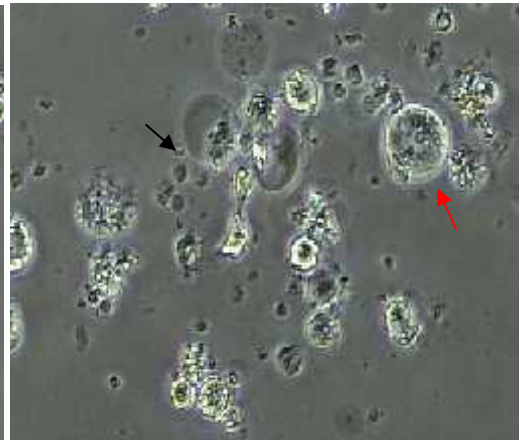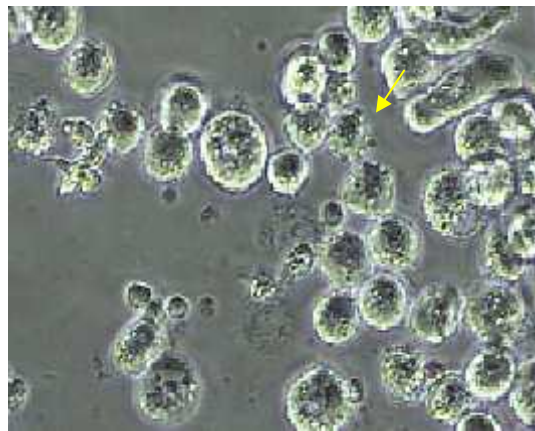

Figure 4.23: Cell killing curve of doxorubicin. Cytotoxicity was determined using MTT assay after 72 hours incubation with 8 concentrations of doxorubicin. Data points represent the mean of 3 individual experiment. The IC_{50} value was determined directly from the graph.
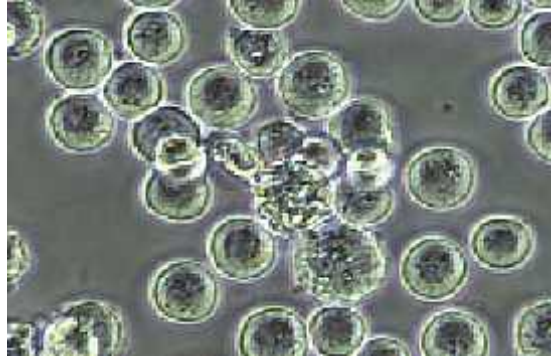
Untreated K-562 cell
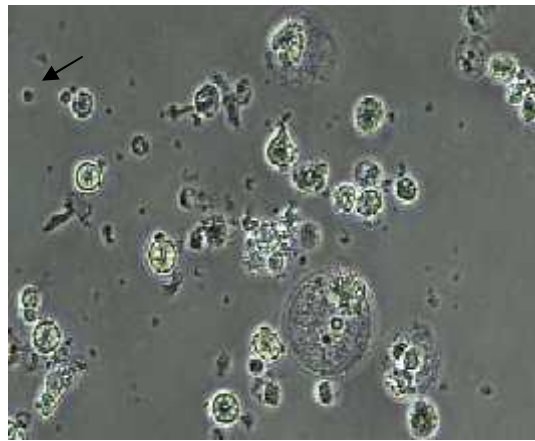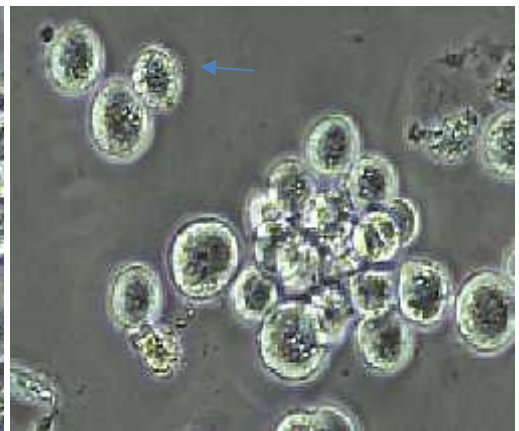
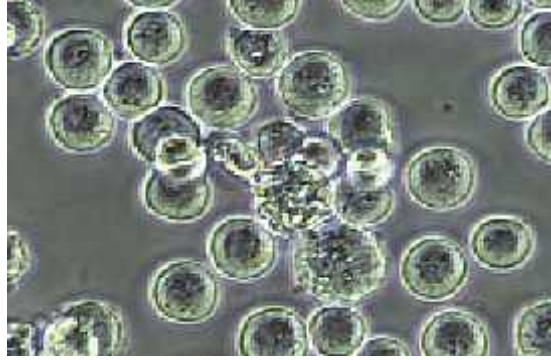Panaxynol 82.0 µM   Panaxynol 41 µM
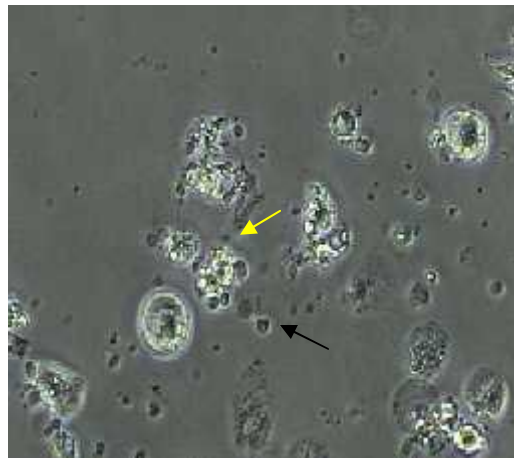
Panaxynol 20.5 µM   Panaxynol 10.25 µM

Figure 4.24: K-562 cells in 200X magnification after treatment with different concentration of panaxynol for 72 hours incubation and the untreated K-562 cells. →: Debris, →: necrotic cell, →: apoptotic cell, →: membrane damage.
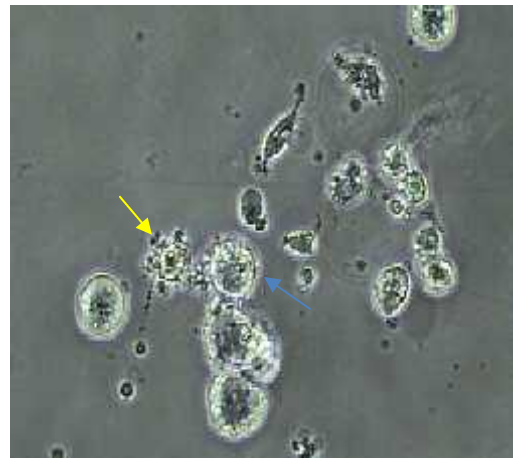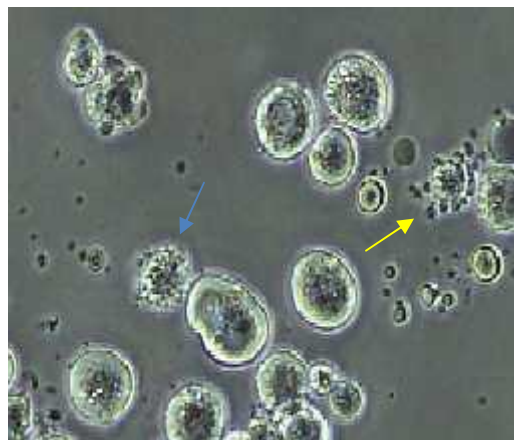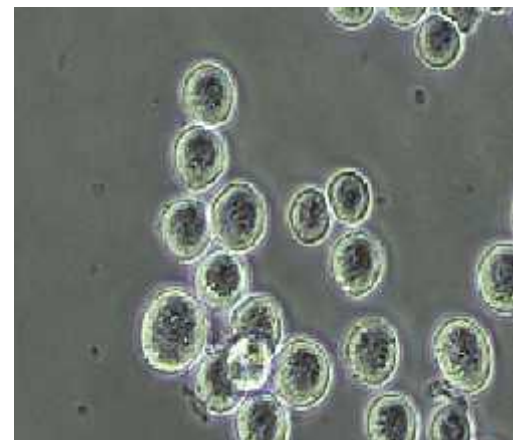
Untreated K-562 cell

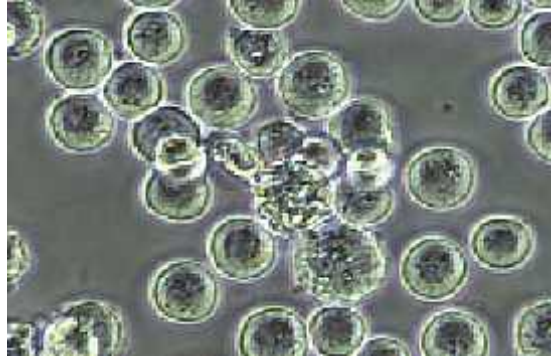C1 30 µg/ml

C1 15 µg/ml

C1 7.5 µg/ml

C1 3.25 µg/ml

Figure 4.25: K-562 cells in 200X magnification after treatment with different concentration of C1 for 72 hours incubation and the untreated K-562 cells.
→: Debris, →: necrotic cell, →: apoptotic cell, →: membrane damage.

Untreated K-562 cell

Cisplatin 33.33 µM

Cisplatin 16.66 µM
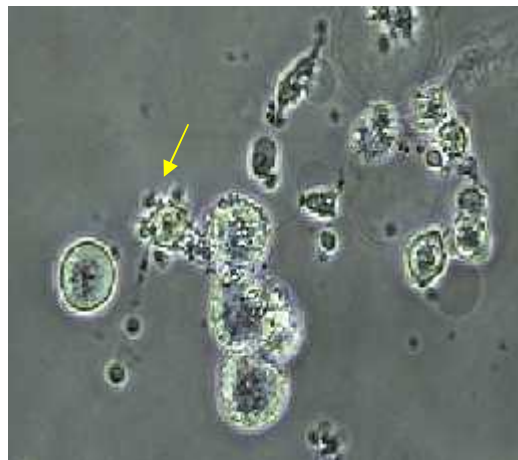
Cisplatin 8.33 µM
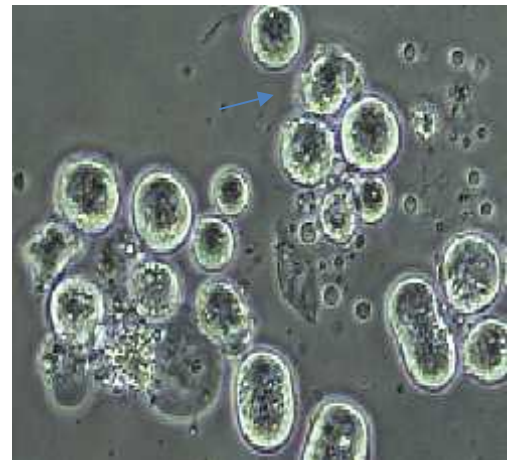
Cisplatin 4.165 µM

Figure 4.26: K-562 cells in 200X magnification after treatment with different concentration of cisplatin for 72 hours incubation and the untreated K-562 cells. →: Debris, →: necrotic cell, →: apoptotic cell, →: membrane damage.
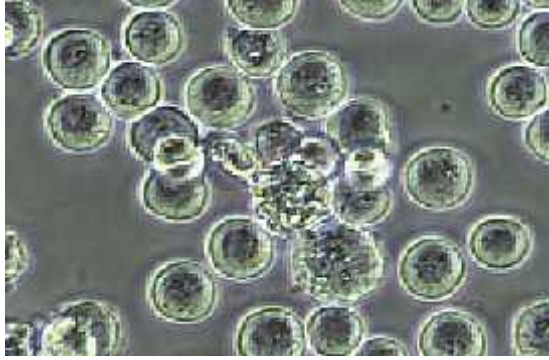
Untreated K-562 cell

Doxorubicin 1.72 µM

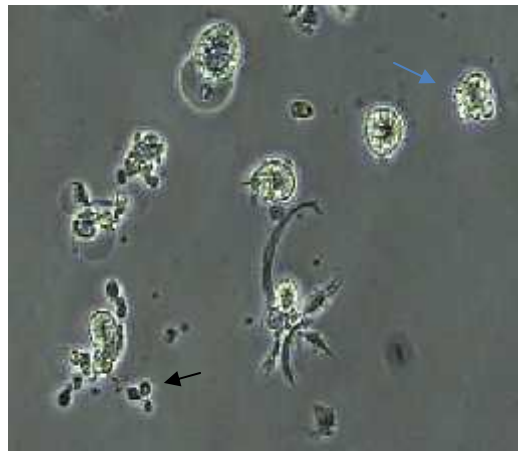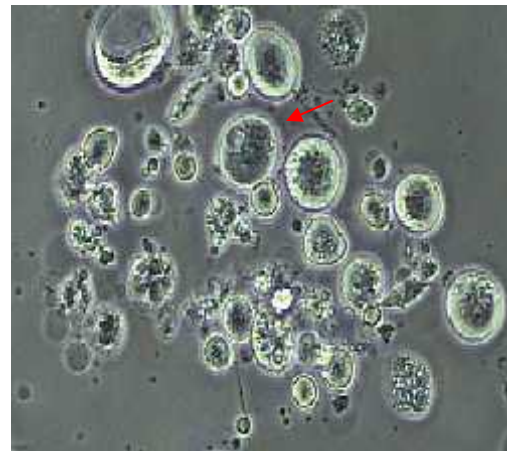Doxorubicin 0.86 µM

Doxorubicin 0.43 µM
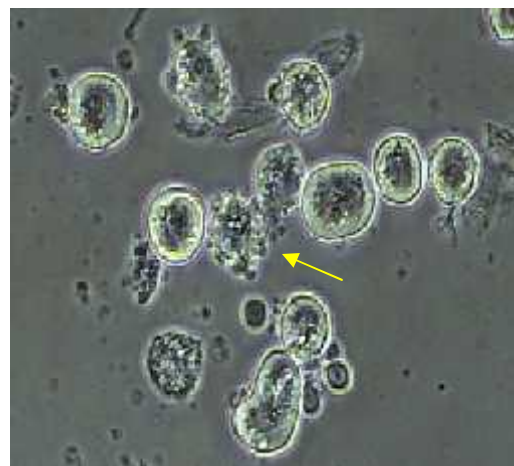
Doxorubicin 0.22 µM

Figure 4.27: K-562 cells in 200X magnification after treatment with different concentration of doxorubicin for 72 hours incubation and the untreated K-562 cells.→: Debris, →: necrotic cell, →: apoptotic cell, →: membrane damage.

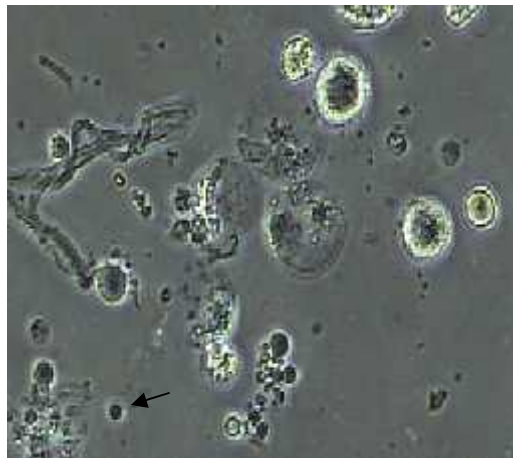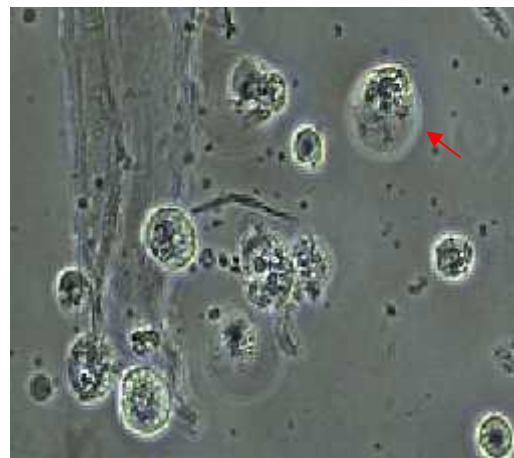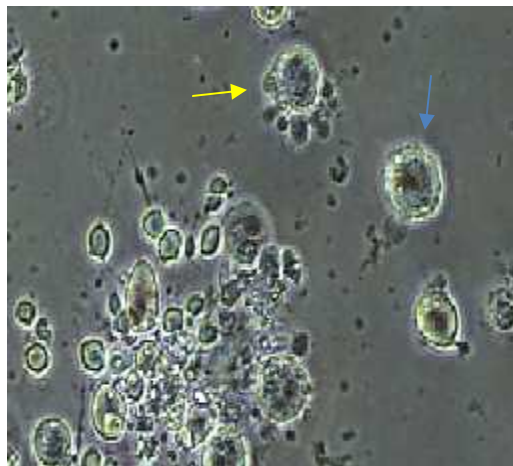## 4.7 Flow Cytometeric Analysis of the Cell Cycle

The DNA content in each cell was determined by PI staining and analysis by flow cytometry. Typically, the first large peak in the histogram represents the cell population at G_0/G_1 while the smaller peak represents cells in the G_2/M phase. G_2/M phase cells have double the amount of DNA and thus has, approximately twice the fluorescence intensity. Replicating cells in S phase have between 2N and 4N amount of DNA.

The histogram and table shown in Figure 4.28 and Table 4.11, represent the distribution of DNA content in the population of untreated K-562 cells and cells treated with IC_{50} and IC_{85} concentrations of panaxynol and IC_{85} concentration of cisplatin, analysed at 12, 24, 48 and 72 hours after treatment. The sub G_0 population of K-562 was treated with IC_{85} concentration of panaxynol increased from 2.99 % at 12 hours incubation to 18.09 % at 72 hours incubation while the S phase population decreased, from 20.91 % at 12 hours incubation to 15.56 % at 72 hours incubation. The population of G_2/M phase cells decreased from 26.36 % at 12 hours incubation to 14.50 % at 48 hours incubation but increased slightly to 16.12 % at 72 hours incubation. The population of G_1 phase cells increased from 51.29 % at 12 hours incubation time to 54.92 % at 48 hours incubation and decreased against to 50.87 % at 72 hours incubation.

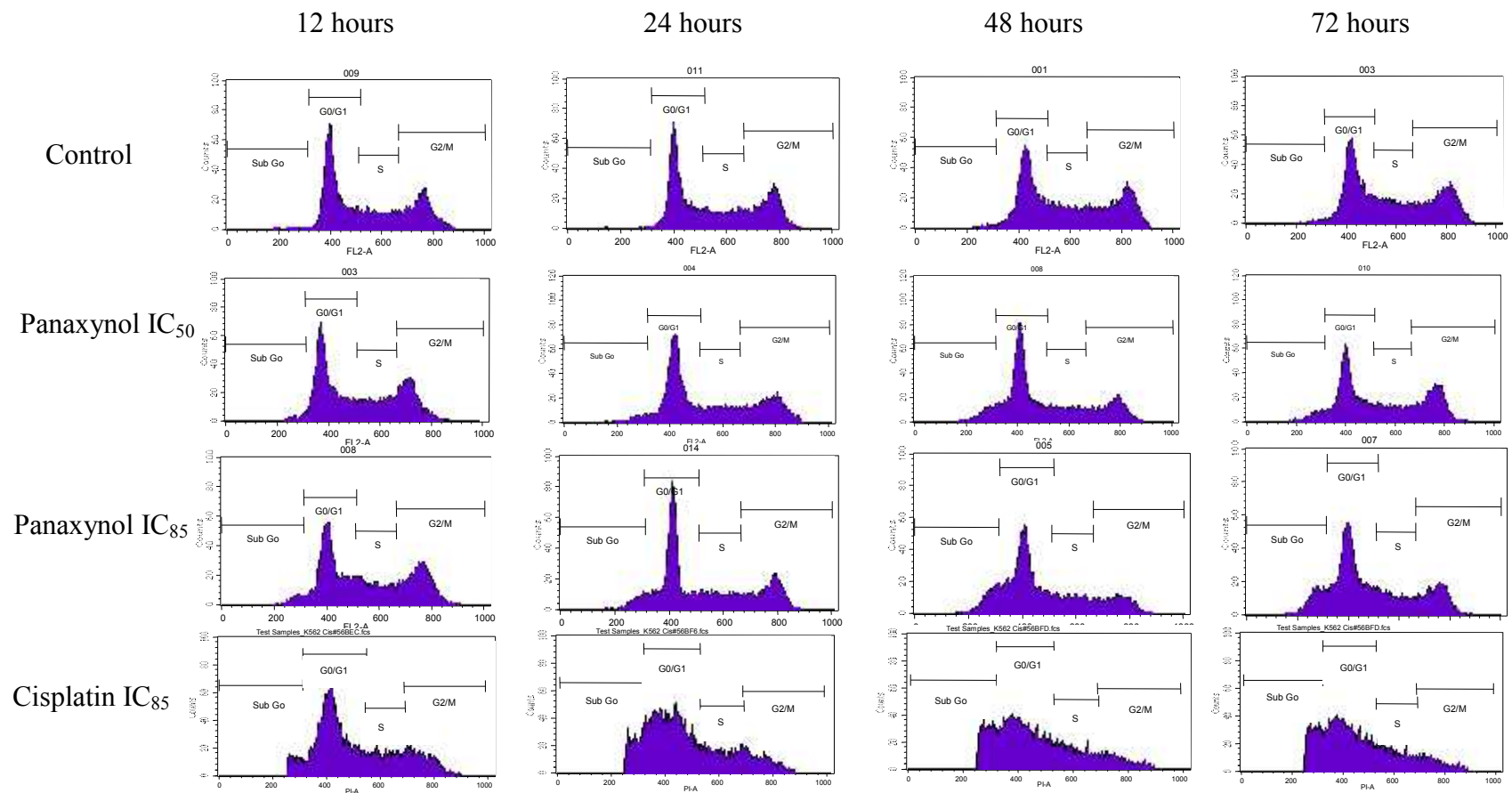Figure 4.28: Flow cytometric determination of DNA content of untreated K-562 and K-562 cell subjected to panaxynol in IC_{50} (13.9 µM) and IC_{85} (24.6 µM) and cisplatin in IC_{85} (32.19 µM). Cells were harvested at 12 hours, 24 hours, 48 hours, and 72 hours. Histograms are representative of three independent experiments.

Table 4.11: Percentage of cell populations of each phase for untreated K-562 cells and K-562 cells treated with Panaxynol in IC_{50} (13.9 µM) and IC_{85} (24.6 µM) and cisplatin in IC_{85} (32.19 µM) in time dependent manner of 12 hours, 24 hours, 48 hours and 72 hours. Datas shown the average of three individual experiment with standard deviation.

Incubation Time (h)	Phase in cell cycle	Control (Untreated cell) (%)	Panaxynol IC_{50} (%)	Panaxynol IC_{85} (%)	Cisplatin IC_{85} (%)
12	Sub G_0	1.71 ± 0.50	2.24 ± 0.33	2.99 ± 0.53	4.15 ± 0.93
	G_0/G_1	46.11 ± 2.34	47.91 ± 3.69	51.29 ± 3.86	61.93 ± 2.19
	S	20.62 ± 1.45	20.75 ± 1.05	20.91 ± 0.69	19.77 ± 1.33
	G_2/M	32.34 ± 2.54	29.89 ± 2.67	26.36 ± 3.63	16.03 ± 1.63
24	Sub G_0	1.17 ± 0.14	4.14 ± 1.87	6.69 ± 0.64	14.85 ± 4.53
	G_0/G_1	47.02 ± 1.56	47.83 ± 4.71	52.21 ± 2.00	55.24 ± 1.65
	S	21.10 ± 1.42	19.03 ± 1.09	18.79 ± 1.97	19.13 ± 1.29
	G_2/M	30.71 ± 3.01	29.65 ± 2.47	23.16 ± 0.48	11.75 ± 3.69
48	Sub G_0	1.39 ± 0.55	7.15 ± 1.72	15.07 ± 2.86	20.08 ± 1.49
	G_0/G_1	47.03 ± 3.14	53.08 ± 2.47	54.92 ± 1.49	55.19 ± 3.60
	S	22.57 ± 1.15	17.36 ± 1.55	16.23 ± 0.57	18.01 ± 2.77
	G_2/M	29.01 ± 2.12	23.20 ± 2.95	14.50 ± 3.18	7.60 ± 2.09
72	Sub G_0	1.27 ± 0.45	5.83 ± 1.90	18.09 ± 4.50	24.36 ± 4.54
	G_0/G_1	47.03 ± 1.95	47.43 ± 2.94	50.87 ± 1.04	54.81 ± 0.59
	S	21.13 ± 0.61	18.23 ± 0.40	15.56 ± 1.20	14.29 ± 2.38
	G_2/M	30.58 ± 3.21	29.34 ± 4.20	16.12 ± 3.59	7.42 ± 2.29

The sub G_0 and G_0/G_1 populations of K-562 cells treated with IC_{50} concentration of panaxynol increased from 2.24 % and 47.91 % at 12 hours incubation to 7.15 % and 53.08 % respectively at 48 hours incubation. However, the populations of sub G_0 and G_0/G_1 cells decreased to 5.83 % and 47.43 % respectively at 72 hours incubation. The population of cells in S phase and G_2/M phase, decreased from 20.79 % and 29.89 % at 12 hours incubation to 17.36 and 23.20 % at 48 hours incubation, but increased slightly to 18.23 % and 29.34 % at 72 hours incubation.

The sub G_0 populations of K-562 cells treated with IC_{85} concentration of cisplatin increased from 4.15 % at 12 hours incubation to 24.36 % at 72 hours incubation. The population of G_0/G_1 phase cell decreased from 61.93 % at 12 hours incubation to 54.82 % at 72 hours incubation. The S and G_2/M phase cells also decreased from 19.77 % and 16.03 % at 12 hours incubation to 14.29 % and 7.42 % respectively at 72 hours incubation.

Panaxynol at IC_{50} and IC_{85} concentrations induced minor cell cycle arrest at G_0/G_1 phase of treated K-562 cells at 48 hours incubation by increasing cell populations at G_0/G_1 phase to 53.08 % and 54.92 % respectively, compared with untreated K-562 cells which maintained G_0/G_1 phase in 47.03 %. The blockage at G_0/G_1 phase of K-562 cells treated at both concentration of panaxynol at 48 hours incubation caused the descreasing cell populations at S phase and G_2/M phase. The S phase

and G_2/M of K-562 cells treated with panaxynol in IC_{50} decreased to 17.36 % and 23.20 %, while the S phase and G_2/M phase of K-562 treated with panaxynol at IC_{85} concentration decreased to 16.23 % and 14.50 % at 48 hours incubation, compared with untreated K-562 which showed the S phase in 22.57 % and G_2/M phase in 29.01 % . Besides, the cisplatin in IC_{85} concentration induced cell cycle arrest at G_0/G_1 phase of K-562 cells at 12 hours incubation, by increasing the G_0/G_1 phase to 61.93 %, compared with untreated K-562 which maintained at G_0/G_1 phase in 46.11 % at 12 hours incubation.

4.8 Flow Cytometeric Analysis of Apoptosis

Apoptosis destroys the asymmetry of the membrane and leads to flipping of phosphatidylserine (PS) from the inner layer to the outer layer of the plasma membrane. External PS can be bound with annexin-V FITC and thus, the extent of apoptosis can be quantified using flow cytometric detection of FITC fluorescence. Double staining with PI allows the distinction between early and late apoptotic cells.

In this study, cells were subjected to panaxynol at IC_{50} and IC_{85} concentrations and cisplatin (as a positive control) at IC_{85} concentration for 4, 8, 12, 16, 24, 48 and 72 hours. Cells were then harvested and stained with annexin-V FITC and PI and analysed immediately by flow cytometer. The X-axis represent FITC fluorescence intensity and Y-axis represent the PI fluorescence intensity. The cell population was gated on forward and side scatter to exclude cell debris and random noise. Data acquisition and analysis were performed using CELLQuest software. The fluorescence intensity distributions are shown in Figure 4.29. The ratio of viable cell (LL), necrosis (UL) and the apoptosis (LR and UR) cells for each time point were extracted from CELLQuest program and tabulated (Table 4.12).

Figure 4.29: K-562 cells subjected to panaxynol IC_{50} (13.9 µM) and IC_{85} (24.6 µM) concentrations and cisplatin IC_{85} (32.19µM) and stained with annexin V- FITC (X-axic) and PI (Y-axis) were analyzed by flow cytometer. Cells were examined at 4, 8, 12, 16, 24, 48 and 72 hours. Viable cell are defined by lower left quadrant (LL), necrotic cell –upper left (UL) quadrant, apoptotic cell – lower right (LR) and late apoptotic cells- upper right (UR). For the purpose of quantification, apoptotic cells are defined by both upper and lower right quadrant. These histograms are representative of 3 independent experiments.

Continued Figure 4.29

Figure 4.29: K-562 cells subjected to panaxynol IC_{50} (13.9 μM) and IC_{85} (24.6 μM) concentrations and cisplatin IC_{85} (32.19μM) and stained with annexin V- FITC (X-axic) and PI (Y-axis) were analyzed by flow cytometer. Cells were examined at 4, 8, 12, 16, 24, 48 and 72 hours. Viable cell are defined by lower left quadrant (LL), necrotic cell –upper left (UL) quadrant, apoptotic cell – lower right (LR) and late apoptotic cells- upper right (UR). For the purpose of quantification, apoptotic cells are defined by both upper and lower right quadrant. These histograms are representative of 3 independent experiments.

Continued Figure 4.29

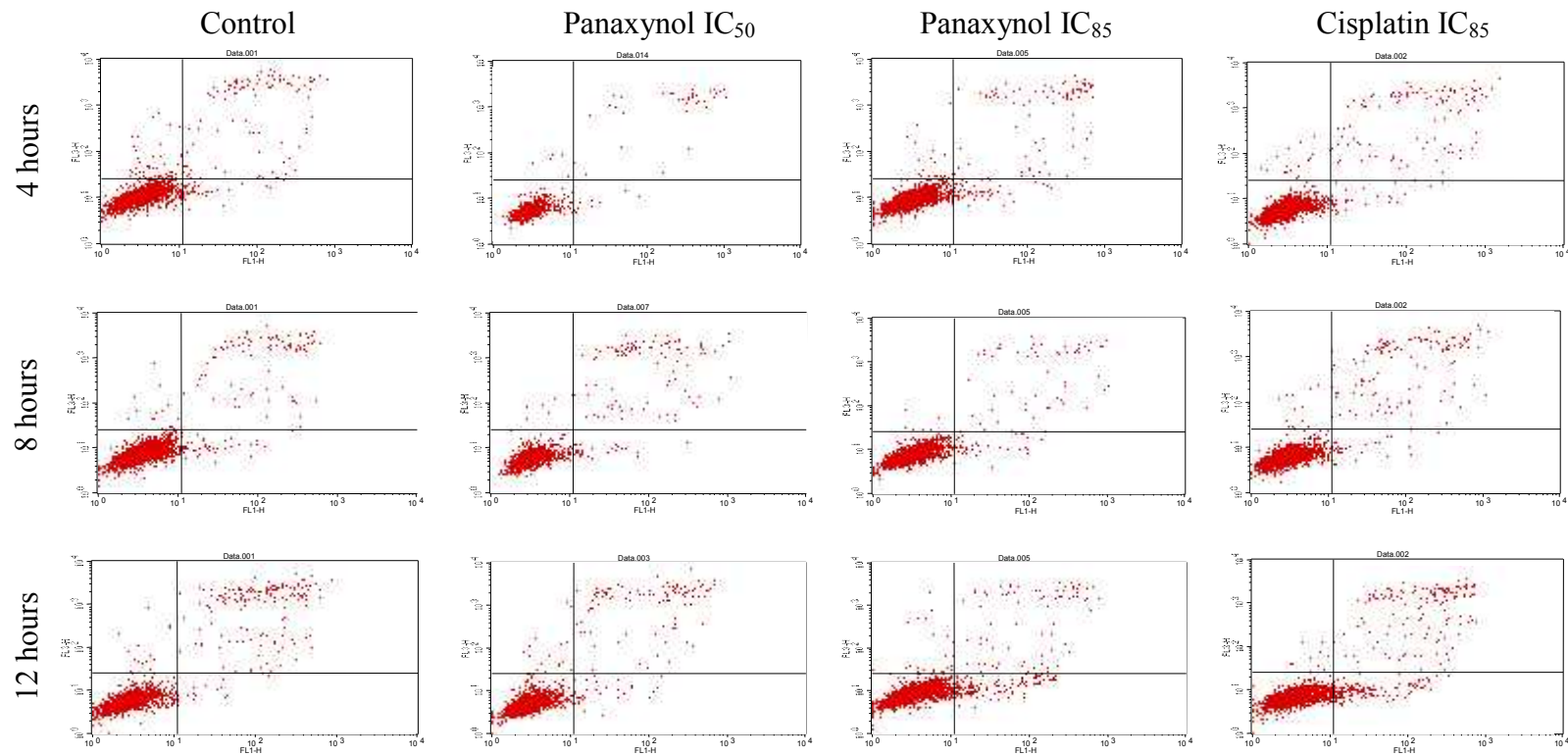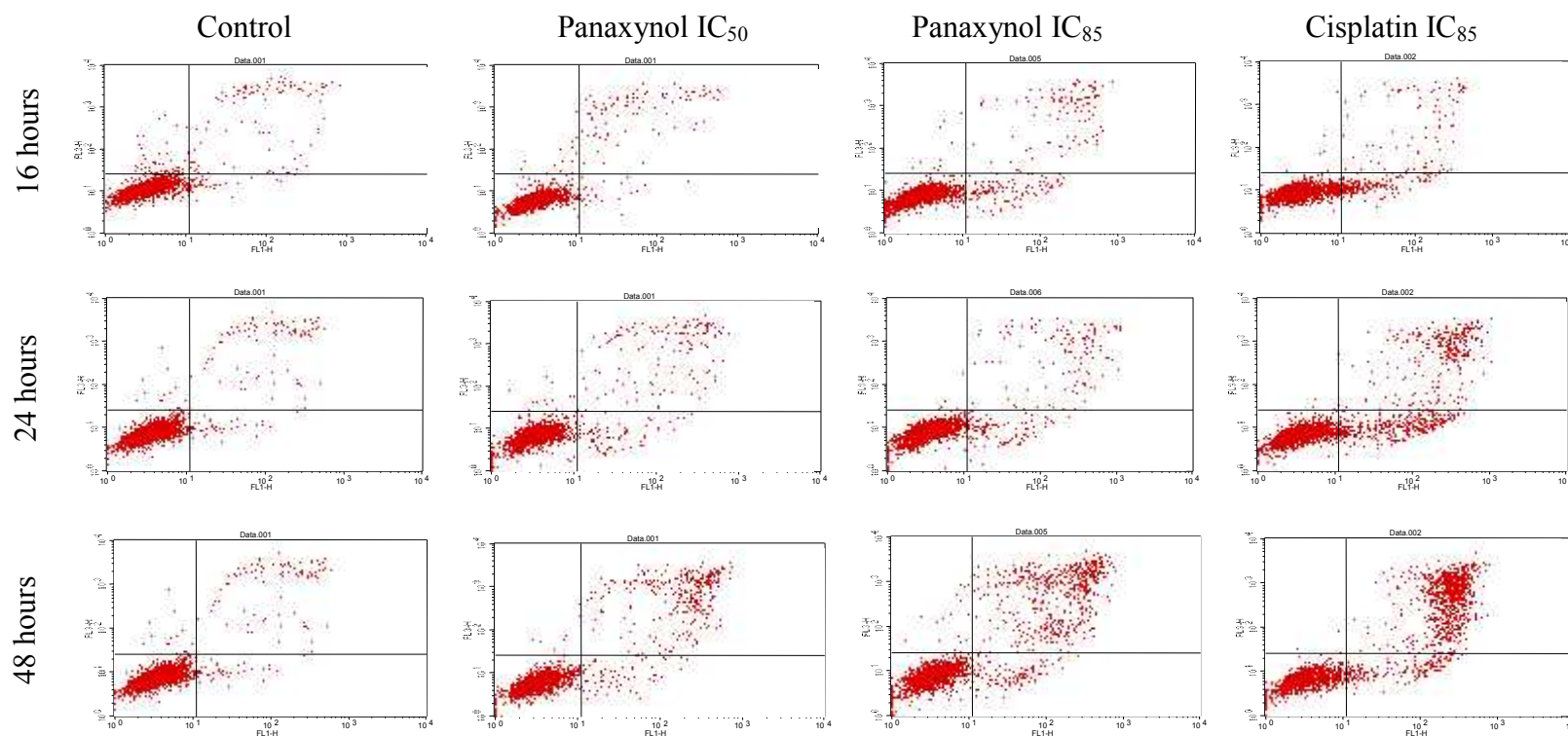| Control | Panaxynol IC$_{50}$ | Panaxynol IC$_{85}$ | Cisplatin IC$_{85}$ |

72 hours

Figure 4.29: K-562 cells subjected to panaxynol IC$_{50}$ (13.9 μM) and IC$_{85}$ (24.6 μM) concentrations and cisplatin IC$_{85}$ (32.19μM) and stained with annexin V- FITC (X-axic) and PI (Y-axis) were analyzed by flow cytometer. Cells were examined at 4, 8, 12, 16, 24, 48 and 72 hours. Viable cell are defined by lower left quadrant (LL), necrotic cell –upper left (UL) quadrant, apoptotic cell – lower right (LR) and late apoptotic cells- upper right (UR). For the purpose of quantification, apoptotic cells are defined by both upper and lower right quadrant. These histograms are representative of 3 independent experiments.

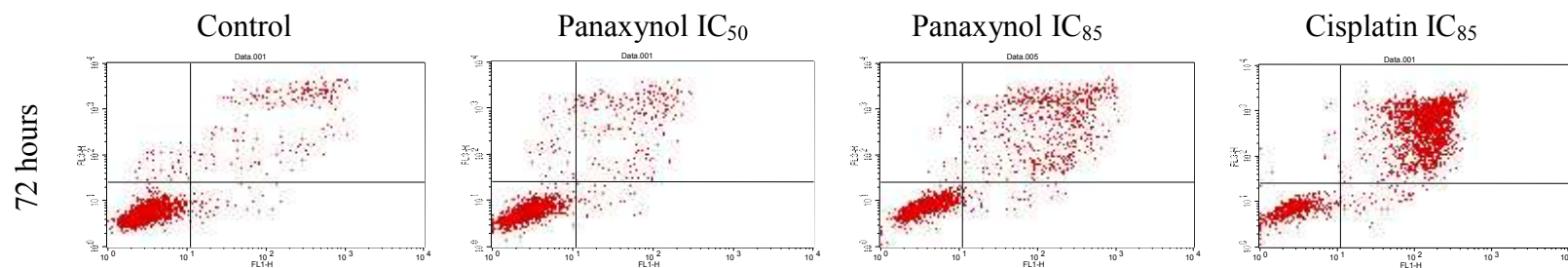Table 4.12: Time course study of K-562 cell populations exposed to panaxynol in IC_{50} (13.9μM) and IC_{85} (24.6μM), cisplatin IC_{85} (32.19μM) and untreated K – 562 cells determined from Annexin V FITC staining which analysis by flow cytometer. Results are expressed as a percentage of the total cell population and represent the mean of 3 independenet experiment.

	Incubation time (h)	Viable Cell (%)	Apoptotic Cell (%)	Necrotic Cell (%)
Control (Untreated cell)	4	93.42 ± 0.25	5.80 ± 0.46	1.01 ± 0.69
	8	93.24 ± 1.74	6.07 ± 1.43	0.61 ± 0.33
	12	93.16 ± 0.46	6.27 ± 0.52	0.63 ± 0.13
	16	94.73 ± 1.48	4.92 ± 1.03	0.42 ± 0.05
	24	93.42 ± 0.53	6.20 ± 0.55	0.50 ± 0.20
	48	93.58 ± 0.90	5.57 ± 0.74	0.78 ± 0.20
	72	93.19 ± 0.72	5.83 ± 0.66	0.99 ± 0.08
Panaxynol IC_{50} (13.9 μM)	4	93.81 ± 1.03	5.64 ± 0.98	0.55 ± 0.13
	8	93.06 ± 0.84	6.24 ± 0.50	0.70 ± 0.34
	12	92.87 ± 0.71	6.57 ± 0.84	0.57 ± 0.29
	16	90.59 ± 1.10	8.31 ± 0.75	1.09 ± 0.79
	24	88.85 ± 3.30	10.37 ± 2.74	0.88 ± 0.62
	48	82.42 ± 3.00	16.57 ± 3.01	1.02 ± 0.14
	72	85.19 ± 0.78	13.32 ± 0.61	1.49 ± 0.25
Panaxynol IC_{85} (24.6 μM)	4	93.91 ± 0.67	5.52 ± 0.56	0.58 ± 0.15
	8	92.86 ± 1.53	6.54 ± 1.49	0.59 ± 0.15
	12	91.51 ± 1.31	7.73 ± 1.21	0.76 ± 0.11
	16	90.96 ± 2.39	8.29 ± 2.23	0.45 ± 0.05
	24	88.98 ± 1.10	10.76 ± 1.14	0.31 ± 0.03
	48	66.00 ± 4.82	32.87 ± 4.54	1.10 ± 0.30
	72	50.70 ± 8.29	47.29 ± 7.80	2.00 ± 0.73
Cisplatin IC_{85} (32.19 μM)	4	92.53 ± 0.33	6.86 ± 0.30	0.61 ± 0.19
	8	92.15 ± 0.78	7.25 ± 0.44	0.60 ± 0.36
	12	87.54 ± 1.39	11.98 ± 1.38	0.48 ± 0.13
	16	81.54 ± 4.53	18.13 ± 4.46	0.34 ± 0.07
	24	70.88 ± 3.46	28.79 ± 3.57	0.33 ± 0.14
	48	50.49 ± 5.62	49.08 ± 5.55	0.43 ± 0.16
	72	22.77 ± 1.08	76.90 ± 1.18	0.33 ± 0.20

More than 90 % of untreated K-562 cells were negative for both Annexin-V FITC and PI (LL quadrant) with a background apoptosis population of between 4-6 % at all time point analysed (Figure 4.30).

Annexin-V FITC positive cells were detected as early as 4 hours following treatement with panaxynol at IC_{50} and IC_{85} concentrations and cisplatin at IC_{85} concentration. From a visual examination of the flourescence intensity quadrants (Figure 4.30), panaxynol and cisplatin treated cells initially progressed from the LL to the LR quadrant as sample incubation time increased. An increase in the population appreasing in the UR quadrant indicated the formation of more secondary necrotic cells overtime. This progress was seen for both panaxynol and cisplatin treated cells over the 72 hours incubation time. The FITC negative and PI positive (UL quadrant) were not detected at any time point. These results suggested that the both IC_{50} and IC_{85} concentrations of panaxynol and cisplatin at IC_{85} increased the percentage of apoptosis populations as the sample incubation time increased. Cisplatin was more effective at inducing apoptosis compared to panaxynol at all time points analysed.

For K-562 cells treated with panaxynol at IC_{50} concentration, the popualtion of viable cells decreased from 93.81 % at 4 hours incubation to 82.42 % at 48 hours incubation and reconvered slightly to 85.19 % at 72 hours. FITC positive apoptosis cells increased from 5.64 % at 4 hours incubation to 16.57 % at 48 hours and decreased to 13.32 % at 72 hours. When treated with IC_{85} concentration (24.6 µM) of panaxynol, viable cells decreased steadily over time from 93.91 % at 4 hours incubation to 50.70 % at 72 hours incubation, while the apoptosis population increased from 5.52 % at 4 hours incubation to 47.29 % at 72 hours incubation, refer Figure 4.30.

For the K-562 cells treated with cisplatin at IC_{85} concentration (32.19 µM), the viable cell population declined steadily from 92.53 % at 4 hours incubation to 22.77 % at 72 hours incubation, while the apoptosis population increased from 6.86% at 4 hours incubation to 76.90 % at 72 hours incubation (Figure 4.27). The necrosis populations of the K-562 cells treated with panaxynol and cisplatin are maintained at the low percentage (0.33 % - 2.00 %). While untreated K-562 shown viable cell populations in the range of 93.16% - 94.73%. Without the treatment from panaxynol and cisplatin, the apoptotic and necrotic cell population of untreated K-562 always maintained in range of 4.92 % - 6.27 % and 0.42 % - 1.01 % at 72 hours sample treatment time.

The morphology of K-562 cells after treatment with IC_{50} (13.9 μM) and IC_{85} concentration (24.6 μM) of panaxynol and cisplatin in IC_{85} concentration and examined (32.19 μM) at 4, 8, 12, 16, 24, 48 and 72 hours following treatment are shown in Figure 4.30-4.32. Untreated K-562 cells maintain their rounded morphology while morphological alternations were seen for K-562 cells treated with panaxynol and cisplatin.

Panaxynol in IC_{50} (13.9 μM) and IC_{85} concentration (24.6 μM) and cisplatin in IC_{85} concentration (32.19 μM) induced membrane blebbing (Figure 4.30-C, pointed by blue arrow) and apoptotic body (Figure 4.31- F, pointed by red arrow) which are hallmark morphological changes of the apoptosis process. Besides, the panaxynol in IC_{50} (13.9 μM) and IC_{85} concentration (24.6 μM) and cisplatin also induce necrosis in K-562 cells.

Figure 4.30: Morphology of untreated cell and Treated K-562 cell with panaxynol in IC_{50} concentration under 200X magnification. →: Apoptotic body, → : viable cell , →: necrotic cell, →: membrane blebbing. A: Untreated cell, B: Panaxynol IC_{50} 4 hours, C: Panaxynol IC_{50} 8 hours, D: Panaxynol IC_{50} 12 hours, E: Panaxynol IC_{50} 16 hours, F: Panaxynol IC_{50} 24 hours, G: Panaxynol IC_{50} 48 hours, H: Panaxynol IC_{50} 72 hours.
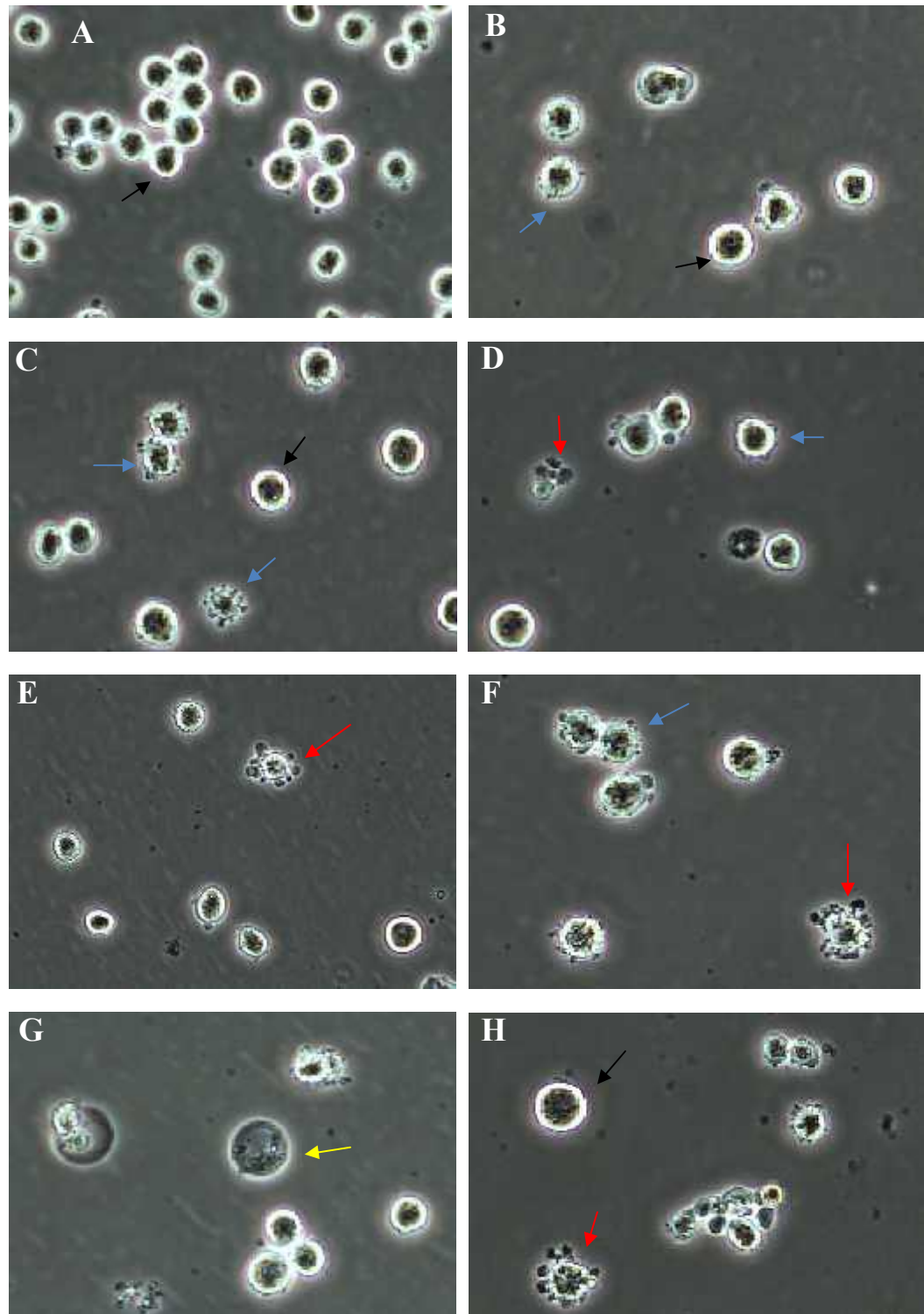
Figure 4.31: Morphology of untreated cell and Treated K-562 cell with panaxynol in IC_{85} concentration under 200X magnification. →: Apoptotic body, → : viable cell , →: necrotic cell, →: membrane blebbing. A: Untreated cell, B: Panaxynol IC_{85} 4 hours, C: Panaxynol IC_{85} 8 hours, D: Panaxynol IC_{85} 12 hours, E: Panaxynol IC_{85} 16 hours, F: Panaxynol IC_{85} 24 hours, G: Panaxynol IC_{85} 48 hours, H: Panaxynol IC_{85} 72 hours.
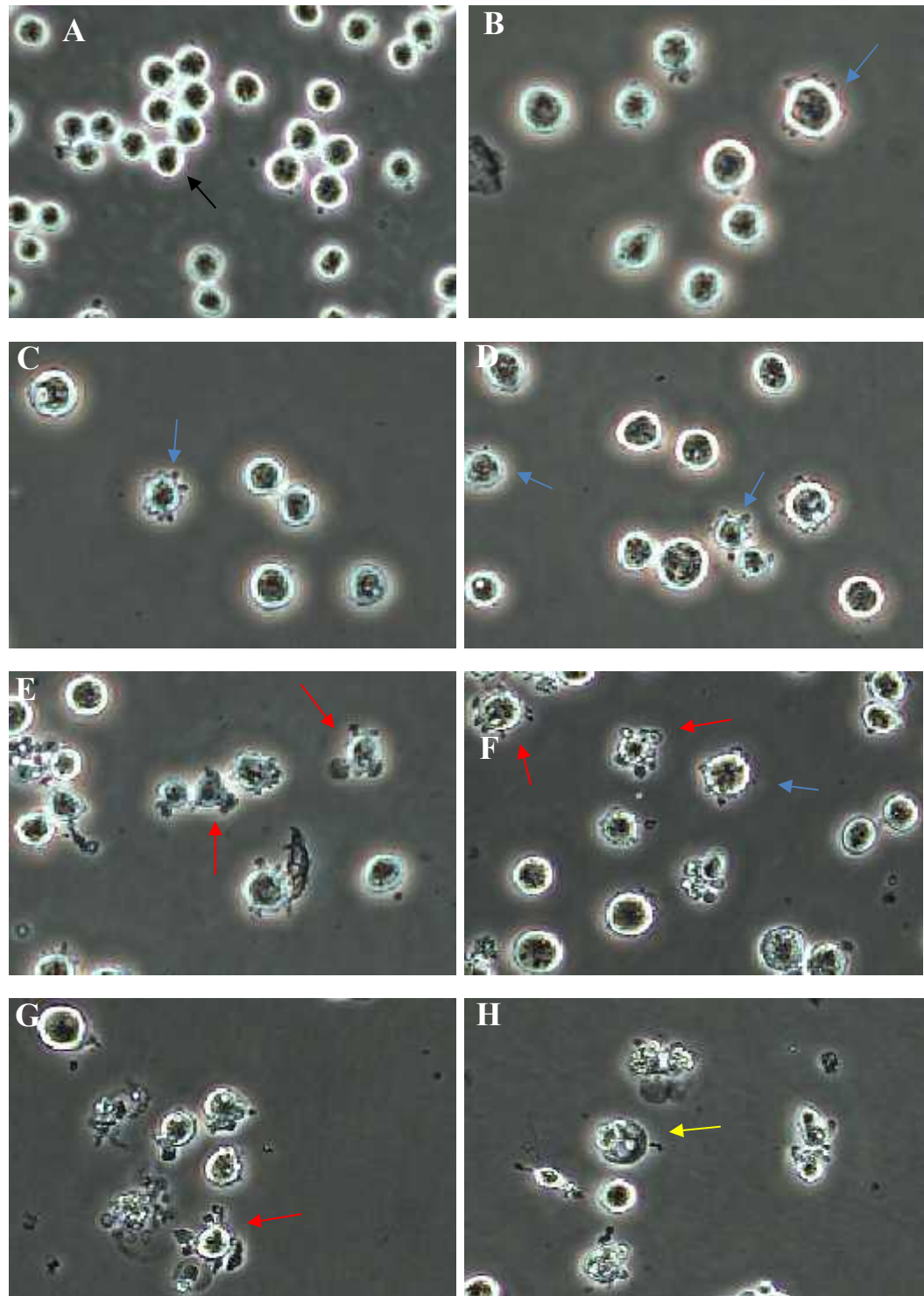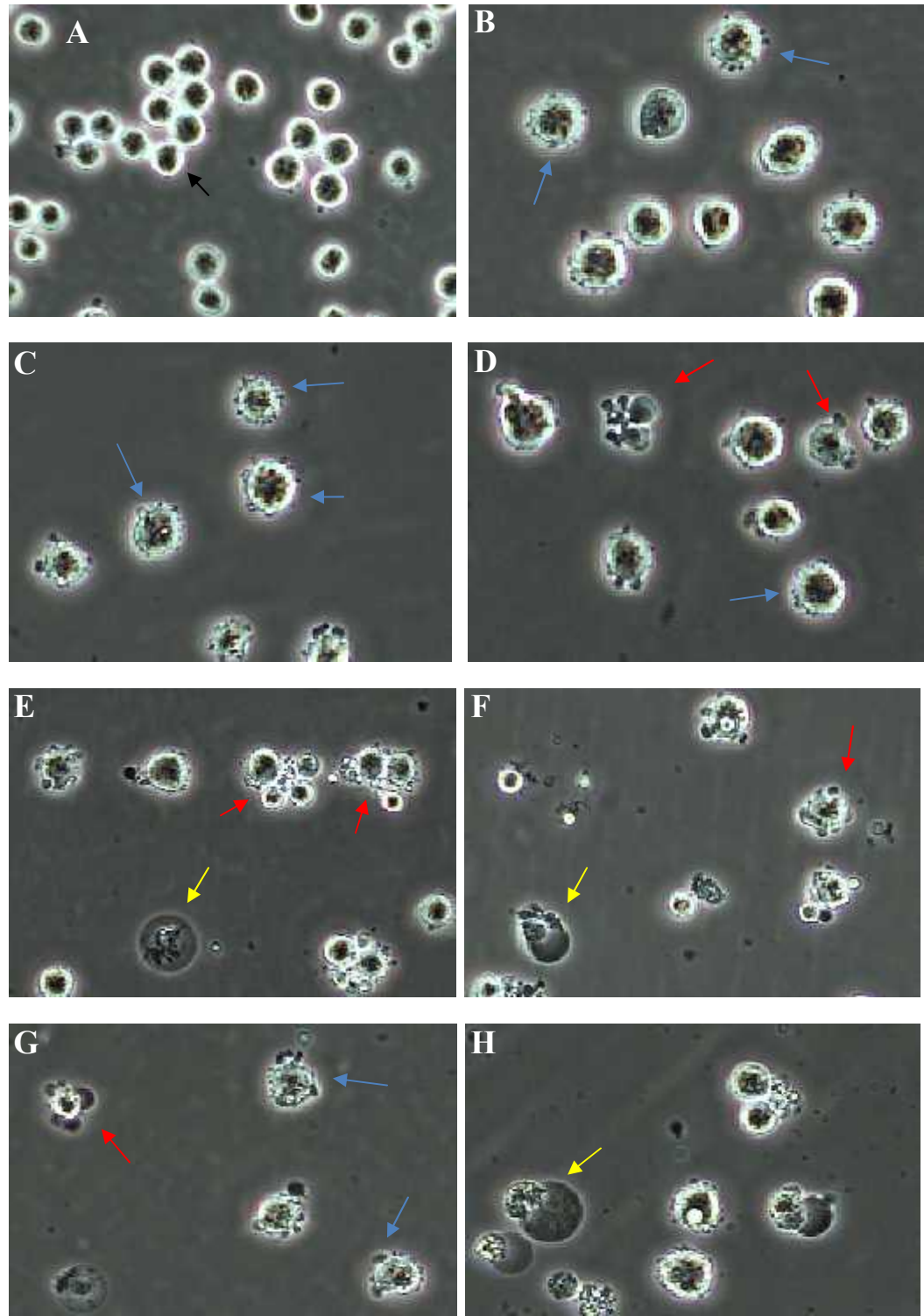
Figure 4.32: Morphology of untreated cell and Treated K-562 cell with cisplatin in IC_{85} concentration under 200X magnification. →: Apoptotic body, → : viable cell , →: necrotic cell, →: membrane blebbing. A: Untreated cell, B: Cisplatin IC_{85} 4 hours, C: Cisplatin IC_{85} 8 hours, D: Cisplatin IC_{85} 12 hours, E: Cisplatin IC_{85} 16 hours, F: Cisplatin IC_{85} 24 hours, G: Cisplatin IC_{85} 48 hours, H: Cisplatin IC_{85} 72 hours.
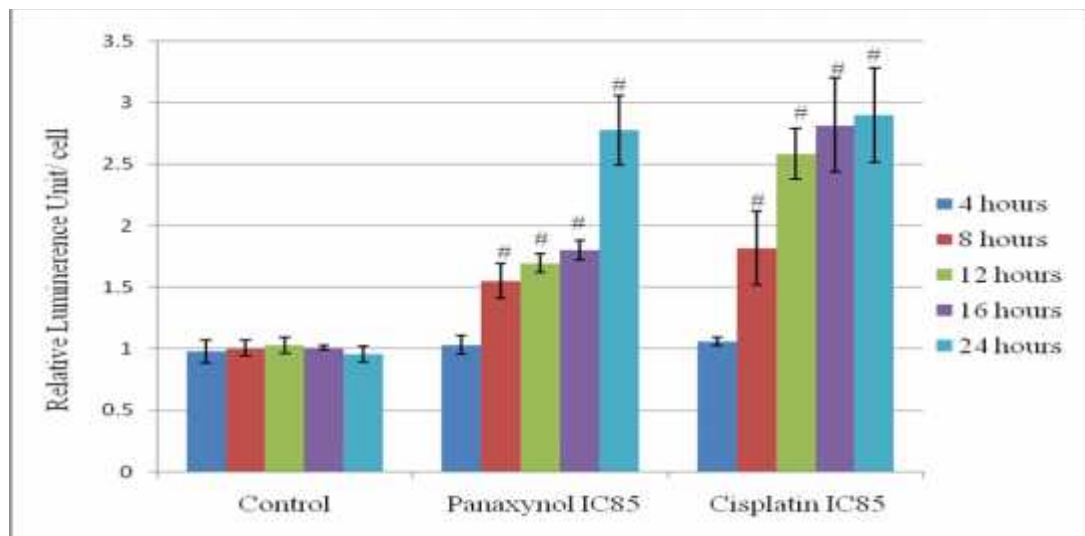
4.9 Caspases Activation by Panaxynol

Caspases play an important role in the activation of apoptosis activities. The initiator caspases like, caspase-8 and caspase-9 are involved in the extrinsic or intrinsic pathway to initiate apoptosis, while the effector caspases (caspase-3 and caspase-7) play a role to execute the destruction of cellular components. Using a luminscent cell based assay specific for caspase-3/7, caspase-8 and caspase-9, mechanism of panaxynol to induce the apoptosis, either through caspase independent pathway or caspase dependent pathway can be determined.

The activation of caspase-8, 9 and 3/7 in K-562 cells induced by panaxynol (24.6 μM) and cisplatin in IC_{85} concentration (32.19 μM) represented in bar chat are shown in Figure 4.33. The caspase-9 activity for untreated K-562 cells showed a base line range from 5.36 RLU/cell to 6.21 RLU/cell from 4 hours to 24 hours sample treatment time. The caspase-9 activity of K-562 cells induced by the panaxynol are increased from 15.31 ± 1.44 RLU/cell at 4 hours to 51.31 ± 5.23 RLU/ cell at 24 hours. Cisplatin induced the caspase-9 activity of K-562 cells from 17.15 ± 1.60 RLU/cell at 4 hours to 53.65 ± 4.77 RLU/ cell at 24 hours. Panaxynol and cisplatin were triggered significant increase of enzyme activities of caspase-9 in K-562 cells, when compared with enzymes activities of caspase-9 of untreated K-562 cells in 4, 8, 12, 16 and 24 hours incubation (* $P<0.05$). The caspase-8 activity in the untreated cells remained at the range of 0.96 RLU/ cell to 1.03 RLU/ cell from 4 hours to 24 hours sample treatment time. For K-562 cells

A

B
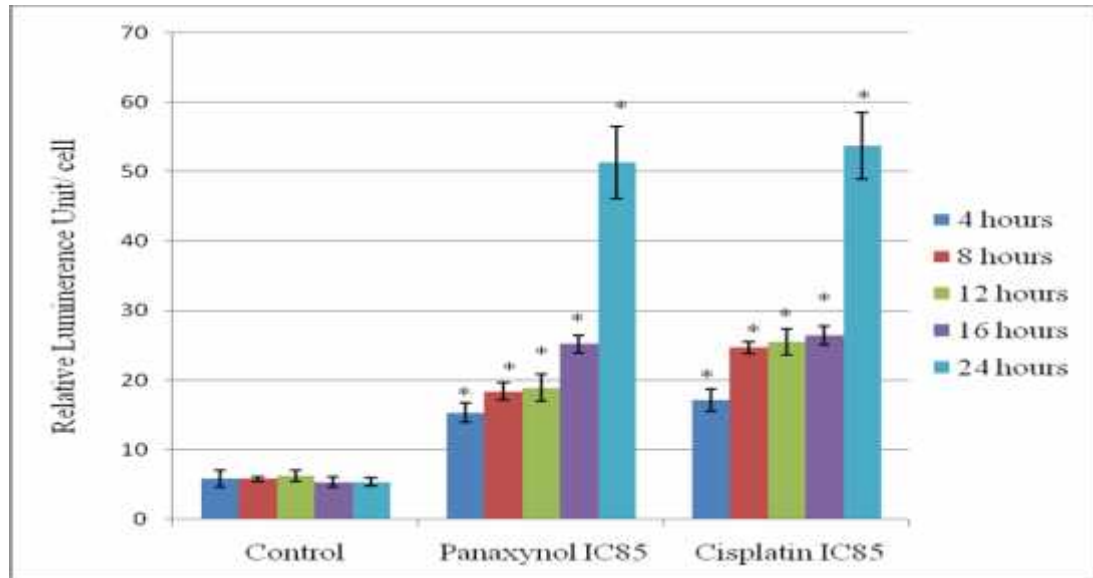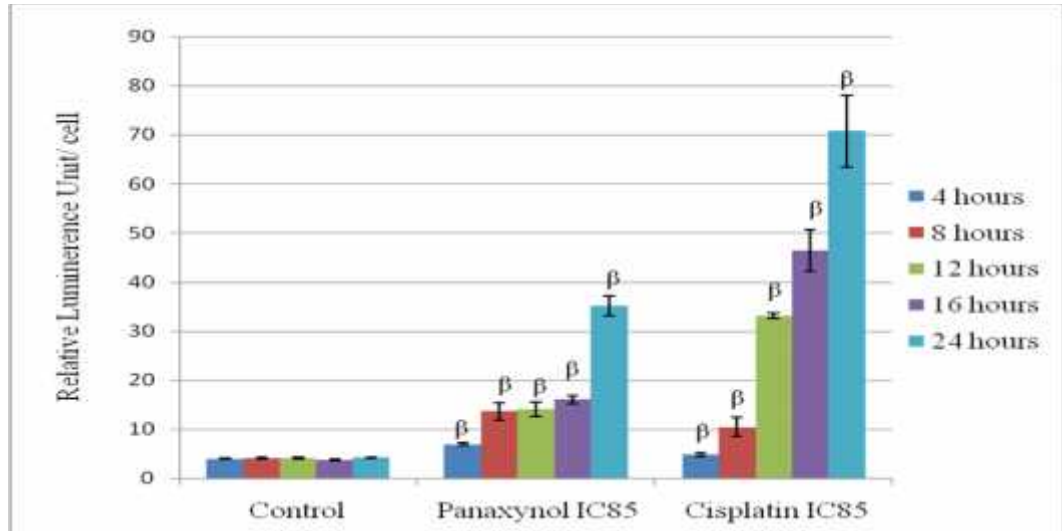
C

Figure 4.33: The caspases activities of panaxynol and cisplatin in IC_{85} concentration treated K-562 for 4, 8, 12, 16, 24 hours incubation and untreated K-562 cell line. A: Ezmymes activities of caspse-9. B: Ezmyme activities of caspase-8. C: Ezmynes activities of caspase-3/7. Date represent the average of three independent experiment. Caspase-9 was significantly increase by panaxynol and cisplatin at 4,8,12,16 & 24 hours incubation (* $P<0.05$). Caspase-8 was significant increased by panaxynol and cisplatin at 8, 12, 16 & 24 hours incubation (# $P<0.05$). Caspase-3/7 was significantly increase by panaxynol and cisplatin at 4, 8, 12, 16 and 24 hours incubation (β $P<0.05$).

subjected to panaxynol, the caspase-8 activity increased from 1.03 ± 0.07 RLU/ cell at 4 hours to 2.78 ± 0.28 RLU/cell at 24 hours. The caspase-8 activity of K-562 cells treated with cisplatin increased from 1.06 ± 0.03 RLU/ cell at 4 hours to 2.90 ± 0.38 RLU/cell at 24 hours.While, caspase-8 activities of K-562 cells was significantly increased by panaxynol and cisplatin at 8, 12 16 and 24 hours treatment time when compared with caspase-8 activities of untreated K-562 in 8, 12, 16 and 24 hours incubation time (# $P < 0.05$). For caspase-3/7 activites, the untreated cells showed a base line level within the range of 3.67 - 4.27 RLU/cell from 4 hours to 24 hours sample treatment time. For panaxynol treated K-562 cells, activated caspase-3 activity increased from 6.91 ± 0.25 RLU/cell at 4 hours to 35.10 ± 2.04 RLU/cell at 24 hours, while cisplatin treated K-562 cells showed caspase-3/7 activity increased from 4.80 ± 0.33 RLU/cell at 4 hours to 70.75 ± 7.34 RLU/cell at 24 hours. Enzymes activities of caspase-3/7 induced by panaxynol and cisplatin were significant higher than enzymes activities of caspase-3/7 of untreated K-562 cells at 4, 8, 12, 16 and 24 hours treatment time (β $P < 0.05$).

CHAPTER 5

DISCUSSION

5.1 *Hydrocotyle vulgaris*

According to the Table 4.1 and Table 4.2, the dry stem of *H. vulgaris* only account for about 21% of the total weight of *H. vulgaris* and the yield of the cytotoxic hexane fraction of stem was also very low (0.57 %). Due to the limited amount of material available, it was not possible to attempt the isolation of the pure bioactive compound from the hexane fraction of stem. One pure, and one partially purified compound was successfully isolated from the dichloromethane fraction of the leaves and the hexane fraction of the root of *H. vulgaris* respectively (Refer to Table 4.6 column 7, row 11). Only 4 mg of C1 compound were isolated from the root of *H. vulgaris*. Only a limited structure elucidation of C1 was possible due to the minute amounts available. GC-MS data suggest that C1 has 79 % similarity with octanoic acid, however, this will require further research to confirm. The dichloromethane fraction of leaves yielded 44.69 mg of Compound L1. L1 was found to be panaxynol from GC-MS, FTIR, polarimeter, and NMR data. Althrough panaxynol is not a novel compound; this is the first report of isolation of panaxynol as the cytotoxic principle in *H. vulgaris*.
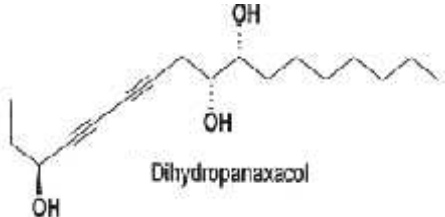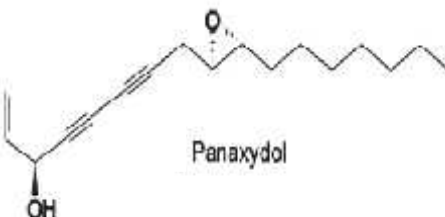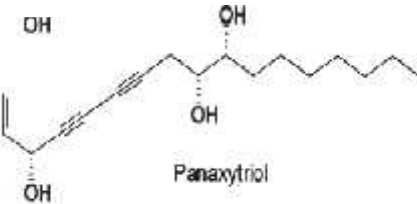
142
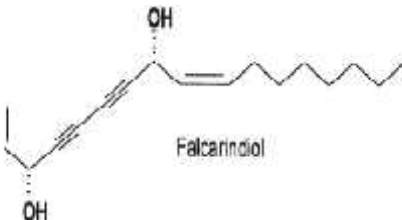
5.2 Panaxynol

Panaxynol, also named as (3S)-heptadeca-1,9(Z)-diene-4,6-diyne-3-ol, is a polyacetylene compound which is found in carrots (Jiang, Lu, Nie & Chen, 2008), the root of Panax ginseng (*Araliaceae*) (Min, Dong, Sang, Young & Kang, 2008), and *Saposhnikovae divaricata* (Kuo, Lin, Huang, Shu & Tsai, 2002). The structure of panaxynol is shown in Figure 4.19. Panaxynol is not a novel organic compound and its bioactivity has already been reported. Examples include the cytotoxic effect on cancer cell lines, like K-562, Raji, Wish, HeLa, Calu-1, vero, CURC II, Caki-1 and A498 (Sohn, Lee, Chung, Park, Kim & Hwang, 1998 ; Tai & Cheung, 2007), G_0/G_1 phase cell cycle arrest (Kuo, Lin, Huang, Shu & Tsai, 2002), inhibiting the platelet-derived growth factor (PDGF) – BB (Jiang, Lu, Nie & Chen, 2008) and inhibiting apoptosis via downregulation of BAX and upregulation of Bcl-2 protein (Nie, Yang, Fu, Jiang, Lu & Lu., 2006 ; Nie et al., 2008).

Figures 4.20, 4.22 and 4.23 show that panaxynol, cisplatin and doxorubicin were cytotoxic with regard to K-562 cells with IC_{50} values of 13.9 μM, 14.13 μM and 0.19 μM, respectively. The cytotoxic effect of doxorubicin against K-562 cells was much higher than both cisplatin and panaxynol, but the cytotoxic effect of panaxynol was higher than cisplatin. Panaxynol gave positive results on MTT assay, might be due to the inhibition for function of mitochondria or destroy the mitochondria in K-562 cells. Kim and his teams (1989) proved that panaxynol is
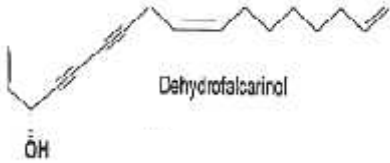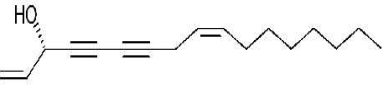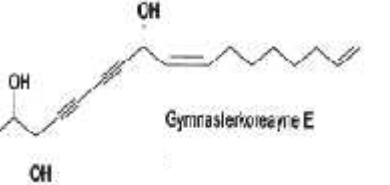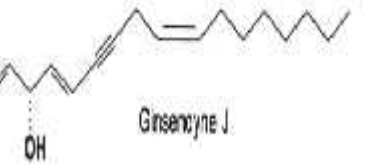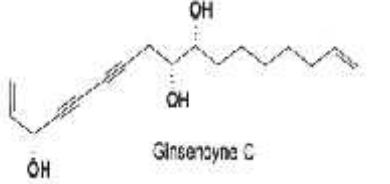
able to damage the membrane of mitochondria of L1210 cells. Panaxynol might conduct the same action to destroy mitochondria of K-562 cells, interrupts succinate dehydrogenase system to catalyse MTT to purple formazan and caused cytotoxic effect against K-562 cells (Berridge & Tan, 1992).

The cytotoxicity properties of panaxynol might be due its chemical structure. Panaxynol is categorised as C-17 polyacetylene and consisted by a long carbon chain and a allylic alcohol. This typical structure (a long carbon chain and a allylic alcohol at the terminus of a compound) also present at other cytotoxic C-17 polyacetylenes (Dembittsky, 2006). The listed of cytotoxic C-17 polyacetylenes are shown at Table 5.1. According to the research of Molinski and Zhou, they found that l-yn3-ol (allylic alcohol) present at terminus of Halicynone (C-33 polyacetylene) as critical structure to provide cytotoxic effect against HCT-116 cells (Human, colon tumour cells). That mean the allylic alcohol present at C-3 position of polyacetylene may be as a critical structure to provide cytotoxic effect against K-562 cells. Radin (2008) also showed that the presence of allylic alcohol in a compound, facilitates the formation of a transient free radical and a reactive carbocation in the dehydrate condition, thereby acting as extremely reactive alkylating agent. Most of alkylating agents provided cytotoxic effect against cancer cell lines.

Table 5.1: The chemical structure of C-17 polyacetylene and cytotoxicity of C-17 polyacetylene against varies type of cancer cell lines (Dembittsky, 2006).

Name of Compound	Chemical Structure of Compound	Cytotoxic effect toward cancer cell lines
Dihydropanaxacol	Dihydropanaxacol	➢ Yoshida sarcoma cells
Panaxydol	Panaxydol	➢ Jurkat cells (Human, leukemia T cells)
Panaxytriol	Panaxytriol	➢ MK – 1 (Human, gastric carcinoma cells ➢ M25 – SF (Human, breast carcinoma cells)
Falcarindiol	Falcarindiol	➢ MK – 1 (Human, gastric carcinoma cells

Continued Table 5.1

Dehydrofalcarinol	Dehydrofalcarinol	➢ LOX cells (Mouse, Melanoma cells)
Falcarinol		➢ CaCo – 2 (Epithelial colorectal adenocarcino ma cells)
Gymnasterkoreayne E	Gymnasterkoreayne E	➢ L – 1201 (Murine leukemia)
Ginsenoyne J	Ginsenoyne J	➢ MCF 7 (Human, breast adenocarcino ma) ➢ L – 1201 (Murine leukemia) ➢ HeLa (Human, epithelial adenocarcino ma)
Ginsenoyne (1,16-heptadecadiene-4,6-diyne-3,9,10-triol)	Ginsenoyne C	➢ HeLa (Human, epithelial adenocarcino ma) ➢ L – 1201 (Murine leukemia)

Panaxynol has an enantiomer compound, named as falcarinol (Figure 5.1) (Zheng et al., 1999). Scientists proved that the enantiomer compounds possessed similar physical properties and similar mechanism to causes cytotoxic effect against cancer cells (Kimball, Turunen, Ellis, Himes & Georg, 2008; Pinto et al., 2011). Falcarinol is a hydrophobic compound easy to penetrate into the membrane of the cells. Besides, falcarinol used the allylic alcohol at C-3 position to facilitate the formation of carbocation and acting as extremely reactive alkylating agent toward various biomolecules, including nucleic acid, amino acid, nucleotide and protein; and generating ROS in cancer cell (Hajnos, Sherma, & Kowalska, 2008; Radin, 2008). The formation of falcarinol to become carbocation compound is shown at Figure 5.2. Furthermore, Purup and colleagues (2009) also showed that the hydroxyl group (allylic alcohol) at C-3 position of falcarinol was a critical function group required for cytotoxic properties. They oxidized falcarinol to falcarinon (Figure 5.1) by removing hydrogen from allylic alcohol of falcarinol and showed that falcarinon was less effective in inhibiting proliferation of Caco-2 cells, compared to falcarinol. That means allylic alcohol at C-3 position as critical function for falcarinol group to cause cytotoxic effect against cancer cells. Panaxynol is enantiomer of falcarinol, may use the allylic alcohol at C-3 position to become carbocation and react as alkylating agent to cause cytotoxic effect at K-562 cells.

According to Figure 4.24, a typical morphological change like apoptotic body was

found in K-562 cells treated by panaxynol (Kerr, Winterford & Harmon, 1994).

That show panaxynol induced cell death of K-562 cells through apoptosis process.

This statement was proved by the present of sub G_0 population in
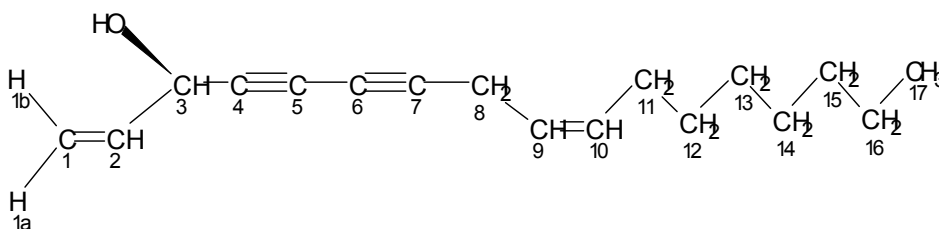
Panaxynol
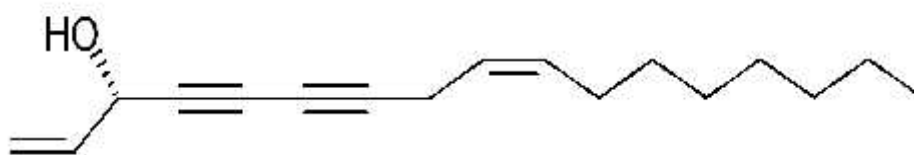
Falcarinol
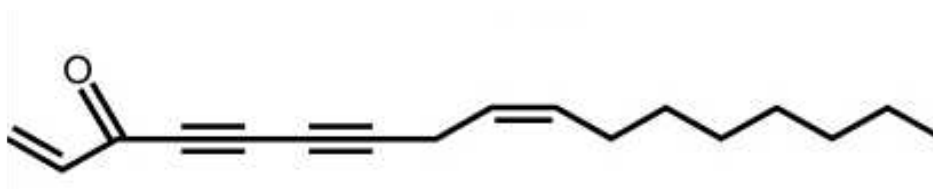
Falcarinon

Figure 5.1: The chemical structure of C-17 polyacetylene, panaxynol, falcarinol and falcarinon (Dembittsky, 2006).
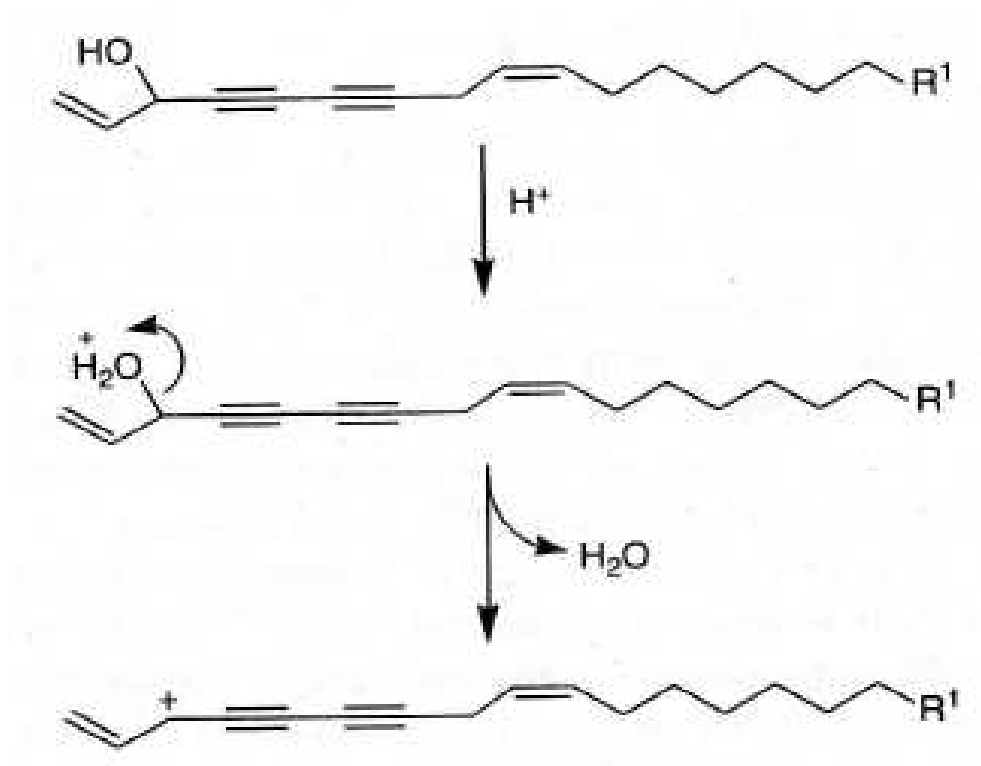
Figure 5.2: The mechanism of falcarinol to produce the carbocation (Hajnos, Sherma, & Kowalska, 2008).

histogram of cell cycle analysis at Figure 4.28 and appearance of K-562 cells

uptake the FITC which quantified at the dot pot of apoptosis test in Figure 4.30.

The sub G_0 DNA population of K-562 cells treated with IC_{50} and IC_{85}

concentrations of panaxynol increased to 7.15 % and 15.07 % respectively after

48 hours incubation compared with untreated K-562 cells which showed 1.39 %. The sub G_0 DNA population cells with reduced DNA content and is mostly due to DNA fragmentation which causes the caspase-3 activation in apoptosis process (Chen, He & Li, 2006). Furthermore, the appearance of Annexin-V FITC positive K-562 cells were detected as early as 4 hours following treatement with panaxynol at IC_{50} and IC_{85} concentrations to 72 hours treatment time. The K-562 cells treated by panaxynol able to uptake the annexin-V FITC cause by externalization of phosphatyserine which induced by activation of caspase-3 in apoptosis process (Frasch et al., 2000; Fujita et al., 2010).

Refer to bioluminescent caspases assay (Figure 4.33), panaxynol is able to induce apoptosis process in K-562 cells through caspase dependent pathway. The activation of enzyme activities of caspase-3/7 and 9 by panaxynol as early as 4 hours treatment time, while caspase-8 was activated by panaxynol started at 8 hours treatment time. So, the caspase-9 (initial caspase) might be the major enzyme to trigger activation of caspase-3 (effector caspase) in apoptosis process, compared with caspase-8. At the same time, activation of caspse-9 is much earlier than the activation of caspase-8. That show panaxynol might not induce activation of caspase-8 to proteolytically activate Bid, which can then facilitate cytochrome c release and further trigger activation of caspase-9 to precede caspase-3/7 activities (Green, 2000; Esposti, 2002). Panaxynol might activate extrinsic pathway and intrinsic pathway to trigger apoptosis process in K-562 cells.

The mechanism of panaxynol to induce apoptosis in K-562 cells is still not fully understood. It is possible that, panaxynol might induce apoptosis in K-562 cells due to the interaction of its allylic alcohol in structure with biological molecules. For example: ceramide (Cer), which possesses allylic alcohol at C-3 position of sphingosine and the Trans-Δ^4-double bond, is able to control cell growth and proliferation, generate reactive oxygen species (ROS) in mitochondria, and release mitochondria protein to induce apoptosis (Radin, 2008). The allylic alcohol of ceramide is oxidized into an allylic ketone in mitochondria, through the interaction with coenzyme Q (CoQ) or a factor closely related to CoQ, with the formation of reactive oxygen species which initiate mitochondria breakdown, and is a vital step in apoptosis (Radin, 2001; Radin 2004). Besides, falcarinol and falcarindiol (chemical structure refers to Table 5.1) possess allylic alcohol at C-3 position and have the ability to generate ROS in myotube culture. This suggests that compounds possessing allylic alcohol groups might have the ability to generate reactive oxygen species which leads to stress in cells that inhibit proliferation by inducing apoptosis.

Two more examples are falcarinol and panaxydol (chemical structure refers to Table 5.1) which belong to the polyacetylene group. Both possess allylic alcohol on the C-3 position in their structure and have a similar structure with panaxynol. Falcarinol and panaxydol are able to induce apoptosis in CaCo-2 (Epithelial colorectal adenocarcinoma cells) and Jurkat cells (Human leukemia T cells)

respectively. Falcarinol at a concentration above 20 μM is able to decrease proliferation of CaCo-2 cells and induce apoptosis by increasing active caspase-3 activity. In addition, falcarinol at a concentration above 10 μM can cause single strand DNA breakage (Young, Duthie, Milne, Christensen, Duthie & Bestwick, 2007). Panaxydol is able to induce apoptosis in Jurkat cells (p53 null cell line) by increasing Ca^{2+} level in Juckat cells and activate JNK and p38 MAPK to generate reactive oxygen species through NADPH oxidase and mitochondria ROS generation. The ROS causes cytochrome c released from mitochondria and activates caspase-3/7, 8 and 9 to induce apoptosis (Kim, Yu, Oh, Lee, Kim & Sohn, 2011). In addition, prolonged JNK protein activation mediates tumour necrosis factor-α dependent apoptosis, often through distinct caspase-8 activation pathway (Wagner & Nebreda, 2009). Panaxynol, which possesses an allylic alcohol and has a similar structure to falcarinol and panaxydol, may activate similar mechanisms of action in inducing apoptosis in K − 562 cells used in this study. The results (Figure 4.33) suggest that panaxynol does activate caspase-3/7, 8 and 9 in K-562 cells (p53 null cells) and this can be correlated with the morphological changes observed in Figure 4.30 and Figure 4.31 that show the classical apoptotic morphology such as the formation of apoptotic bodies, DNA fragmentation, chromatin condensation, membrane blebbing and induction of the externalization of phosphotidyserine.

According to the histogram in Figure 4.28, the G_0/G_1 DNA populations of K-562 cells treated with panaxynol at IC_{50} and IC_{85} concentration was increased to 53.08 % and 54.92 % respectively after 48 hours of incubation compared with untreated K-562 cells which showed 47.03 %. That means that panaxynol was able to induce a small G_0/G_1 cell cycle arrest of K-562 cells. This finding supports earlier studies that show that panaxynol downregulated cyclin E concentration in K-562 cells and blocked the cell cycle to enter S phase for DNA synthesis (Kuo et al., 2002).

Based on the literature and results in this study, it is hypothesised that panaxynol may activate JNK pathway as upstream process to cause cytotoxic effect to K-562 cells (p53 null). This is consistent with the pathway activated by panaxydol to induce cytotoxic effect on Jurkat cells (p53 null), in the absence of wild-type p53 protein. The activation of JNK pathway in K-562 cells may be due to allylic alcohol at C-3 position of panaxynol. The allylic alcohol of panaxynol is able to form a carbocation with the loss of water and acts as a reactive alkylating agent. The reactive alkylating agent in turn is able to generate ROS in cancer cells (Cooklin, 2004; Panasci & Alaoui-Jamali, 2004). Moreover, falcarinol and falcarindiol have the ability to generate ROS in myotube culture (Young, Christensen, Theil & Oksbjerg, 2008). Panaxynol, which possesses similar structure with these two compounds, may be able to generate ROS in cancer cells in a similar manner. Therefore, in order to activate ROS, panaxynol may induce

upstream process of JNK pathway by increasing the Ca^{2+} level and activate JNK and p38 MAPK in K-562 cells. The activation of JNK and p38 MAPK in K-562 cells is able to generate ROS. Kim and his team discovered that panaxynol is able to damage the membrane of mitochondria of L1210 cells (Kim, Jin, Kim & Hahn, 1989). Panaxynol may use ROS to damage the membrane of mitochondria. The damaged mitochondria interrupt succinate dehydrogenase system to catalyse MTT to purple formazan (Kyoung et al., 2011). Therefore, panaxynol treated K-562 cells showed reduced formazan formation. (Figure 4.20) The damaged membrane of mitochondria is believed to further released cytochrome c from mitochondria and activated downstream caspase 9 and 3, and triggered apoptosis process in K-562 cells. The biochemical apoptosis markers measured in K-562 cells was correlated with morphological changes observed in Figure 4.30 and Figure 4.31 which shows the classical apoptotic morphology such as formation of apoptotic bodies, membrane blebbing, chromatin condensation, and biochemical change like externalization of phosphotidyserine (Figure 4.29) and DNA fragmentation (Figure 4.28)

5.3 Future Work

Future research for this project should concentrate on isolating the active pure compound from the hexane fraction of stem and root of *Hydrocotyle vulgaris*. These pure bioactive compounds should be characterized using a nuclear magnetic resonance, mass spectrometer and FTIR. Once that has been accomplished, the mechanism of cytotoxicity employed by those active compounds can be studied.

Meanwhile, researchers can also study the mechanism of allylic alcohol in the structure of panaxynol to induce apoptosis with the activation of caspases-8, 9 and 3/7 in K-562 cells (p53 mutant cells) should be conducted. And hence, this could help to determine whether panaxynol is able to activate the JNK pathway to induce apoptosis in K-562 cells or generate a carbocation to produce changes in kinase activity and phosphoprotein level in K-562.

CHAPTER 6

CONCLUSION

In this study, cytotoxic compounds were found in the hexane fraction of stem and root; and the dichloromethane fraction of the leaf of *Hydrocotyle vulgrais*. One pure cytotoxic compound and one partial pure cytotoxic compund were successfully isolated from the leaf and root of *Hydrocotyle vulgaris* and are named as L1 (panaxynol) and C1 compound. The cytotoxicity of panaxynol and C1 compound were tested with an *in vitro* cytotoxic assay (MTT assay) against K-562 cells with IC_{50} values: 13.90 μM and 34.22 μM respectively. Due to an insufficient amount of C1 compound (4 mg), further structure elucidation and mechanism studies were not carried out. Flow cytometry studies of cell cycle analysis showed that panaxynol at IC_{50} concentration (13.9 μM) resulted in a 7.15 % ± 1.72 of the K-562 cell population detected in sub G_0 and 53.08 % ± 2.47 in G_0/G_1 phase of the cell cycle at 48 hours incubation. Panaxynol at IC_{85} concentration (24.6 μM) at the same incubation time resulted in the doubling of the sub G_0 (15.07 % ± 2.86) population while the G_0/G_1 phase population remained almost the same at 54.92 % ± 1.49. Untreated K-562 cells showed a small (1.39 % ± 0.55) sub G_0 population and a 47.03 % ± 3.14 of the population in G_0/G_1. That means panaxynol able to induce minor cell cycle arrest and activate

apoptosis process in K-562 cells. Panaxynol at IC_{50} and IC_{85} concentrations resulted, morphological changes in K-562 cells such as the formation of apoptotic bodies, membrane blebbing and chromatin condensation from 4 hours to 48 hours of incubation. Panaxynol at IC_{50} and IC_{85} concentration caused an increase in the apoptotic population of K-562 cells from 16.57 % ± 3.01 at 4 hours to 32.87 % ± 5.45 at 48 hours incubation, compared with untreated K − 562 cells which showed small amount (5.57 % ± 0.74) of apoptotic cells. Panaxynol at IC_{85} concentration (24.6 μM) increased the enzyme activities of caspase-3/7 (6.91 RLU/cell ± 0.25 at 4 hours to 35.10 ± 2.04 RLU/cell at 24 hours), caspase-8 (1.03 RLU/ cell ± 0.07 at 4 hours to 2.78 ± 0.28 RLU/cell at 24 hours) and caspase-9 (15.31 RLU/cell ± 1.44 at 4 hours to 51.31 RLU/ cell ± 5.23 at 24 hours) of K-562 cells from 4 hours of incubation to 24 hours of incubation, compared with untreated K-562 cells which maintained the enzyme activities of caspase-3/7,caspase-8 and caspase-9 in base line range from 3.67 - 4.27 RLU/cell, 0.96 - 1.03 RLU/ cell and 5.36 - 6.21 RLU/cell respectively over the same incubation period. Due to the fact that K-562 cells are p53 null, we hypothesise that panaxynol could induces apoptosis in K-562 cells via a caspase dependent pathway which is independent of p53 activation.

REFERENCE

Abcam. (2010). *Propidium iodide staining of cells to assess DNA cell cycle*. URL: http://www.abcam.com/index.html?pageconfig=resource&rid=13432. Accessed: 12th October 2011

Ahuja, S. (2003*).* Relating chromatography to separation 4th .*Chromatography and separation scicence,* (pp.1-16). California: Academic Press.

American Cancer Society. (2010). *Cancer Facts & Figures 2010*. Atlanta: American Cancer Society; 2010.

Ariffin Omar, Zainudin Mohd Ali & Nor Saleha Ibrahim Tamin. (2006). *Malaysian cancer statistics – Data and figure Peninsular Malaysia 2006*. Kuala Lumpur: National Cancer Registry, Ministry of Health Malaysia. URL: http://www.makna.org.my/ MalaysiaCancerStatistics.pdf . Accessed 29 April 2009).

Balunas, M. J. & Kinghorn, A.D. (2005). Drug discovery from medicinal plants. *Life Sciences*, 78 (5), 431-441.

BD Bioscience. (2006). *Technical data sheet: FITC Annexin V*. San Jose: Becton, Dickinson and Company.

Becker, W. M., Kleinsmith, L. J. & Hardin, J. (2003).The cell cycle: DNA replication, mitosis, and cancer, *The world of the cells* (pp. 564-569). San Francisco: Benjamin Cummings.

Berridge,V.M. & Tan, S.A. (1992). Characterization of the cellular reduction of 3-(4,5-dimethylthiazol-2-yl)-2,5-diphenyltetrazolium bromide (MTT): subcellular localization, substrate dependence, and involvement of mitochondria electron transport in MTT reduction. *Arch. Biochem. Biophys*, 303, 474–482.

Bourgaud, F., Gravot, A., Milesi, S. & Gontier, E. (2001). Production of plant secondary metabolites: a historical perspective. *Plant Science*, 161, 839-851.

Bunz, F. (2001). Cell death and cancer therapy. *Current Opnion in Pharmacology*, 1, 337-341.

Burton, J. M. (2002). *Hydrocotyle vulgaris (L) Mash Pennywort.* URL: http:// http://www.spookspring.com/Umbels/Hydro.html. Accessed: 10th November 2010.

Cali, J. J., Niles, A., Valley, M. P., O'Brien, M. A., Riss, T. L. & Shultz, J. (2008). Bioluminescent assay for ADMET. *Toxicol*, 4, 103-120.

Cannell, R. J. P. (1998). Isolation by planar chromatography, *Natural product isolation* (pp. 209-246). New Jersey: Humana Press Inc.

Chabner, B. A. & Longo, D. L. (2006).Clinical and High Through Dose Alkylating agents, *Cancer chemotherapy and biotherapy: principles and practice* (pp. 283-309). USA: Lippincott Williams & Wilkins.

Chavasiri, W., Prukchareon, W., Sawasdee, P. & Zungsontiporn, S. (2005). *Allelochemicals from Hydrocotyle umbellata Linn*. URL: http://www.regional.org.au/au/allelopathy/2005/2/1/2628_warinthorn.htm. Accessed on 6th June 2010.

Chen, W., He, F. Y. & Li, Y. Q. (2006). The apoptosis effect of hispolon from Phellinus linteus (Berkeley & Curtis) Teng on human epidermoid KB cells. *Journal of Ethnopharmacology*, 105, 280-285.

Chen, W. L., Tang, W. D., Lou, L. G. & Zhao, W. M. (2006). Pregnane, coumarin and lupine derivatives and cytoxic constituents from *Helictere*s *angustifolia*. *Photochemistry*, 67, 1041-1047.

Cheng, Y., Wang, Y. & Wang, X., W. (2006). A causal relationship discovery-based approach to identifying active components of herbal medicine. *Computational Biology and Chemistry*, 30, 146-154.

Chu, W. L. & Radhakrishnan, A. K. (2008). Research on bioactive molecules: achievement and the way forward. *IcJSME*, 2, 21-24.

Cooklin, K. A. (2004). Chemotherapy-associated oxidative stress: impact on chemotherapeutic effectiveness. *INTEGRATIVE CANCER THERAPIES*, 3 (4), 294 -300.

Crews, P., Rodríguez, J. & Jaspars, M. (1998). Interpretation and use of proton and carbon chemical shifts, *Organic structure analysis* (pp. 53-101). New York: Oxford University Press, Inc.

Dembitsky, V. M. (2006). Anticancer activity of natural and synthetic acetylenic lipid. *Lipids*, 41, 883-924.

Denault, J. B. & Salvesen, G. S. (2002). "Caspases: keys in the ignition of cell death." *Chem Rev*, 102(12), 4489-500.

Duke, J. A. (1996). *"Specific queries of the phytochemical database"(Dr.Duke's phytochemical and ethnobotanical databases)*. URL: http://www.ars-grin.gov. Accessed on 7th May 2010.

Elmore, S. (2007). Apoptosis: a review of programmed cell death. *Toxicol Pathol*, 35, 495-516.

Esposti, M. D. (2002). The roles of Bid. *Apoptosis*, *7*, 433–440.

Fadeel, B., Gleiss, B., Hongstrand, K., Chandra, J., Wiedmer, T., Sims, P. J., Henter, J. I., Orrenius, S. & Samali, A. (1999). "Phosphatidylserine exposure during apoptosis is a cell-type-specific event and does not correlate with plasma membrane phospholipid scramblase expression."*Biochem Biophys Res Commun*, 266 (2), 504-511.

Fan, F. & Wood, K. V. (2007). Bioluminescent assay for high –throughput screening. *ASSAY and Drug Development Technologies*, 5, 127-136.

Felter, H. W. & Lloyd, J. U. (1989). *Hydrocotyle.—Water Pennywort*. URL: http://69.163.135.204/eclectic/kings/centella.html. Accessed on 7th September 2010.

Fouche, G., Cragg, G. M., Pillay, P., Kolesnikova, N., Maharaj, V.J. & Senabe, J. (2008). In vitro anticancer screening of South African plants. *Journal of Ethnopharmacology*, 119, 455-461.

Foster, I. (2008). Cancer: A cell cycle defect. *Radiography*, 14, 144-149.

Frasch, S. C., Henson, P. M., Kailey, J. M., Richter, D. A., Janes, M. S., Fadok, V. A. & Bratton, D. L. (2000). Regulation of phospholipid scramblase activity during apoptosis and cell activation by protein kinase Cδ*. *The Journal of Biological Chemistry*, 275 (30), 23065-23073.

Fujita, H., Shiva, D., Utsumi, T., Ogino, T., Ogawa, T., Abe, K., Yasuda, T., Utsumi, K & Sasaki, J. (2010). α-Tocopheryl succinate induces rapid and reversible phosphatidylserine externalization in histiocytic lymphoma through the caspase-independent pathway. *Mol Cell Biochem*, 333, 137-149.

Fulda, S. & Debatin, K. M. (2006). Extrinsic versus intrinsic apoptosis pathway in anticancer chemotherapy. *Oncogene*, 25, 4798-4811.

Fulda, S., Meyer, E., Friesen, C., Susin, S. A., Kroemer, G., & Debatin, K. M. (2001). Cell type specific involvement of death receptor and mitochondrial pathways in drug-induced apoptosis. *Oncogene*, *20,* 1063-1075

Gewies, A. (2003). Introduction of apoptosis. *ApoReview*, 1-26.

Gewirtz, D. A., Holt, S.E. & Grant, S. (2007). Evaluating the importance of apoptosis and other determinants of cell death and survival, *Apoptosis, senescence, and cancer* (pp. 55-72). New Jersey: Humana Press Inc.

Gewirtz, D. A., Holt, S.E. & Grant, S. (2007). The extrinsic pathway of apoptosis, *Apoptosis, senescence, and cancer* (pp. 31-54). New Jersey: Humana Press Inc.

Givan, A. L. (2001). Cells from within: DNA in life and death, *Flow cytometry: first principles* (pp.123-154). Canada: Wiley-Liss, Inc.

Gore, M. & Russell, D. (2003). Principle of cancer care, *Cancer in primary care* (pp. 47-88). London: Martin Dunitz, an imprint of Taylor & Francis Group plc.

Graham, J. G., Quinn, M. L., Fabricant, D. S., & Farnswort, N. R. (2000). Plants used against cancenr – an extension of the work of Jonathan Hartwell. *Journal of Ethnopharmacology*, 73, 374-377.

Gray, J. W. & Darzynkiewicz, Z. (1987). Multivariate cell analysis: techniques for correlated measurements of DNA and other cellular constituents, *Techniques in cell cycle analysis* (pp. 163-199). United State of America: The Humana Press Inc.

Green, D. R. (2000). Apoptosis pathways: paper wraps stone blunts scissors. *Cell, 102,* 1-4.

Gurib-Fakim, A. (2006). Medicinal plants: traditions of yesterday and drug of tomorrow. *Molecular Aspects of Medicine*, 27(1), 1-93

Hajnos, M. W., Sherma, J. & Kowalska, T. (2008). Polyacetylenes: Distribution in higher plant, pharmacological effects and analysis, *Thin layer chromatography in phytochemistry* (pp. 758-801). United State: CRC Press Taylor & Francis Group.

Hanahan, D. & Weinberg, R. A. (2000). The hallmarks of cancer. *Cell*, 100, 57-70

Harborne. J.B. (1998a). Methods of plant analysis, *Phytochemical methods: A guide to modern techniques of plant analysis* (pp.1-32). London: Chapman & Hall.

Harborne. J.B. (1998b). Organic acids,lipid and related compounds, *Phytochemical methods: A guide to modern techniques of plant analysis* (pp.151-179). London: Chapman & Hall.

Harborne, J. B. (1999). Perspectives on Secondary Plant Products, *Classes and functions of secondary product, Chemicals from plants* (pp. 1-25) New Jersey: Walton, D.E. Brown (Eds.) Imperial College Press.

Haupt, S., Berger, M., Goldberg, Z. & Haupt, Y. (2003). Apoptosis – the p53 network. *Journal of Cell Science*, 116, 4077-4085.

He, M., Rennie, P. S., Dragowska, V., Nelson, C. C. & Jia, W. (2002). A mutant p53 can activate through a mechanism distinct from those induced by wild type p53. *FEBS Letters*, 517, 151-154.

Hector, S. & Prehn, J. H. M. (2009). Apoptosis signaling proteins as prognostic biomarker in colorectal cancer: A review. *Biochimica et Biophysica Acta*, 1795, 117-129.

Israels, E.D. & Israels, L. G. (2000). The cell cycle. *The Oncology*, 5, 510-513.

Itokawa, H., Morris-Natschke, S., Akiyama, T. & Lee, K. H. (2008). Plant-derived natural product research aimed at new drug discovery. *J Nat Med*, 62, 263-280.

Ito, N., Hasegawa, R., Imaida, K., Hirose, M., Asamoto, M. & Shirai, T. (1995). Concept in multistage carcinogenesis. *Oncology/Hematology*, 21, 105-133.

Jiang, L. P., Lu, Y., Nie, B. M. & Chen, H. Z. (2008). Antiproliferative effect of panaxynol on RASMCs via inhibition of ERK1/2 and CREB. *Chemico-Biological Interactions*, 171, 348-354.

Kerr, J. F., Winterford, C.M. & Harmon, B. V. (1994). Apoptosis. Its significance in cancer and cancer therapy. *Cancer*, 73, 2013-2026.

Kessler, C. (2000). In vivo labeling of DNA probe with 5- Brdu. 2nd Edition, *Nonradioactive analysis of biomolecule* (pp. 168-179) Germany: Springer-Verlag Berlin Heidelberg.

Kim, J. Y., Yu, S. J., Oh, H. J., Lee, J. Y., Kim, Y. & Sohn, J. (2011). Panaxydol induces apoptosis through an increased intracellular calcium level, activation of JNK and p38 MAPK and NADPH oxidase – dependent generation of reactive oxygen species. *Apoptosis*, 16(4), 347 – 358.

Kim, Y. S., Jin, S. H., Kim. S. I. & Hahn, D. R. (1989). Studies on the mechanism of cytotoxicities of polyacetylenes against L1210 Cell. *Arch.Pharm.Res*, 12(3), 207-213.

Kimball, F. S., Turunen, B. J., Ellis, K. C., Himes, R. H. & Georg, G. I. (2008). Enantiospecific synthesis and cytotoxicity of 7-(4-methoxyphenyl)-6-phenyl-2,3,8,8a-tetrahydroindolizin-5(1H)-one enantiomers. *Bioorg Med Chem*, 16(8), 4367-4377.

Kinghorn, A. D., Carcache de Blanco, E. J., Chai, H. B., Orjala, J., Farnsworth, N. R., Soejarto, D. D., Oberlies, N. H., Wani, M. C., Kroll, D. J., Pearce, C. J., Swanson, S. M., Kramer, R. A., Rose, W. C., Fairchild, C. R., Vite, G. D., Emanuel, S., Jarjoura, D. & Cope, F. O. (2009). Discovery of anticancer agents of diverse natural origin. *Pure Appl Chem*, 81(6), 1051-1063.

Kintzios, S.E. & Barberaki, M. G. (2003). What do we know about cancer and its therapy?*Plant that fight cancer*(pp.1-10). Washington, D.C: CRC Press LLC.

Kuo, Y. C., Lin, Y. L., Huang, C. P., Shu, J. W. & Tsai, W. J. (2002) *Cancer Investigation*, 20. 955-964.

Kyoung, A. K., Jin, S. K., Rui, Z., Mei, J. P., Young, H. M., Mi, Y. K., In, K. L., Bum, J. K. & Jin, W. H. (2011). KIOM – 4 protects against oxidative stress – induced mitochondrial damage in pancreatic β – cells via its antioxidant effect. *Evidence – Based Complementary and Alternative Medicine*, 2011, 1-11.

Lam, K. S. (2007). New aspects of natural product in drug discovery. *TRENDS in Microbiology*, 15, 6.

Law, J. C., Ritke, M. K., Yalowich, J. C., Leder, G. H. & Ferrel, R. E. (1993). Mutational inactivation of the p53 gene in the human erythroid leukemic K562 cell line. *Leukemia Research*, 17 (12), 1045-1050.

Maddika, S., Ande, S. R., Panigrahi, S., Paranjothy, T., Weglarczyk, K., Zuse, A., Eshraghi, M., Manda, K. D., Wiechec, E. & Los, M. (2007). Cell survival, cell death and cell cycle pathways are interconnected: Implications for cancer therapy. *Drug Resistance Updates*, 10, 13-29.

M A K N A . (2 0 0 6) . *A b o u t m y w o r k – M A K N A* . U R L : http://www.makna.org.my/news/news_161006_01.asp. Accessed: 11th November 2010.

Malumbres, M. & Barbacid, M. (2009). Cell cycle, CDK and cancer a changing paradigm. *Cancer*, 9,153-166.

Medical Univercity of Vienna. (2005). *Cell Cycle Analysis by Propidium Iodide (PI) Staining*. URL: http://www.meduniwien.ac.at/user/johannes.schmid /PIstaining3.htm. Accessed: 6th November 2011.

Mendelsohn, J., Howley, P. M., Israel, M. A., Gray. J. W. & Thompson. C. B. (2008a). Apoptosis, Autophagy, and Necrosis. 3rd Edition, *The Molecular Basis of Cancer* (pp 205-220). Philadelphia, PA : Saunders, an imprint of Elsevier Inc.

Mendelsohn, J., Howley, P. M., Israel, M. A., Gray, J. W. & Thompson, C. B. (2008b). Regulation of the cell cycle. 3rd Edition, *The molecular basis of cancer* (pp 177-188). Philadelphia, PA : Saunders, an imprint of Elsevier Inc.

Min, C. Y., Dong, S. S., Sang, U. C., Young, H. P. & Kang, R. L. (2008). Polyacetylenes from the roots of cultivated-wild ginseng and their cytotoxicity *In Vitro*. *Arch Pharm Res*, 31(2), 154-159.

Mishra, K. P., Ganju, L., Sairam, M., Banerjee, P. K. & Sawhney, R. C. (2008). A review of high throughput technology for the screening of natural product. *Biomedicine & Pharmacotherapy*, 62, 94-98.

Mishra, R. C. (2011). Mircotubule binding natural substances in cancer chemotherapy. *Research Signpost*, 37/661 (2), 269-282.

Mohammad Shoeb (2006). Anticancer agents from medicinal plants. *Bangladesh J Pharmacol*, 1, 35-41.

N C I . (2 0 0 9) . *D e f i n i n g   o f   c a n c e r* .   U R L : http://www.cancer.gov/cancertopics/cancerlibrary/what-is-cancer, Accessed, 9th April 2010.

Newman, D.J., Cragg, G.M., & Snader, K.M. (2003). Natural products as sources of new drugs over the period 1981-2002. *J Nat Prod*, 66, 1022-1037.

Nie, B. M., Yang, L. M., Fu, S. L., Jiang, X. Y., Lu, P. H. & Lu, Yang. (2006). Protective effect of panaxydol and panaxynol on sodium nitroprusside-induced apoptosis in cortical neurons. *Chemico-Biological Interactions*, 160, 225-231.

Nie, B. M., Jiang, X. Y., Cai, J. X., Fu, S. L., Yang, L. M., Lin, L., Hang, Q., Lu, P. L. & Lu, Y. (2008). Panaxydol and panaxynol protect cultured cortical neurons against Ab25e35-induced toxicity. *Neuropharmacology*, 54, 845-853.

Panasci, L. C. & Alaoui – Jamali, M. A. (2004). Regulation of DNA repair and apoptosis by p53 and its impact on alkylating drug resistance of tumor cells, *DNA repair in cancer therapy* (pp 73-108). New Jersey: Humana Press Inc.

Pieters, L. & Vlietinck, A. J. (2005). Bioguided isolation of pharmacologically active plant component, still a valuable strategy for the finding of new lead compound? *Journal of Ethnopharmacology*, 100, 57- 60.

Pinto, M. C. X., Dias, D. F., Puerto, H. L., Martins, A. S., Teixeira-Carvalho, A., Martins-Filho, O., Badet, B., Durand, P., Alves, R. J. & Souza-Fagundes, E. (2011). Discovery of cytotoxic and pro-apoptotic compound against leukemia cells: Tert-butyl-4-[(3-nitrophenoxy)methyl]-2,2-dimethyloxazolidine-3-carboxylate. *Life Scinece*, 89, 786-794.

Plant of a Future. (2000). *Hydrocotyle vulgaris*. URL: http://www.ibiblio.org/pfaf/cgibin/arr_html?Hydrocotyle+vulgaris&CAN =LATIND, Accessed 10th August 2009.

Prasad, P. N. (2003). Flow cytometry, *Introduction to biophotonics* (pp 390-432). New Jersey: John Wiley & Sons, Inc, Hoboken.

Promega. (2009).*Technical bulle: Caspase-Glo® 3/7 Assay*. USA: Promega Corporation.

Proskuryakov, S. Y., Konoplyannikov, A. G. & Gabai, V. L. (2003). Necrosis: a specific form of programmed cell death? *Experimental Cell Research*, 283, 1-6.

Purup, S., Larsen, E. & Christensen. L. P. (2009). Differential effect of falcarinol and related aliphatic C_{17}- polyacetylenes on intestinal cell proliferation. *J. Agric. Food Chem*, 57, 8290-8296.

Puthalakath, H. & Strasser, A. (2002). "Keeping killers on a tight leash: transcriptional and post-translational control of the pro-apoptotic activity of BH3-only proteins." *Cell Death Differ*, 9 (5), 505 – 12.

Radin, N. S. (2001). Apoptosis death by ceramide: will the real killer please stand up? *Medical Hypotheses*, 67(1), 96-100.
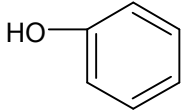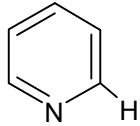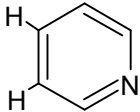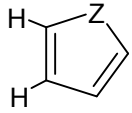
Radin, N. S. (2004). Poly – drug cancer therapy based on ceramide. *Exp Oncol*, 26(1), 3-10.

Radin, N. S. (2008). Drug design: hiding in full view. *Drug Development Research*, 69, 15 – 25.

Ramlan, A. A. (2003). *Turning Malaysia into a global herbal producer, a personal perspective.* URL: http:// www.penerbit .utm.my/cgi-bin/syarahan/print.cgi?id= sepintas lalu, Accessed 15th August 2009.

Reed, J. C. & Tomaselli, K. J.(2000). Drug discovery opportunities from apoptosis research. *Current Opnion in Biotechnology*, 11, 586-592.

Richardson, H. & Kumar, S. (2002). "Death to flies: Drosophila as a model system to study programmed cell death." *J Immunol Methods*, 265(1-2), 21-38.

Rimando, A. M., Olofsdotter, M., Dayan, F. E. & Duke. S. O. (2001). Searching for rice allelochemicals: An example of bioassay-guided isolation. *Agronomy Journal*, 93, 16-20.

RÍOS, J. L., RECIO, M. C., MÁÑEZ, S. & GINER, R. M., (2000). Natural Triterpenoids as Anti-inflammatory Agents, *Study of natural product chemistry* (pp 93-144) Netherlands: Elsevier Science B. V.

Robert, G & Johnson, M. D., (2009). *Surgery*. URL: http://www.merckmanuals.com/home/special_subjects/surgery/surgery.html?qt=&sc=&alt=. Accessed: 5th January 2011.

Rouessac, F. & Rouessac, A. (2000). Chemical analysis, *Modern instrumental methods and techniques*. England: John Wiley & Sons.

Ruddon, R. W. (2007). Cause of cancer. 4th Edition, *Cancer biology* (pp 17-61). New York: Oxford University Press, Inc.

Sarker, S. D., Latif, Z. & Gary. A. I.(2006a). Natural product isolation. 2nd Edition, *Natural product isolation* (pp 1-26). New Jersey: Humana press lnc.

Sarker, S. D., Latif, Z. & Gary. A. I. (2006b). *Isolation of Natural Product by Low-Pressure Column Chromatography*. 2nd Edition, *Natural product isolation* (pp 117-158). New Jersey: Humana press Inc.

Scholzova, E., Malik, R., Evcik, J. S. and Kleibl, Z. (2007). RNA regulation and cancer development. *Cancer Letter*, 246, 12-23.

166

Shriner, R. L., Hermann, C. K. F., Morrill, T. C., Curtin, D. Y. & Fuson. R. C. (2004). Mass spectrometry.8th Edition, *The systematic identification of organic compounds* (pp 228-246). Singapore: John Wiley & Sons (Asia) Pte.Ltd.

Skoog, D. A., Holler, F. J. & Nieman, T. A. (2004a). Molecular mass spectrometry. 5th Edition, *Principles of instrumental Analysis* (pp 498-534). United State: Thomson Learning, Inc.

Skoog, D. A., Holler, F. J. & Nieman. T. A. (2004b). Nuclear magnetic resonance spectroscopy. 5th Edition, *Principles of instrumental Analysis*(pp 445- 497) United State: Thomson Learning, Inc.

Sohn, J., Lee, C. H., Chung, D. J., Park, S. H., Kim, I. & Hwang, W. L. (1998). Effect of petroleum ether extract of Panax ginseng root on proliferation and cell cycle progression of human renal cell carcinoma cells. *Experimental and Molecular Medicine*, 30(1), 47-51.

Tai, J. & Cheung, S. (2007). Anti- proliferative and antioxidant activities of *Saposhnikovia divaricata*. *Oncology Reports*, 18, 227-234.

Tan, M. L., Ooi, J. P., Nawfal Ismail., Ahmed Ismail Hassan Moad. & Tengku Sifzizul Tengku Muhammad. (2009). Programmed cell death pathway and current antitumor target. *Pharmaceutical Research*, 26, 1547-1560.

Tannock, I. F., Hill, R. P., Bristow, R. G. & Harrington, L. (2005). Chemical and Radiation Carcinogenesis. 4th Edition, *The basic science of oncology* (pp 25-49). United State: McGraw-Hill.

Tee, S. L. (2007). Bioassay – guided isolation of cytotoxic compound from *Hydrocotyle vulgaris*. Unpublished degree's thesis, Universiti Tunku Abdul Rahman, Malaysia.

Thornberry, N. A., Rano, T. A., Peterson, E. P., Rasperi, D. M., Timkey, T., Garcia-Calvo, M., Houtzageri, V. M., Nordstromi, P. A., Royi, S., Vaillancourti, J. P., Chapman, K. T. & Nicholsoni. D. W. (1997). A Combinatorial approach defines specificities of members of the caspase family and granzyme B. *The journal of biological chemistry*, 272, 17907-17911.

Van Cruchten, S. &Van Den Broeck, W. (2002). Morphological and biochemical aspects of apoptosis, oncosis and necrosis. *Anat Histol Embryol*, 31(4), 214-23.
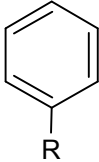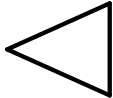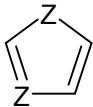
Villas-BOAS, S. G., Roessner, U., Hansen, M. A. E., Smedsgaard, J. & Nielsen, J. (2007). Analytical Tool, *Metabolome analysis: An introduction* (pp 83-145) New Jersey: John Wiley & Sons, Inc.

Vlietinck, A. J., Pieters, A. C. & Vander Berghe, D. A. (1995). Bioassay guided isolation and structure elucidation of pharmacologically active plant substances, *Photochemistry in medicine plant* (pp 113-132). New York: Plenum press.

Wagner, E. F. & Nebreda, Á. R. (2009). Signal integration by JNK and p38 MAPK pathways in cancer development. *Nature Review*, 9, 537 – 549.

Watts, D. C. (2007). *Elsevier's Dictonary of Plant Lore. P* (pp 283-310). United Kingdom: Elsevier. Inc.

Weyermann, J., Lochmann, D. & Zimmer, A. (2005). A practical note on the use of cytotoxic assays. *International Journal of Pharmaceutical*, 28, 369-376.

Wong, C. P. (2006). Cytotoxicity of some selected Chinese Malaysian herbs on Raji, HL-60, and U – 2 OS cell lines. Unpublished degree's thesis, Universiti Tunku Abdul Rahman, Malaysia.

Young, J. F., Christensen, L. P., Theil, P. K & Oksbjerg, N. (2008). The polyacetylene falcarinol and falcarindiol affect stress responses in myotube cultures in a biphasic manner. *Dose-Response*, 6, 239-251.

Young, J. F., Duthie, S. J., Milne, L., Christensen, L. P., Duthie, G. G. & Bestwick, C. S. (2007). Biphasic effect of falcarinol on CaCo – 2 cell proliferation, DNA damage, and apoptosis. *J.Agric.Food Chem*, 55, 618 – 623.

Yuan, R. & Lin. Y. (2000). Traditional Chinese medicine: an approach to scientific proof and clinical validation. *Pharmacology & Therapeutic*, 86, 191-198.

Zheng, G., Lu, W., Aisa, H. A. & Cai, J. (1999). Absolute configuration of falcarinol, a potent antitumor agent commonly occurring in plants. *Tetrahedron Letter*, 40, 2181-2182.

Zhou, G. X. & Molinski, T. F. (2003). Long – chain acetylenic ketones from the Micronesian sponge haliclona sp. Importance of the 1-yn-3-ol group for antitumor activity. *Mar.Drugs*, 1, 46-53.

APPENDIX A

^{1}H NMR Chemical Shifts in Organic Compounds. (Crews, Rodríguez, & Jaspars, 1998)

Name of Proton Character	Proton Character	Chemical shift (ppm)
Phenol – OH		4.0 – 10.0
Alcohols – OH	R – OH	1.0 – 5.4
Thiols – SH	HS – R	3.3 – 4.0
Amines – NH_2	R – NH_2	3.4 – 4.8
Amides	$RCONH_2$	4.9 – 7.0
	RCONHR	6.0 – 9.5
Carboxylic acids – OH	$HO_2 C$ -	9.0 – 12.0
Aldehydes	HCO -	9.5 – 10.5
Heteroaromatic		8.1 – 9.0
		6.5 – 7.4
	 Z = O, N, S	6.3 – 8.0

^{1}H NMR Chemical Shifts in Organic Compounds. (Crews, Rodríguez, & Jaspars, 1998)

Name of Proton Character	Proton Character	Chemical shift (ppm)
Aromatic	 R	6.4 – 8.3
Alkenes	$HRC = CR_2$	4.4 – 8.0
	$H_2C = CR_2$	4.4 – 6.6
	$-HC - O -$ or $- CH_2 - X$	3.8 – 5.2
Alcohol, Halogens	$-CH_2 - O -$ or $-CH_2 - X$	3.5 – 4.9
Amines	$-CH-N-$ or $CH_2 - N$	2.7 – 3.5
Alkynes	$R - C \equiv C - R$	2.2 – 3.0
Methyl group (R – Me)	$CH_3 - O -$	3.3 – 4.0
	$CH_3 - N -$	2.2 – 3.5
	$CH_3 - S -$	2.3 – 2.7
	$CH_3 - Ph$	2.3 – 2.6
	$CH_3 - C - X$	0.8 – 2.0
	$CH_3 - CO -$	1.9 – 2.2
	$CH_3 - C = C -$	1.5 – 2.0
Methylenes (- CH$_2$ -)	$Ph - CH_2 -$	2.6 – 2.9
	$- CO - CH_2 -$	2.2 – 2.8
	$-CH_2 - C = C -$	1.7 – 2.1
	$R - CH_2 - R$	1.2 – 1.9
Cyclopropyl		-0.9 – 0.8
Metals	$M - CH_3$	-0.1 – 0.1
	 Z = O, N, S	7.1 – 9.0

APPENDIX B

^{13}C NMR Chemical Shifts in Organic Compounds. (Crews, Rodríguez, & Jaspars, 1998)

Type of hybridisation	Type of carbon atom	Name of Carbon Character	Carbon Character	Chemical shift (ppm)
sp	-	Alkyne	$C \equiv C$	75 – 95
	-	Nitrile	$C \equiv N$	119 - 127
sp[2]	-	Ketone	$C = O$	204 – 230
	-	Aldehyde	$C = O$	186 - 208
	-	Acid	$C = O$	171 - 183
	-	Ester, Amide	$C = O$	160 - 175
	-	Thioketone	$C = S$	190 - 201
	-	Azomethine	$C = N -$	146 – 161
	-	Heteroaromatic	$C = N -$	145 - 154
	-	Alkene	$C = C$	106 - 142
	-	Aromatic	$C = C$	112 - 134
	-	Heteroaromatic	$C = C$ (*sp*[2])	117 – 140
	-	Alkyne	$C \equiv C$ (*sp*)	75 – 96
	-	Nitrile	$C \equiv N$ (*sp*)	119 – 127
sp[3]	4°		C Quat	118 – 127
	4°		$C – O$	74 – 85
	4°		$C – N$	61 – 77
	4°		$C – S$	51 – 71
	4°	Halogen	$C – X$	34 – 79

^{13}C NMR Chemical Shifts in Organic Compounds. (Crews, Rodríguez, & Jaspars, 1998)

Type of hybridisation	Type of carbon atom	Name of Carbon Character	Carbon Character	Chemical shift (ppm)
sp^3	3°		CH – C	32 – 60
	3°		CH – O-	65 – 78
	3°		CH – N-	56 – 69
	3°		CH – S-	57 – 65
	3°	Halogen	CH – X-	34 – 62
	2°		CH_2 – C	25 – 45
	2°		CH_2 – O-	56 – 69
	2°		CH_2 – N-	44 – 55
	2°		CH_2 – S-	28 – 43
	2°	Halogen	CH_2 – X-	5 – 39
	1°		CH_3 – C	7 – 28
	1°		CH_3 – O-	49 – 60
	1°		CH_3 – N-	11 – 41
	1°		CH_3 – S-	11 – 20
	1°	Halogen	CH_3 – X-	3 – 29

The equation to calculate cell viability is shown below:

A_B = Average of absorbance of blank

A_C = Average of absorbance of cell control

A_S = Average of absorbance of cell treated with extract

Percentage of cell viability = $\dfrac{A_S - A_B}{A_C - A_B}$ X 100

Example:

A_B: 0.14

A_C: 1.15

A_S: 0.21

Percentage cell viability: $\dfrac{0.21 - 0.14}{1.15 - 0.14}$ X 100

: 6.93 %

APPENDIX D

The equation to calculate the amount of caspase activity

A_B: Average of luminescent signal for blank

A_S: Average of luminescent signal for cells treat with panaxynol or cisplatin

Amount of caspase activity of 20000 cells treat with panaxynol or cisplatin: $A_S - A_B$

Amount of caspase activity per cell: $\dfrac{A_S - A_B}{200000}$

Example:

A_B: 30928.67 Relative luminescent units (RLU)/20000 cells

A_S: 335326.67 Relative luminescent unit (RLU)/20000 cells

Amount of caspase − 9 activity for 20000 K-562 cells treated with IC_{85} concentration of panaxynol: 335326.67 RLU/20000 cells - 30928.67 RLU/20000 cells

: 304398 RLU/20000 cells

Amount of caspase activity per K-562 cell treated with with IC_{85} concentration of panaxynol: 304398/ 20000

: 15.22 RLU/cell